National Library of Canada — Bibliothèque nationale du Canada

CANADIAN THESES ON MICROFICHE — THÈSES CANADIENNES SUR MICROFICHE

NAME OF AUTHOR/NOM DE L'AUTEUR [illegible]

TITLE OF THESIS/TITRE DE LA THÈSE The Ground Temperatures [illegible] and [illegible] [illegible] [illegible] [illegible] [illegible] River and Environmental Boundary Conditions

UNIVERSITY/UNIVERSITÉ University of Alberta, Edmonton

DEGREE FOR WHICH THESIS WAS PRESENTED/GRADE POUR LEQUEL CETTE THÈSE FUT PRÉSENTÉE M.Sc.

YEAR THIS DEGREE CONFERRED/ANNÉE D'OBTENTION DE CE GRADE [illegible]

NAME OF SUPERVISOR/NOM DU DIRECTEUR DE THÈSE Prof. K. N. [illegible]

DATED/DATÉ [illegible] SIGNED/SIGNÉ [illegible]

PERMANENT ADDRESS/RÉSIDENCE FIXE [illegible] Dyer [illegible] Road,

Penang, Malaysia

THE UNIVERSITY OF ALBERTA

THE [illegible] AND ITS

RELATIONSHIP TO SOIL PROPERTIES, [illegible] OF

COVER [illegible] CONDITIONS

by

(C) [illegible]

A THESIS

SUBMITTED TO THE FACULTY OF GRADUATE STUDIES AND RESEARCH

IN PARTIAL FULFILMENT OF THE REQUIREMENTS FOR THE DEGREE

OF MASTER OF SCIENCE

DEPARTMENT OF MECHANICAL ENGINEERING

EDMONTON, ALBERTA

SPRING, 1975

UNIVERSITY OF ALBERTA

FACULTY OF GRADUATE STUDIES AND RESEARCH

The undersigned certify that they have read, and recommend to the Faculty of Graduate Studies and Research, for acceptance, a thesis entitled "THE GROUND TEMPERATURE REGIME AND ITS RELATIONSHIP TO SOIL PROPERTIES, SURFACE COVER AND ENVIRONMENTAL BOUNDARY CONDITIONS," submitted by WONG, BOON-KENG in partial fulfillment of the requirements for the degree of Master of Science.

. . . .
Supervisor

. . . .

. . . .

. . . .

Date . January 20th, 1975 . . .

ABSTRACT

A study is made of the problem of periodic heat flow to the ground in a freeze thaw situation. Analytic and numerical models are developed for the purpose of studying the effects of various parameters on the ground thermal regime. In particular, the effects of surface cover, soil properties and meteorological parameters on the average ground temperature below the active layer are studied. The main emphasis has been toward obtaining an indication of the effects of the parameters rather than an overall predictive model.

The results obtained indicate the relative importance of the various parameters. They also indicate that under certain conditions simplifying approximations can be made to the environmental boundary conditions. Analytical methods of estimating the quantitative effects of surface disturbances are proposed.

The results are in general agreement with field observations.

ACKNOWLEDGMENTS

The author would like to express his appreciation to Dr. K.R. Gilpin for his guidance and supervision. Thanks are due also to Mrs. Elaine Weisenburger for typing this thesis.

TABLE OF CONTENTS

TABLE OF CONTENTS (continued)

TABLE OF CONTENTS (continued)

Page

TABLE OF CONTENTS (continued)

TABLE OF CONTENTS (continued)

LIST OF TABLES

LIST OF TABLES (Continued)

LIST OF FIGURES

LIST OF FIGURES (continued)

NOMENCLATURE

LETTER SYMBOLS

Symbol	Definition
c	Specific heat
d	Insulating layer thickness
D	Diffusivity
e_a	Air vapor pressure
erf	Error function
erfc	Complementary error function
f	Variable associated with D
F	Constant associated with D
G	Heat flux to the ground
h	Enthalpy
h_{eff}	Effective 'heat transfer coefficient'
k	Thermal conductivity
L	Latent heat flux
L_1	Latent heat
M	Constant associated with height of cloud cover
M_1	Moisture content
P	Total pressure
R	Radiation
r	Reflectivity
S	Sensible heat flux
S_1	Stefan constant

NOMENCLATURE (continued)

Symbol	Definition
t	Time
T	Temperature
U	U factor
u	Wind velocity
u_{nf}	Unfrozen moisture content
w	Relative humidity
w_c	Cloud cover
x	Depth
y	Depth of the fusion front

GREEK LETTERS

τ	Time (normalized)
α	Thermal diffusivity
ε	Thermal emissivity
η	Depth of fusion front (normalized)
θ	Temperature (normalized)
ϕ	Enthalpy (normalized)
ζ	Depth (normalized)
ω	Frequency
σ	Stefan-Boltzmann constant
ρ	Density

NOMENCLATURE (continued)

SUBSCRIPTS

Symbol	Definition
so	Soil
a	Air
s	Surface
gs	Ground surface
gw	Point just beneath the active layer
c	Constant
F	Freezing
f	Frozen
uf	Unfrozen

PART I

INTRODUCTION

The problem of heat flow into a thawing and freezing soil has been studied rather extensively in the past especially by those countries close to the Arctic Region namely, Russia, Canada, United States and the Scandinavian countries. Despite these efforts, an exact mathematical solution to any practical thermal soil problem is still unavailable. General solution of the temperature distribution in the soil involves analysis of the transient heat flow in the soil which is affected by the thermal properties, namely, the specific heat, latent heat and conductivity, all of which are temperature-dependent. Therefore in order to find an exact mathematical solution, the specific problem must first be idealized. Problems of this nature are boundary value problems and therefore accurate specific boundary conditions must be applied to the surface where the heat flow is known.

1.1 Review of some analytical techniques

The first mathematical solution obtained for this problem is by Neumann (1) but was later adapted to the calculation of frost depth penetration in soil by Berggren (2). The first published literature on the rate of ice formation in still water was by Stefan (3) and thus hence originate the title "Stefan Problem". Most of the theoretical frost depth equations used even today can be shown to be a modified form or a variation of the "Berggren formula" (or Neumann) even the "Stefan formula". Later Aldrich and Paynter (4, 5) presented the "Berggren formula" in a modified form so that it could be adapted to layered systems. Since then the "modified Berggren formula" has been adopted by the Corps of Engineers and the Highway Research Board in the United States with some modifications to accommodate the specific conditions.

Consider now Neumann's solution applied to a semi infinite soil initially at constant temperature, T_c. Then assume that the surface temperature drops below freezing and remains so for all $t > 0$. There exists now two phases, the frozen and the unfrozen region.

The temperature distributions for the frozen and the unfrozen regions are given by:

$$T_f = (T_F/\mathrm{erf}\,\lambda)\ \mathrm{erf}(y/2(\alpha_f t)^{1/2}) \tag{1.1}$$

$$T_{uf} = T_c - \{[(T_c - T_F)/\mathrm{erfc}\ \lambda(\alpha_f/\alpha_{uf})^{1/2}]\ \mathrm{erfc}(y/2(\alpha_{uf} t)^{1/2})\} \tag{1.2}$$

where T_F is the freezing temperature of the liquid and,

λ is the proportional constant which is determined from:

$$(e^{-\lambda^2}/\mathrm{erf}\,\lambda) - \{[k_{uf}(\alpha_f)^{1/2}(T_c - T_F)\ e^{-(\alpha_f/\alpha_{uf})\ \lambda^2}]/$$

$$[k_f(\alpha_{uf})^{1/2}\ T_F\ \mathrm{erfc}\ \lambda(\alpha_f/\alpha_{uf})^{1/2}]\} = (\lambda L\sqrt{\pi})\alpha_f T_s \tag{1.3}$$

The interface position y is obtained from

$$y = 2\lambda(\alpha_f t)^{1/2} \tag{1.4}$$

Apart from Neumann (1, 6) and Stefan (3), the only two known exact solutions available, there are others solutions but they do not give the exact closed form solutions. The Variational Technique was used by Biot and Daughaday (18) to study the heat conduction in a melting semi infinite solid with constant properties. Goodman (19) used the Heat-Balance Integral Technique to solve cases of melting in a semi infinite solid with a fixed boundary temperature and with a given heat flux at the boundary. The Heat-Balance Integral Technique changes the energy equation from a partial differential equation into an ordinary differential equation.

$$\int_0^x \rho c \frac{\partial T}{\partial t} dx = \int_0^x \nabla . k \nabla T dx \tag{1.5}$$

The temperature profile is then assumed to be of a general polynomial form which is substituted into the integral equation. Integration produces an ordinary differential equation with time t as an independent variable. Poot (21) used the integral method to study a moving two dimensional solidification problem. The complexity of this heat transfer problem is increased if the latent heat effect no longer occurs at a certain single temperature, but over a temperature range. The problem was described by Rubinshtein (22) and Weiner (23), both considering the soil undergoing "n" phase changes. In 1967 Tien and Geiger (27) obtained a solution for the above problem using the Neumann approach by modifying the boundary conditions.

1.2 Review of some of the numerical techniques used

As reviewed previously, there are relatively few analytical solutions available for the practical heat transfer problems involving a change in phase of the soil due to freezing and thawing. In order to obtain a more general solution, other techniques have to be adopted.

Numerical methods are the most powerful and accurate of all the techniques available.

Many of the existing numerical solutions to the practical heat transfer problem involving change of phase use a continuous description on the movement of the fusion front as well as a description of the temperature distributions. Modifying the conventional finite difference procedure, various authors developed different ways of solving the problem. Cochran (24) developed a simplified analysis by using a single lump of variable thickness to represent the frozen region. While the technique works the inaccuracies resulted from the lumping severely hindered its use. Otis (25) extended the works of Lightfoot by using the concept of a moving heat source to account for the latent heat. Forster (26) modified the conventional finite difference equation for fixed grid so that the travel of the fusion front is continuously computed, but the method is limited for soil initially or finally at the fusion temperature only. Murray and Landis (12) later developed two numerical approaches with a wider range of applicability and a greater degree of accuracy. One approach utilizes the variable space network where the number of grid points in each phase (frozen and unfrozen) remains constant. The second method was a refinement of the Forster work. It lead to a more accurate prediction of the temperature distribution and it also continuously computed the fusion front movement.

Most of the above mentioned methods have difficulty in handling the situation where a fusion front overtakes a thawing front or vice versa. This occurs in the case where the surface temperature is periodic and its range includes 0°C. The numerical model presented in this thesis will be free of this limitation.

1.3 Recent Interest

Building of engineering structures such as oil and gas pipelines, roads and etc. in permafrost regions such as Alaska and Northern Canada, has been and still is a big problem for any contractor especially now with the present development and discovery of large energy resources. With the rapid growth of development, a growing concern for the arctic environment has caused both the government and industry to increase their rate of research on developing suitable methods for constructing and operating in permafrost areas. A considerable amount of work has been, and continues to be done in the area of developing comprehensive models of heat flux in freezing and thawing soils. Numerical methods have been, and continue to be developed by universities, government and industry to model ground thermal regime. The choice of numerical methods used depends on the problem under consideration. For one-dimensional analysis, finite difference methods are in common use. The finite difference methods used are: ordinary forward difference, backward difference and the alternating direction. The forward difference has been used by many authors whereas the backward difference has been rarely used. The alternating-direction explicit methods were employed by Lachenbruch (13) and Doherty (14) while Fleming (15) used the alternating-direction implicit methods for solving the problem. The recent trend is towards the use of finite element methods, as were used by Hwang et al (16) and Charlwood (17). These have been designed for engineering predictions of temperatures around engineering structures.

1.4 Proposed program

The purpose of this thesis will be to assess the effects of each of a number of parameters in this very complicated problem of periodic heat transfer to the ground in a freeze and thaw situation. This will be done by breaking the problem into three subproblems. They are:

I. Ground temperature distributions with imposed surface temperatures. Here, the main objective will be to look at the effects that the various individual soil parameters have on the ground temperatures and the active layer.

II. Ground temperature distributions with an insulating layer and an imposed insulating layer surface temperature. Here the main objective will be to look at the effects the insulating layer have on the ground temperatures and the active layer.

III. As in (II) but with the environmental heat fluxes at an insulating layer surface boundary. Here, the main objective will be to look at the effects the main parameters have on the various temperatures.

PART II

IMPOSED SURFACE TEMPERATURE

2.1 Analytical model for the ground temperature distributions with imposed surface temperature

2.1.1 Formulation of the model

Assume the ground to be a semi infinite domain in which two phases exist as shown in Figure 1. Soil properties will be assumed to be uniform throughout a given phase, however conductivity, specific heat and the temperature gradient will be different for the two phases.

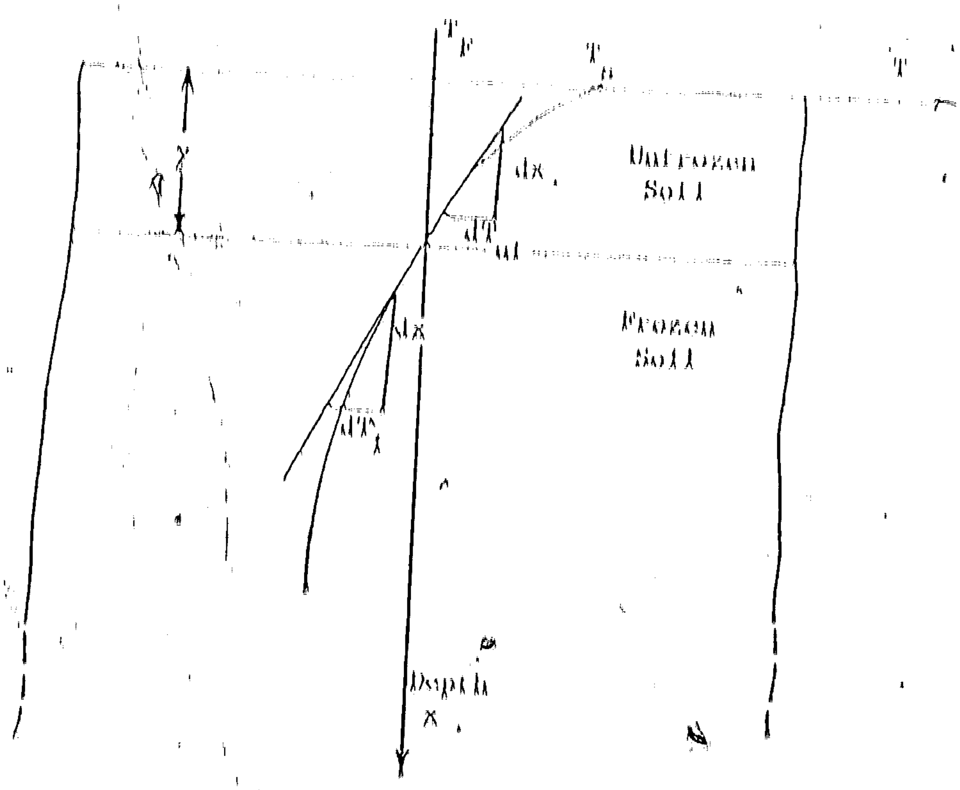

FIGURE 1

Applying the classical theory of heat transfer to the above conditions, the temperature distribution within a given phase may be calculated.

Using the Fourier approximation for one-dimensional heat conduction and the first law of thermodynamics, the equation for the temperature, T_{uf} in the unfrozen region becomes

$$\alpha_{uf}(\partial^2 T_{uf}/\partial x^2) = \partial T_{uf}/\partial t \tag{2.1}$$

where $\alpha_{uf} = k_{uf}/\rho c_{uf}$.

At the moving interface between the frozen and the unfrozen regions, the heat flow into the interface equal to the heat flow out plus the latent heat of fusion associated with the interface motion. The conditions will be satisfied by the equations

$$k_{uf}\ \partial T_{uf}/\partial x + \rho L(\partial y/\partial t) = k_f\ \partial T_f/\partial x \tag{2.2}$$

where y is the position of the interface.

In the frozen region the diffusion equation is

$$\alpha_f(\partial^2 T_f/\partial x^2) = \partial T_f/\partial t \tag{2.3}$$

The boundary condition at the ground surface will be assumed to be that of an imposed temperature varying sinusoidally during the year, that is

$$T_s = \bar{T}_s + \Delta T \sin 2\pi t$$

where $\bar{T}_s$ is the average temperature and

ΔT is the amplitude of variation

The boundary condition at $x \to \infty$ is $\partial T/\partial x = 0$, that is zero heat flux. Non-dimensionalizing equations (2.1), (2.2) and (2.3), the three equations become :

$$\partial^2\theta_{ul}/\partial\xi^2 = S_{ul}(\partial\theta_{ul}/\partial\tau) \qquad (2.4)$$

$$(k_{ul}/k_l)\ \partial\theta_{ul}/\partial\xi = -\partial\eta/\partial\tau + \partial\theta_l/\partial\xi \qquad (2.5)$$

and

$$\partial^2\theta_l/\partial\xi^2 = S_l(\partial\theta_l/\partial\xi) \qquad (2.6)$$

where $\theta = (T - T_f)/\Delta T$

$\xi = x/x_c$

$\eta = y/x_c$

$\tau = t/t_c$ (and $t_c = 1$ year)

$S_l = \rho c_l \Delta T/\rho L$

$= \rho c_l x_c^2/k_l t_c$

where $x_c = (k_l t_c \Delta T/\rho L)^{1/2}$

similarly

$S_{ul} = \rho c_{ul} x_c^2/k_l t_c$

The boundary conditions in non dimensional form become :

at $\zeta = 0$ $\qquad \theta = \theta_a + \sin 2\pi\tau$

and

at $\zeta \to \infty$ $\qquad \partial\theta/\partial\zeta = 0$

For the purposes of obtaining an approximate analytical solution, the above problem can be simplified down to "Stefan Problem" which is the simplest form of approximation. It will be used to predict the frost penetration depth and the average ground temperature. In this simplification it is assumed that the volumetric heat capacities of both the frozen and the unfrozen soil are negligible with respect to the latent heat of fusion of the soil water. This condition is satisfied when the Stefan Number ($c\Delta T/L$) is small. When this condition is satisfied, the three governing equations become respectively

$$\partial^2\theta_{uf}/\partial\zeta^2 = 0 \qquad (2.7)$$

$$(k_{uf}/k_f)\ \partial\theta_{uf}/\partial\zeta = -\,d\eta/d\tau + \partial\theta_f/\partial\zeta \qquad (2.8)$$

$$\partial^2\theta_f/\partial\zeta^2 = 0 \qquad (2.9)$$

Equations (2.7) and (2.9) with the unfrozen and the frozen phases can thus be integrated to give

$$\theta_{uf} = C_1 + C_2\,\zeta \qquad (2.10)$$

[illegible] (2.1

that is within a given phase the temperature profiles are linear

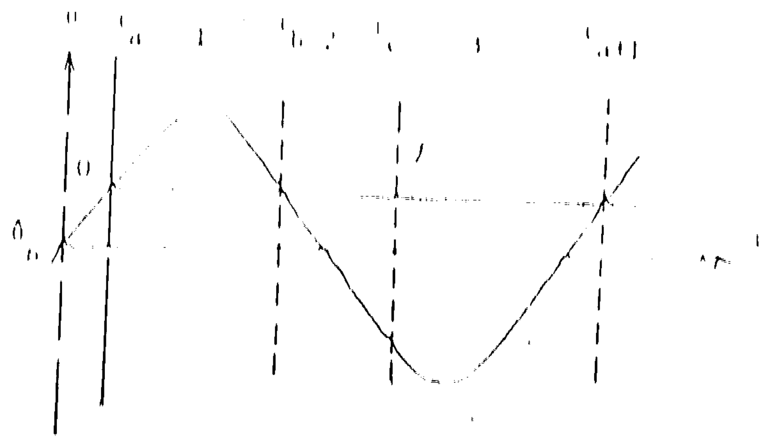

(i)

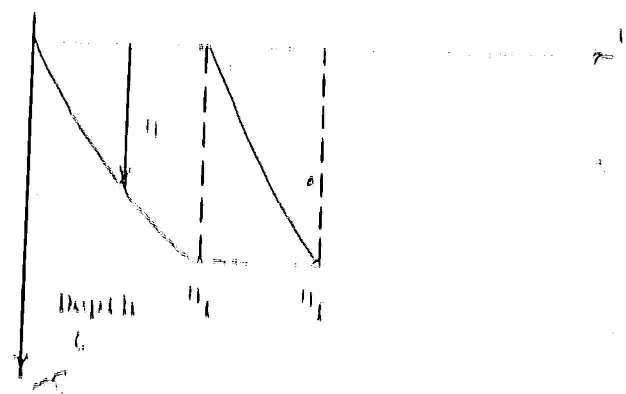

(ii)

FIGURE 2

For the assumption of the surface temperature, three different time domains may exist throughout the year (Figures 2 and 3).

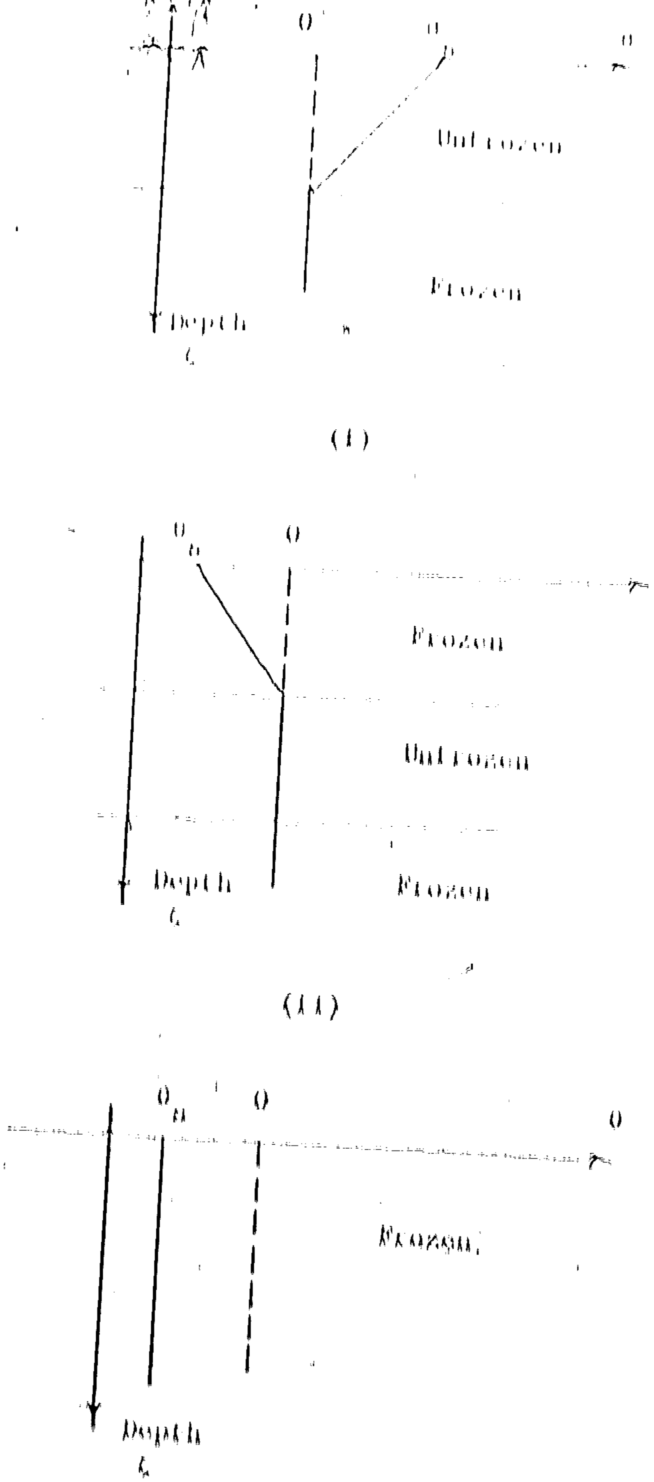

FIGURE 3

Applying the boundary conditions to equation (2.10) and (2.11)

$$\zeta = 0, \quad \theta_{ul} = \theta_s$$

$$\zeta = m, \quad \partial\theta_f/\partial\zeta = 0$$

$$\zeta = n, \quad \theta_{ul} = \theta_f = 0$$

Considering first equation (2.10)

$$\theta_{ul} = C_1 + C_2\,\zeta$$

at $\zeta = 0, \quad \theta_{ul} = \theta_s$

$$\therefore C_1 = \theta_s$$

at $\zeta = n, \quad \theta_{ul} = 0$

$$\therefore C_2 = -\theta_s/n$$

hence

$$\theta_{ul} = \theta_s(1-\zeta/n) \tag{2.12}$$

Considering now equation (2.11)

$$\theta_f = C_3 + C_4\,\zeta$$

at $\zeta = n, \quad \theta_f = 0$

$$\therefore 0 = C_3 + C_4\,n$$

at $\zeta = m, \quad \partial\theta_f/\partial\zeta = 0$

implying $C_4 = 0$

$\therefore C_3 = 0$

hence $u_1 = 0$ (2.13)

Substituting equations (2.12) and (2.13) into equation (2.8), it becomes

$$(k_{ut}/k_l)\ \theta_s/\eta = d\eta/dt \qquad (2.14)$$

Equation (2.14) is the governing equation for this simplified problem.

2.1.2 Solution

Considering first region (1) and Figure 2(1), the boundary conditions are

at $\eta = 0, \quad t = t_a$

and at $\eta = \eta_1, \quad t = t_b$

The governing equation is

$$(k_{ut}/k_l)\ \theta_s\ dt = \eta d\eta$$

but $\theta_s = \bar{\theta}_s + \sin 2\pi t$

where $\bar{\theta}_s = (\bar{T}_s - T_F)/\Delta T$

Integrating equation (2.14), it gives

$$\eta^2/2 = (k_{ut}/k_l)\ (-\cos 2\pi t/2\pi + \bar{\theta}_s t) + \text{const}$$

From the boundary conditions, when $\eta = 0, t = t_a$

$$\therefore \text{const.} = (k_{ut}/k_t)[\cos 2\pi t_a/2\pi - \theta_s t_a]$$

hence $$\eta^2/2 = (k_{ut}/k_t)[(\cos 2\pi t_a - \cos 2\pi t)/2\pi + \theta_s(t - t_a)]$$

when $$\eta = \eta_t, \quad t = t_b$$

$$\therefore \eta_t^2/2 = (k_{ut}/k_t)[(\cos 2\pi t_a - \cos 2\pi t_b)/2\pi + \theta_s(t_b - t_a)] \qquad (2.15)$$

From Figure 2(1)

$$\dot{\eta} = 0$$

when $t = t_a$ and $t = t_b$

$$\therefore \sin 2\pi t_a = -\theta_s$$

hence $$t_a = \sin^{-1}(-\theta_s)/2\pi \ ;$$

$$t_b = 1/2 - t_a$$

$$\cos 2\pi t_a = (1-\theta_s^2)^{1/2}$$

$$\cos 2\pi t_b = \cos(\pi - 2\pi t_a)$$

$$= -(1-\theta_s^2)^{1/2}$$

Substituting the above expressions into equation (2.15), it becomes

$$\eta_t^2 = (2k_{ut}/k_t)[(1-\theta_s^2)^{1/2}/\pi + \theta_s(1/2 - \sin^{-1}(-\theta_s)/\pi)] \qquad (2.16)$$

Equation (2.16) gives the depth of the claw penetration. Considering now region (2) of Figure 2.

$$\therefore u_1^2/2 = -\int_{t_b}^{t_c} \theta_s \, dt$$

from region (1),

$$u_t^2/2 = k_{u1}/k_1 \int_{t_a}^{t_b} \theta_s \, dt \qquad (2.18)$$

but $\quad u_t^2/2 = u_1^2/2$

$$\therefore \int_{t_b}^{t_c} \theta_s \, dt = - k_{u1}/k_1 \int_{t_a}^{t_b} \theta_s \, dt \qquad (2.19)$$

Considering all the 3 regions

$$\theta_s = \int_{t_c}^{t_a+1} \theta_s \, dt \qquad (2.20)$$

$$\int_{t_a}^{t_a+1} \theta_s = \theta_s$$

$$\therefore \int_{t_a}^{t_b} \theta_s \, dt + \int_{t_b}^{t_c} \theta_s \, dt + \int_{t_c}^{t_a+1} \theta_s \, dt = \bar{\theta}_s$$

hence

$$\int_{t_c}^{t_a+1} \theta_s \, dt = - \int_{t_a}^{t_b} \theta_s \, dt - \int_{t_a}^{t_b} \theta_s \, dt + \bar{\theta}_s \qquad (2.21)$$

Substituting equation (2.21) into equation (2.19), it gives

$$\bar{\theta}_s = - \int_{t_a}^{t_b} \theta_s \, dt - \int_{t_b}^{t_c} \theta_s \, dt + \bar{\theta}_s$$

$$\therefore \theta_g - \theta_s = \zeta \int_{t_a}^{t_b} \theta_s \, dt - \int_{t_b}^{t_a} \theta_s \, dt$$

$$= -(1-k_{uf}/k_f) \int_{t_a}^{t_b} \theta_s \, dt$$

but from region (1),

$$-\int_{t_a}^{t_b} \theta_s \, dt = -(1-\theta_s^{\,2})^{1/2}/\pi - \theta_s(1/2 - \sin^{-1}(-\theta_s)/\pi)$$

$$\therefore (\theta_g - \theta_s) = (k_{uf}/k_f - 1)[\theta_s[1/2 - \sin^{-1}(-\theta_s)/\pi]$$

$$+ (1-\theta_s^{\,2})^{1/2}/\pi] \tag{2.22}$$

Equation (2.22) gives the average ground temperature for the case when $T_s < T_F$.

Solutions to the above problem are for the case when the average temperature $\bar{T}_s$ is less than the freezing temperature T_F. Using the same approach as above, the solutions for the case when the average temperature, $\bar{T}_s$ is greater than the freezing temperature T_F, are:

$$\eta_F^{\,2} = -2[(1-\bar{\theta}_s^{\,2})^{1/2}/\pi + \bar{\theta}_s[1/2 - \sin^{-1}(-\bar{\theta}_s)/\pi]] \tag{2.23}$$

and,

$$(\bar{\theta}_g - \bar{\theta}_s) = (1-k_f/k_{uf})[\bar{\theta}_s[1/2 - \sin^{-1}(-\bar{\theta}_s)/\pi + (1-\bar{\theta}_s^{\,2})^{1/2}/\pi] \tag{2.24}$$

Equation (2.23) and (2.24) gives the frost penetration and the average ground temperature for the case when $\bar{T}_s > T_F$. These analytic results will be compared with the numerical results later in this part of the thesis.

2.1.3 Limitations of this analytic model

i. The assumptions that the properties of the soil are uniform is not true in many cases. This is because of the different soil textures, moisture content, soil compositions and other soil properties at different regions in the soil. All these properties contribute to the volumetric heat capacities, latent heat of fusion and the thermal conductivities of the soil.

ii. Though the air temperature is not a true periodic function of time owing to the variability of the weather, it has many features in common with a periodic function, such as the fluctuations caused by the succession of day and night or winter and summer.

2.2 Numerical Model

2.2.1 Formulation of the model

The main difference between the proposed method and most of the existing methods will be, instead of continuously computing the travel of the fusion front, this proposed method will keep track of the enthalpy h, as well as the temperature T, at any time t. Governing Equations:

$$\partial h/\partial t = k(\partial^2 T/\partial x^2) \qquad (2.25)$$

where

$$\left.\begin{aligned} h/\rho L &= (T-T_f)\rho c_f/\rho L & T < T_f \\ h/\rho L &= (T-T_f)\rho c_{uf}/\rho L + \rho L/\rho L & T > T_f \end{aligned}\right\} \qquad (2.26)$$

The boundary conditions are

$$\left.\begin{array}{ll} x = 0, & T = T_s \\ x \to \infty, & \partial T/\partial x = 0 \end{array}\right\} \qquad (2.27)$$

At $T = T_F$, the enthalpy is not a single valued function of temperature, thus equation (2.26) cannot be substituted directly into equation (2.25) as in the case where no phase change occurs. This difficulty can be overcome either by keeping track of the position of the fusion fronts or by keeping track of the enthalpy. The later method will be used.

Equation (2.26) is true when the entire phase change occurs at a single temperature. If the phase change happens to occur over a temperature range, equations (2.25) and (2.26) will be modified to take into account the unfrozen water content. The modifications will be presented at the end of this section.

2.2.2 Normalizing the equations

Writing

$\phi = h/\rho L$

$\theta = (T-T_F)/\Delta T$

$\xi = x/x_o$

$\tau = t/t_o$ where $t_o = 1$ year

Equation (2.26) becomes

$$\phi = (\rho c_f \Delta T/\rho L)\theta \qquad \theta < 0$$

$$\phi = (\rho c_{uf} \Delta T/\rho L)\theta + 1 \qquad \theta > 0$$

ie: $$\phi = S_f \theta \qquad \theta < 0$$

$$\phi = S_{uf}\theta + 1 , \qquad \theta > 0 \qquad (2.28)$$

where $S_f = (\rho c_f \Delta T)/\rho L$

and $S_{uf} = (\rho c_{uf} \Delta T)/\rho L$

Equation (2.25) becomes

$$(\rho L/t_c)\ \partial\phi/\partial t = (k\Delta T/x_c^{\ 2})\ \partial^2\theta/\partial\xi^2$$

$$\therefore\ \partial\phi/\partial\tau = [k t_c \Delta T/\rho L x_c^{\ 2}]\ \partial^2\theta/\partial\xi^2 \qquad (2.29)$$

For the frozen and unfrozen regions, the respective equations are:

$$\partial\phi/\partial\tau = [k_f t_c \Delta T/\rho L x_c^{\ 2}]\ \partial^2\theta/\partial\xi^2 \qquad (2.30)$$

and $$\partial\phi/\partial\tau = [k_{uf} t_c \Delta T/\rho L x_c^{\ 2}]\ \partial^2\theta/\partial\xi^2 \qquad (2.31)$$

choosing

$$[k_f t_c \Delta T/\rho L x_c^{\ 2}] = 1$$

then equations (2.30) and (2.31) become

$$\partial\phi/\partial\tau = \partial^2\theta/\partial\xi^2 \qquad (2.32)$$

and $\quad \partial \theta/\partial t = (k_{ut}/k_f)\ \partial^2\theta/\partial \xi^2$ (2.33)

i.e.: $\quad \partial\phi/\partial t = k'(\partial^2\theta/\partial\xi^2)$ (2.34)

where $\quad k' = 1 \qquad \theta < 0$

$\qquad = k_{ut}/k_f \qquad \theta > 0$ (2.35)

Rewriting the governing equations with the given boundary conditions, the equations are

$$\partial\phi/\partial t = k'(\partial^2\theta/\partial\xi^2) \tag{2.34}$$

$\phi = S_f\theta \qquad \theta < 0$

$\phi =$ [illegible] $\qquad \theta > 0$ (2.28)

$x = 0,$ [illegible] $\theta = \theta_1$

$x = x_s,$ [illegible] $(\theta_n - \theta_{n-1})/\Delta\xi = 0$ (2.36)

2.2.3 Solution

Considering now equation (2.34)

$$\partial\phi/\partial t = k'(\partial^2\theta/\partial\xi^2)$$

writing it in the finite difference form, it becomes

$$d\phi/dt\big|_{t_m} = (\phi^{m+1} - \phi^m)/\Delta t$$

where ϕ^{m+1} is one time step ahead of ϕ^m

$$K'(\partial^2\theta/\partial z^2) = ((\theta_{m+1} - \theta_n) K'/\Delta z - (\theta_n - \theta_{n-1}) K'/\Delta z)/\Delta z$$

or

$$\phi^{m+1} - \phi^m = (K'(\theta_{n+1} - \theta_n) - K'(\theta_n - \theta_{n-1}))\Delta t/\Delta z^2 \qquad (2.37)$$

but

$$\phi^{m+1} - \phi^m = \Delta\phi^m$$

$$\therefore \phi^{m+1} = \phi^m + \Delta\phi^m \qquad (2.38)$$

Hence equation (2.37) can be written as

$$\Delta\phi^m = (K'(\theta_{n-1} - \theta_n) - K'(\theta_n - \theta_{n+1}))\Delta t/\Delta z^2 \qquad (2.39)$$

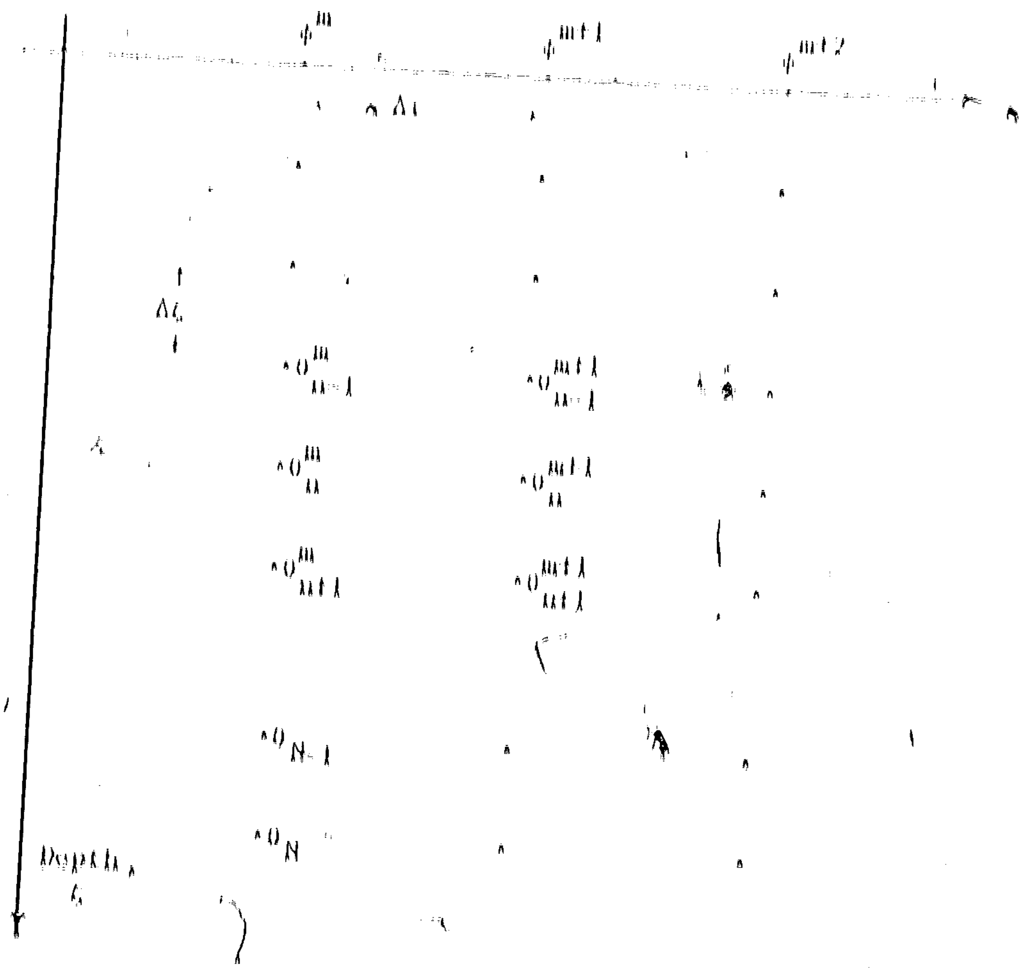

where $\phi^{m+1}_{n,1}$ is one time step ahead of $\phi^{m}_{n,1}$.

Initially all the temperatures at the nodal points were assumed to be at a constant temperature T_s. New enthalpies and hence the new temperatures, one time step forward, were then found by applying the boundary conditions to the governing equations. The time interval $\Delta\tau$ was chosen to be so small that only the local temperature and the temperature of the adjacent reference points need to be considered in calculating the local temperature. It was found that if $\Delta\tau$ was greater than $\frac{1}{2} S_1 (\Delta x)^2$, numerical instabilities resulted because of the use of an explicit computation scheme.

Briefly the steps are:

I. Set all temperatures equal to θ (i.e. $\theta_n = \theta$) and then change it into ϕ using equation (2.28).

$$\phi^m = S_{ul}\,\theta + L \qquad \text{if } \theta > 0$$

$$= S_1\,\theta \qquad \text{if } \theta < 0$$

II. Apply the boundary conditions equation (2.36) and solve for the enthalpy changes at each nodal point using equation (2.39). Then using enthalpies from the last time step and these enthalpy changes, new values of the enthalpies at each nodal are calculated. Enthalpy changes only apply for node 2 to node N since this is an imposed surface temperature problem. The temperature at the surface therefore is always equal to the imposed temperature, which in this case is the air temperature.

So for node 2 to (N-1), using equation (2.19)

$$\Delta\phi_n^m = R11(\theta_{n-1} - \theta_n) - R12(\theta_n - \theta_{n+1})$$

where $R11 = \Delta t/\Delta z^2$ if $\theta_{n-1} + \theta_n > 0$

$= (k_u/k_f)\,\Delta t/\Delta z^2$ if $\theta_{n-1} + \theta_n < 0$

and $R12 = \Delta t/\Delta z^2$ if $\theta_n + \theta_{n+1} > 0$

$= (k_u/k_f)\,\Delta t/\Delta z^2$ if $\theta_n + \theta_{n+1} < 0$

$$\phi_n^{m+1} = \phi_n^m + \Delta\phi_n^m$$

For node N, assuming the heat flux from deep in the ground to be negligible

$$\Delta\phi_N^m = (\theta_{N-1} - \theta_N)\,RT \times 2$$

where $RT = \Delta t/\Delta z^2$ if $\theta_{N-1} + \theta_N > 0$

$= (k_u/k_f)\,\Delta t/\Delta z^2$ if $\theta_{N-1} + \theta_N < 0$

$$\phi_N^{m+1} = \phi_N^m + \Delta\phi_N^m$$

iii. Then use enthalpy ϕ_n^{m+1} to calculate θ_n^{m+1} by using equation (2.28).

$\theta_n^{m+1} = \phi_n^{m+1}/S_f$ if $\phi_n^{m+1} > 0$

$= (\phi_n^{m+1} - 1)/S_u$ if $\phi_n^{m+1} < 0$

θ_n^{m+1} are then the new temperatures one time step ahead of θ_n^m. Both the new temperatures θ_n^{m+1} and enthalpies ϕ_n^{m+1} are stored.

iv. Proceed as before, as the time step advances, but now the initial temperatures and enthalpies are those just computed, θ_n^{m+1} and ϕ_n^{m+1} respectively.

As for the surface temperature, $\theta_1 = \theta_n$.

v. The computation is over when the average temperature distribution over a year approaches steady state. This numerical approach provides one with a continuous computation of the temperature distribution and also the travel of the fusion front with a minimum of complications.

2.2.4 For the case when the phase change occurs over a temperature range instead of at a single temperature, equation (2.34) becomes

$$\partial\phi/\partial t = k'(\partial^2\theta/\partial z^2) \tag{2.40}$$

where

$$k' = (1 - unf/M_{so}) + (k_{uf}/k_f)\,unf/M_{so} \qquad \theta < 0$$
$$= k_{uf}/k_f \qquad \theta \geq 0 \tag{2.41}$$

and equation (2.28) becomes

$$\phi = S_f\theta + unf/M_{so} \qquad \theta < 0$$
$$= S_{uf}\theta + 1 \qquad \theta \geq 0 \tag{2.42}$$

where unf is the unfrozen fraction and M_{so} is the soil moisture content. Proceed as before, using new equations (2.40), (2.41) and (2.42).

2.2.5 Comments

In this thesis the steady periodic solution will only be of interest, the transient behavior produced by starting from a constant ground temperature will not be considered. Rigorously speaking, the steady periodic solution is obtained only when the temperatures at all times during the yearly cycle are the same in two consecutive years. However, since this work is primarily concerned with the temperatures averaged over a yearly cycle, a somewhat less rigorous test was used to determine if the steady periodic state had been reached. The criterion used was that the change of the averaged temperatures from one year to the next must be small. In practice the calculations were always carried out through five yearly cycles of temperature variation. If the change in the averaged temperatures was greater than 0.02°C between the fourth and the fifth years, the calculations were extended to the tenth or the fifteenth years as required.

Input data for this model includes the ground surface temperature variation during the year and the physical properties of the soil. The ground surface temperature is assumed to be equal to the air temperature, which is approximated by the harmonic function fitted to meteoralogical data, Appendix I. Temperature conditions of Edmonton, Norman Wells, and Inuvik were used as the basic cases. For soil properties data compiled by Lunardini (28) was used, Appendix II. The basic conditions used for calculating effects of soil property variations were taken as a fine grained soil, dry density 1.2×10^3 kg./m^3., with moisture contents of 15%, 30% and 45%.

2.3 Results of the numerical calculations

2.3.1 Temperature distributions in the ground

Figures (4) and (5) show the temperature distribution in the ground for two cases, Edmonton and Norman Wells, both with 30% moisture content in a fine grained soil. The temperature profiles were drawn for the various time intervals of the fourth year.

The temperature profiles for the two cases display the characteristic features of all ground temperature profiles, that is the amplitude of the temperature variation decreases with depth and the phase of the temperature variation lags behind the phase at the surface. The overall temperature profiles do not appear to resemble those for the idealized analytic model, where Stefan number was zero. It will be noted however, for both the cases, the temperature profiles that cross the 0°C line tend to be linear from that point to the surface temperature value. This is particularly striking in the case for Edmonton where the average air temperature of 2.56°C, is very close to the freezing point. Since it is the region where phase change occurs, it is thus the most important region in determining the thermal behavior of the ground. Thus, it is reasonable to expect that the analytical model will give satisfactory results for some calculations. Also, note that in the temperature profiles in Figures (4) and (5), the average temperature deep in the ground appears to be different from the average temperature at the surface. This is the result predicted by the analytical model.

Figure (6) shows the variation of the average soil temperature with depth. It will be observed that the variation occurs only in the

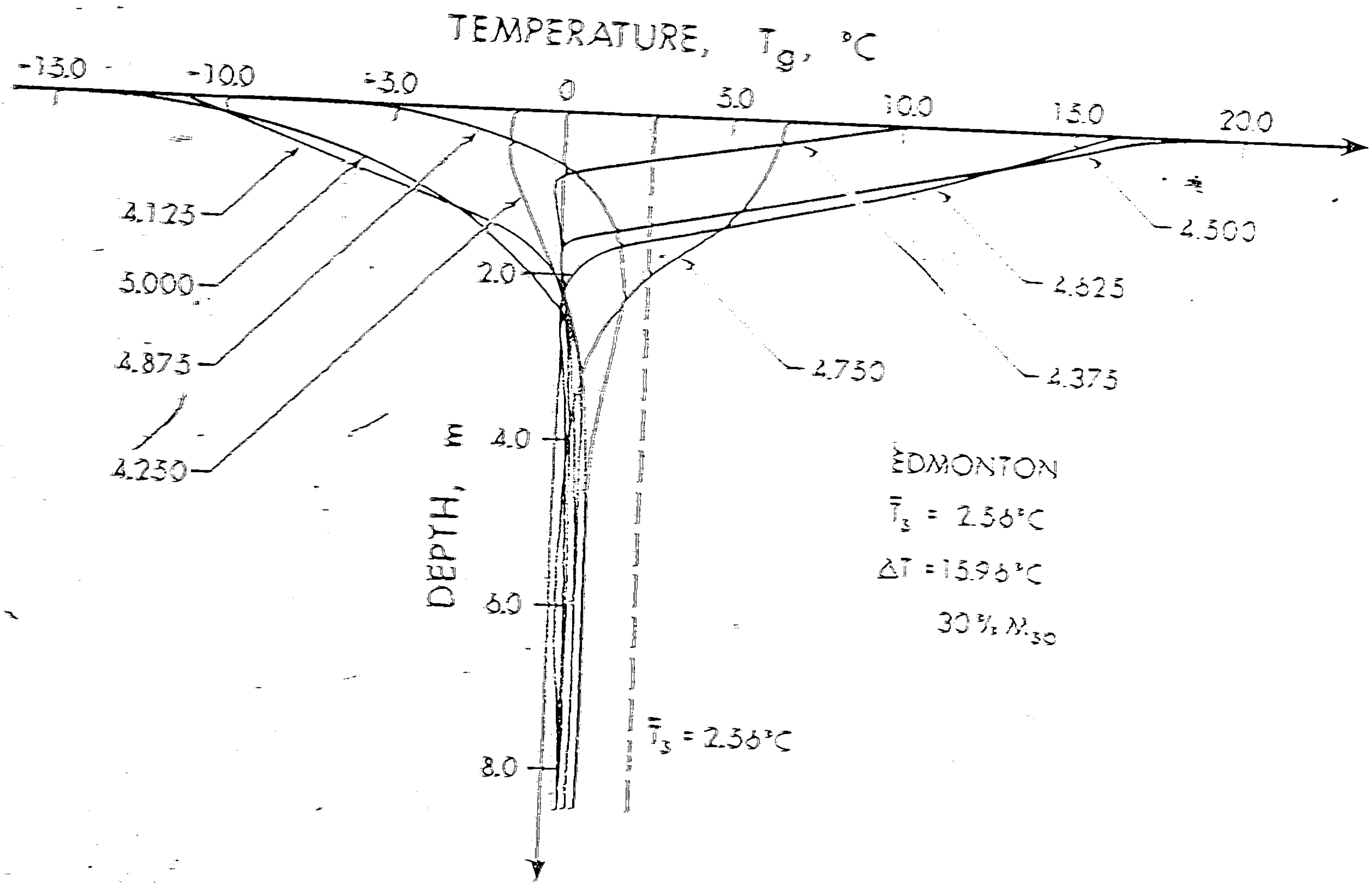

FIGURE 4 — Temperature distributions in the ground at Edmonton with imposed surface temperature

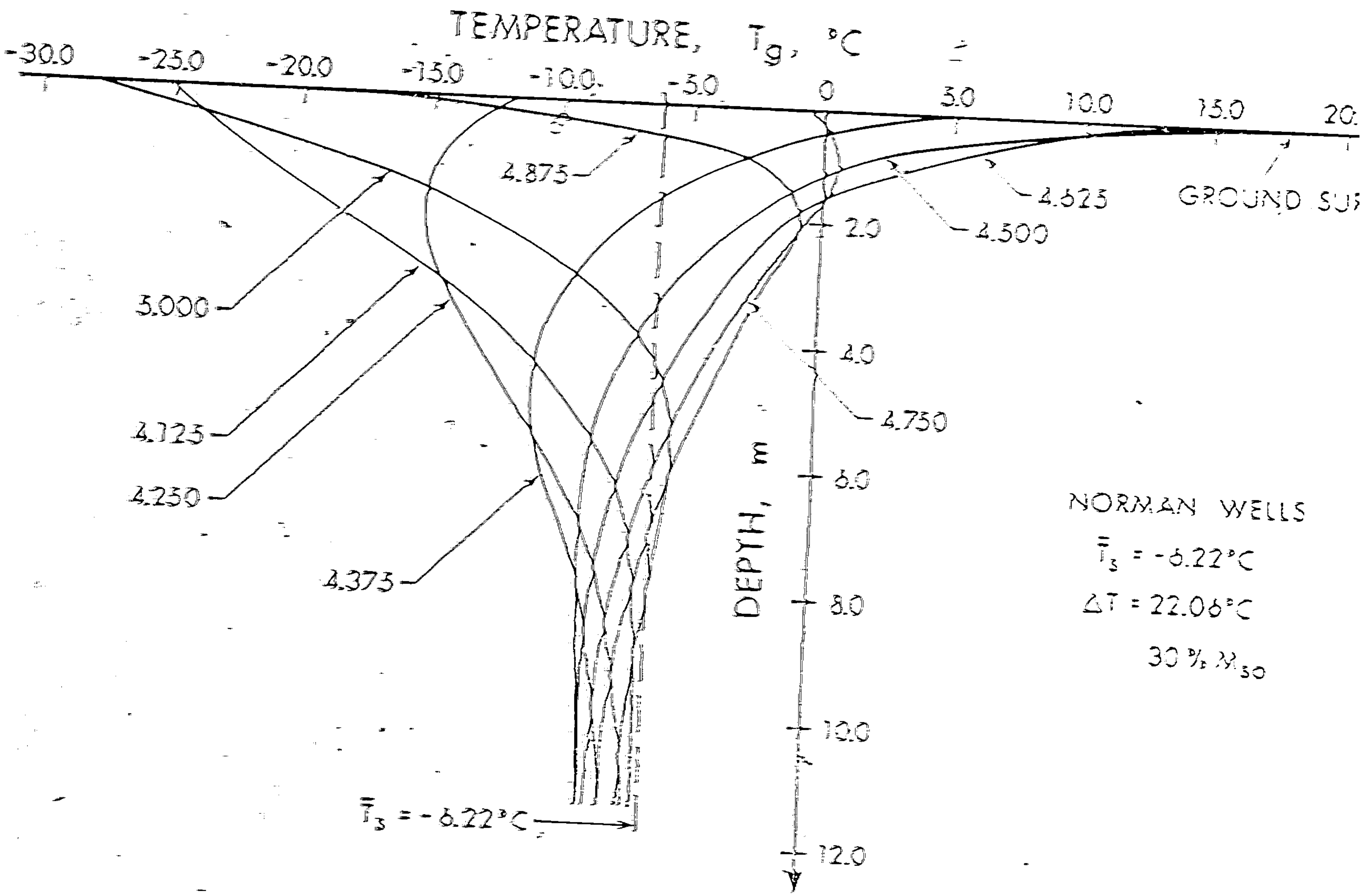

FIGURE 5 — Temperature distributions in the ground at Norman Wells with an imposed ground surface temperature

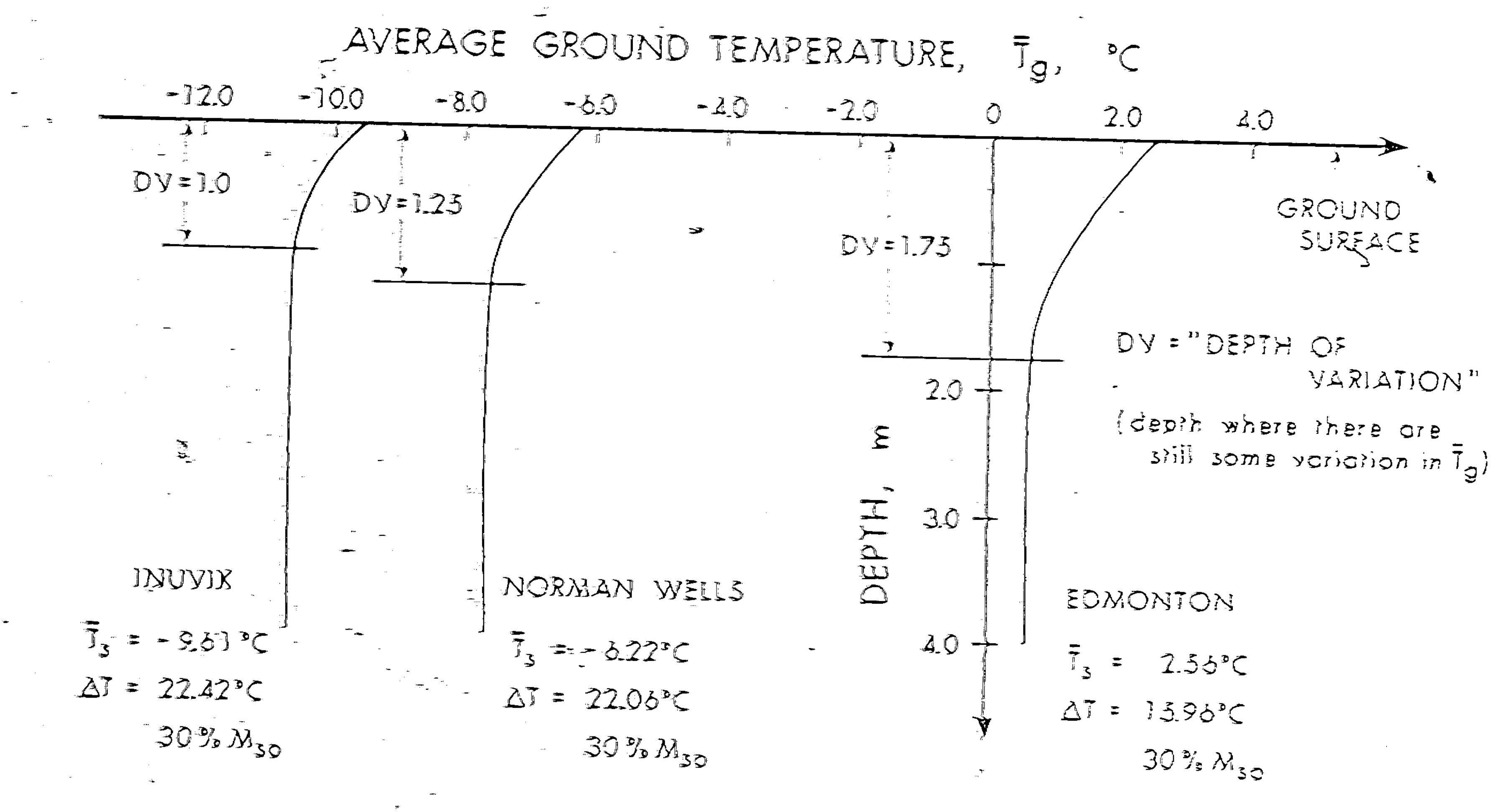

FIGURE 6 — Profiles of average temperature with imposed ground surface temperature

top few meters of the soil. This depth will be observed later to correspond to the depth of penetration of the phase change. This indicates that, the phase change or rather the conductivity change that results from phase change is responsible for the change in the average ground temperature with depth.

The absolute determination of the ground temperature in practice is almost impossible because of the large number of variabilities involved. However it is possible to predict the change in the ground temperature that would result from a change in one of its controlling parameters. This section will deal with the effects the main parameters namely, average surface temperature $\bar{T}_s$, volumetric heat capacities of the soil L_f, thermal heat conductivities ratio k_{uf}/k_f and the soil moisture content M_{mo}, have on the differences between the average surface temperature $\bar{T}_s$ and the average ground temperature $\hat{T}_g$.

The effects that changes in the average surface temperature have on the temperature difference $\hat{T}_g - \bar{T}_s$, is shown in Figure 7. Here the temperature differences have been normalized by ΔT, the amplitude of the temperature oscillation at the surface. These results are for a ratio of conductivities between the unfrozen and frozen soil, k_{uf}/k_f, of 0.647 which corresponds to a fine grained soil with 30% moisture content. It will be noted that for this ratio of conductivities, the temperature below the active layer is always colder than the average surface temperature and the maximum difference occurs when $\bar{T}_s$ is slightly greater than the freezing temperature. The theoretical curves indicated by the solid lines in Figure 7 meet at a value of $(\hat{T}_g-\bar{T}_s)/\Delta T = -0.14$.

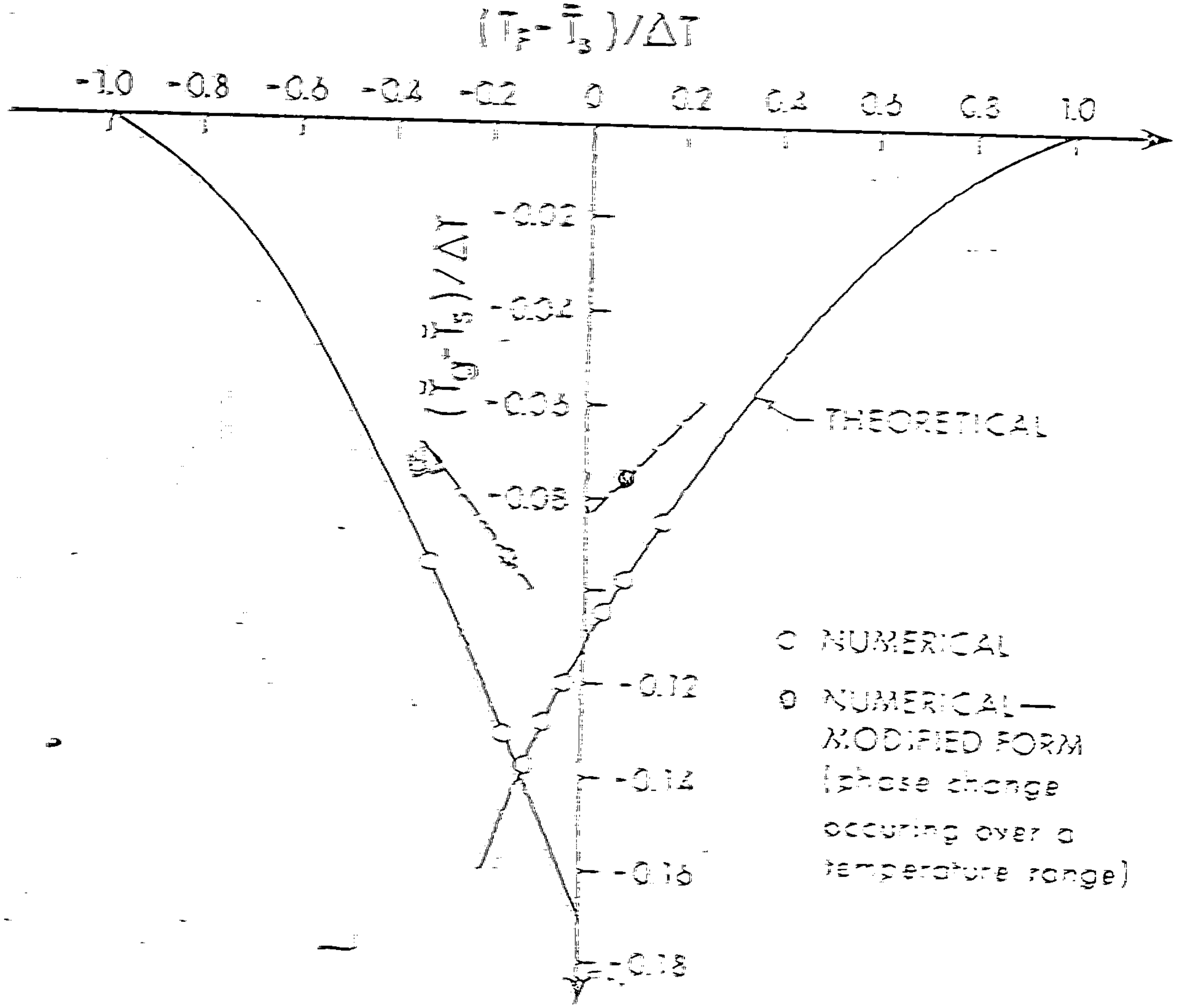

FIGURE 7 — Variation of $\bar{\bar{T}}_3$ with $\bar{\bar{T}}_F - \bar{\bar{T}}_3/\Delta T$

The curve on the left corresponds to a soil temperature deep in the ground that is above 0°C and the one on the right corresponds to a soil temperature below 0°C (that is permafrost grounds). The intersection of these curves and thus the minimum value of the parameter $(T_g - T_s)/\Delta T$, corresponds to the condition under which the greatest difference exists between the average surface and ground temperatures. The minimum value of $(T_g - T_s)/\Delta T$ for this case is -0.14, which for a typical temperature range $\Delta T = 20°C$ would correspond to a difference between average surface and ground temperatures of 2.8°C. The position of this minimum value and thus the minimum value of $(T_g - T_s)/\Delta T$ is a complex function of the conductivity ratio k_{uf}/k_f. It can be calculated by equating equations (2.22) and (2.24) of the analytic model.

The results of the numerical calculations for $L_f = 1.2 \times 10^8$, that is $M_{uu} = 30\%$, agree with the analytic results except near the minimum point in Figure 7. Here calculations must be run through 15 yearly cycles before a steady periodic state is reached.

An increase in the unfrozen moisture causes a decrease in $(T_g - T_s)/\Delta T$, as indicated in Figure 7. This is due to a decrease in the range of conductivity.

A change in the moisture content of the soil affects both the latent heat of fusion L_f and the ratio of the conductivities k_{uf}/k_f in the soil. These effects of the two parameters will first be looked at separately.

Figure (8) indicates that if the calculations are carried out through enough yearly cycles, approximately 15, the value of $(T_g - T_s)/\Delta T$ obtained is independent of the volumetric heat capacity of the soil L_f.

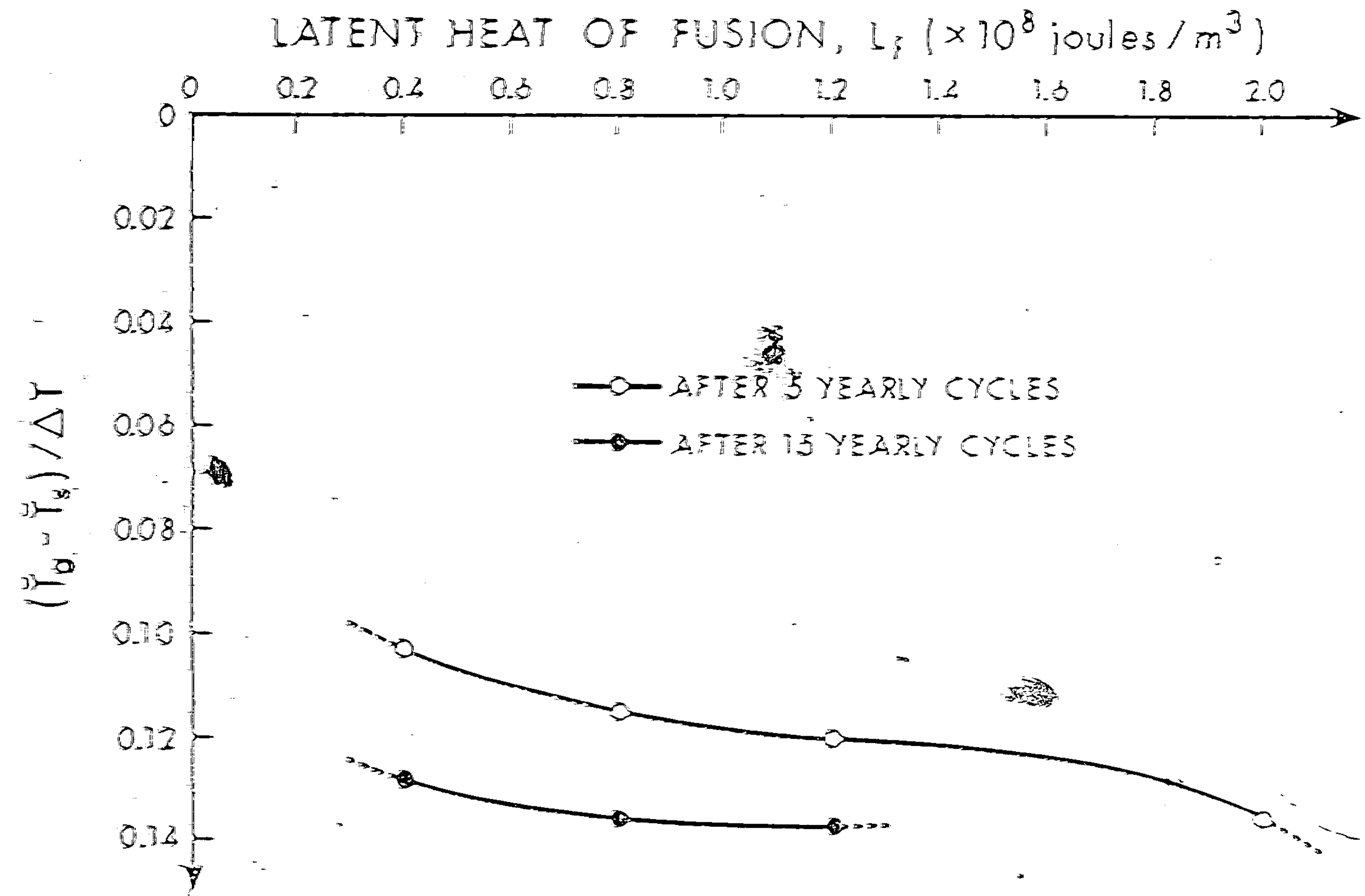

FIGURE 8 – Variation of L_f with $(\bar{T}_g - \bar{T}_s)/\Delta T$

The result is in agr[illegible] the analytic model.

The ratio of conductivities, k_{uf}/k_f, has a much more significant effect. The relationship between k_{uf}/k_f and $(T_g - T_s)/\Delta T$ is linear, that is as k_{uf}/k_f increases, $(T_g - T_s)/\Delta T$ increases, as indicated by Figure [illegible]. For every unit increase in k_{uf}/k_f, there result a corresponding 0.166 units increase in $(T_g - T_s)/\Delta T$. This is at a value of $(T_g - T_s)/\Delta T = 0.341$.

The graph of $(T_g - T_s)/\Delta T$ versus the moisture content M_{so} in Figure (10) will only confirm the results of the two previous findings. The graph shows that an increase in moisture content will result in an increase in the magnitude of $(T_g - T_s)/\Delta T$. This results because of the increased difference between k_{uf} and k_f that occurs at the higher moisture content. Also changes in moisture content have less effect on the ground temperature in the colder region such as Inuvik than the comparatively warmer region such as Edmonton. This is because as shown in Figure (7), the effects of conductivity differences between frozen and unfrozen soil are the greatest when the soil is near 0°C.

2.4 Depth of the active layer

2.4.1 Depth of frost or thaw penetration

Figure (11) shows the frost or thaw penetration depth during the fourth year for the three locations, Edmonton, Norman Wells and Inuvik, with 30% moisture content. The method of obtaining the frost

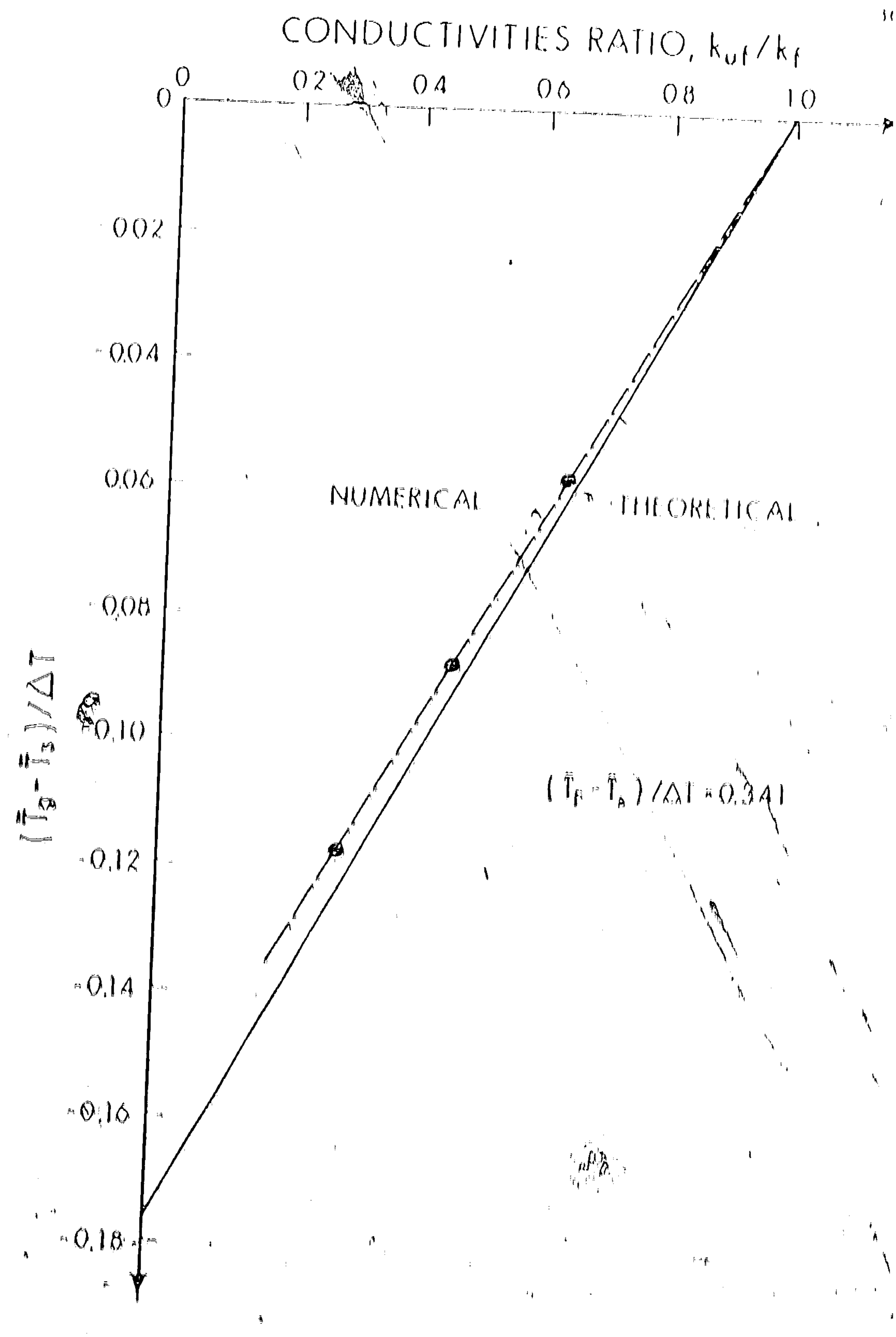

FIGURE 9 – Variation of k_{uf}/k_f with $(\bar{T}_B - \bar{T}_A)/\Delta T$

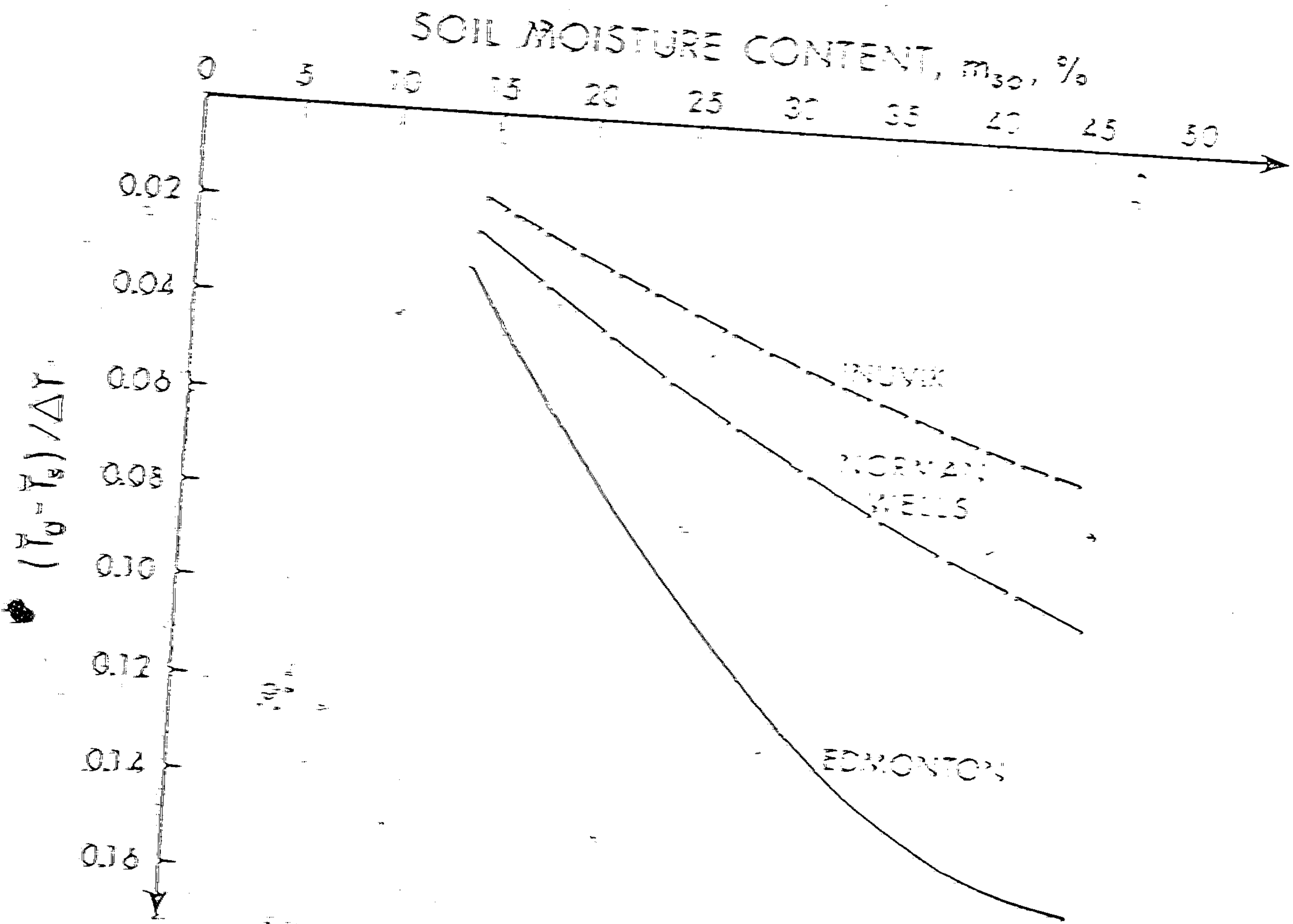

FIGURE 10 – Variation of M_{30} with $(\bar{T}_g - \bar{T}_s)/\Delta T$

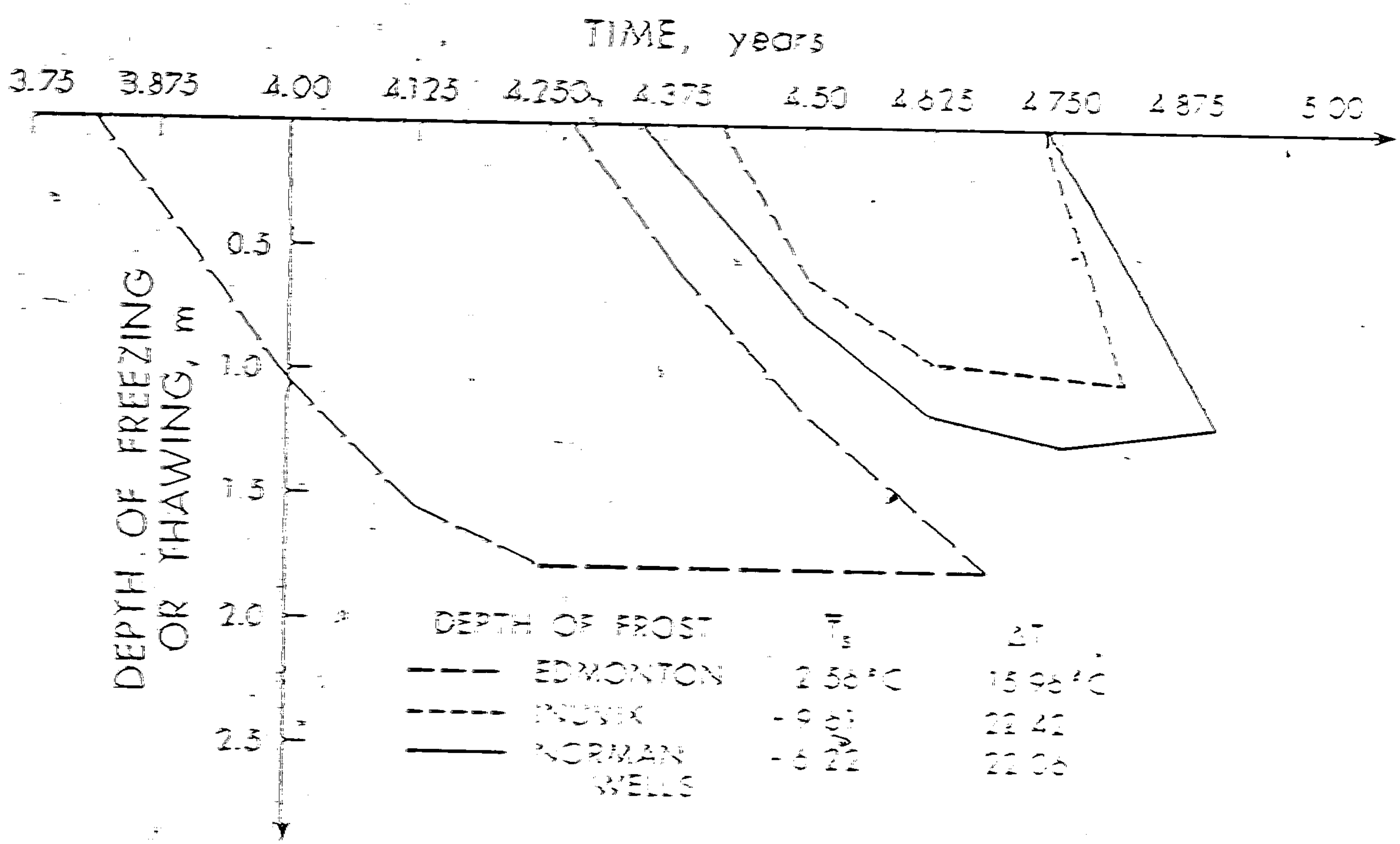

FIGURE 11 — Frost or thaw depth penetration with imposed ground surface temperature and 30% W_{sc}

of thaw penetration depth will be discussed briefly below.

2.4.1 Method of calculating the depth of thaw or frost penetration

Consider first the case where there is frost penetration, that is a frozen phase over an unfrozen phase.

If T_n 0, then T_{n+1} 0

and the depth to the fusion front is

$$y^* = n - 0.5 - \phi_n$$

The 0.5 occurs because the first nodal point represent only 1/2(Δx). The latent heat of the nth nodal point is ϕ_n and it represents the fraction of that element unfrozen. For thaw penetration, that is an unfrozen phase over a frozen phase,

If T_n 0, then T_{n+1} 0

and the depth to the fusion front is

$$y^* = n - 1.5 + \phi_n$$

The depth of thaw or frost penetration, y, is given by

$$y = y^* \times \Delta x$$

Example:

Considering now the Edmonton case, that is frozen/unfrozen.

Time = 4th year

Nodal Points	Region	Temperatures	Enthalpies
	Ground Surface		
1	↑	12.89658	0.17128
2		10.79542	0.14394
3		8.74095	0.11655
4	Frozen Region	6.77457	0.09033
5		4.93179	0.06562
6		3.19098	0.04255
7		1.56498	0.02087
8		0.0	0.94294
		$\phi = 1.000$	
9	Unfrozen Region ↓	0.18144	1.00363

$$y^* = 8 - 0.5 - 0.94294$$

$$= 6.56$$

$$y = y^* x_e \Delta t$$

$$\Delta t = 0.06$$

$$x_e^2 = \frac{k_f \, t_e \, \Delta T}{\rho L}$$

$$= \frac{1.7 \times 3.156 \times 10^7 \times 15.96}{1.2 \times 10^8} = 7.136$$

$$\therefore x_e = 2.6713$$

Hence the depth of frost penetration,

$$y = (6.56 \times 0.06 \times 2.6713) \text{ meters}$$

$$= 1.05 \text{ meters}$$

As indicated in Figure (8), for the stated conditions, that is imposed surface temperature, average temperature $T_a = 2.56°C$, amplitude of oscillation $\Delta T = 15.96°C$ and with 30% moisture content, the maximum frost penetration depth is 1.8 meters, about 5.9 feet. The generally accepted and known frost penetration depth in Edmonton is about 8 feet. For the cases of Norman Wells and Inuvik, both of which are naturally permafrost locations, the maximum depths of thaw are 1.225 m (about 4 feet) and 1.00 m (about 3 feet) respectively. It will be observed that these depths of the active layer correspond to the depths over which the variation in the average ground temperature occurred in Figure (6). This is the expected result, in that it is the conductivity variations that accompany the phase change that causes the average ground temperature to vary with depth.

2.4.2 Effects the various parameters have on the active layer

As it is possible to predict the change in the ground temperatures, it is also possible to predict the change in the depth of the active layer that would result from a change in one of its controlling parameters.

Figure (12) shows the effects the changes in the average surface temperature have on the depth of the active layer. A collation with Figure (7) shows that they exhibit the same behavior with the

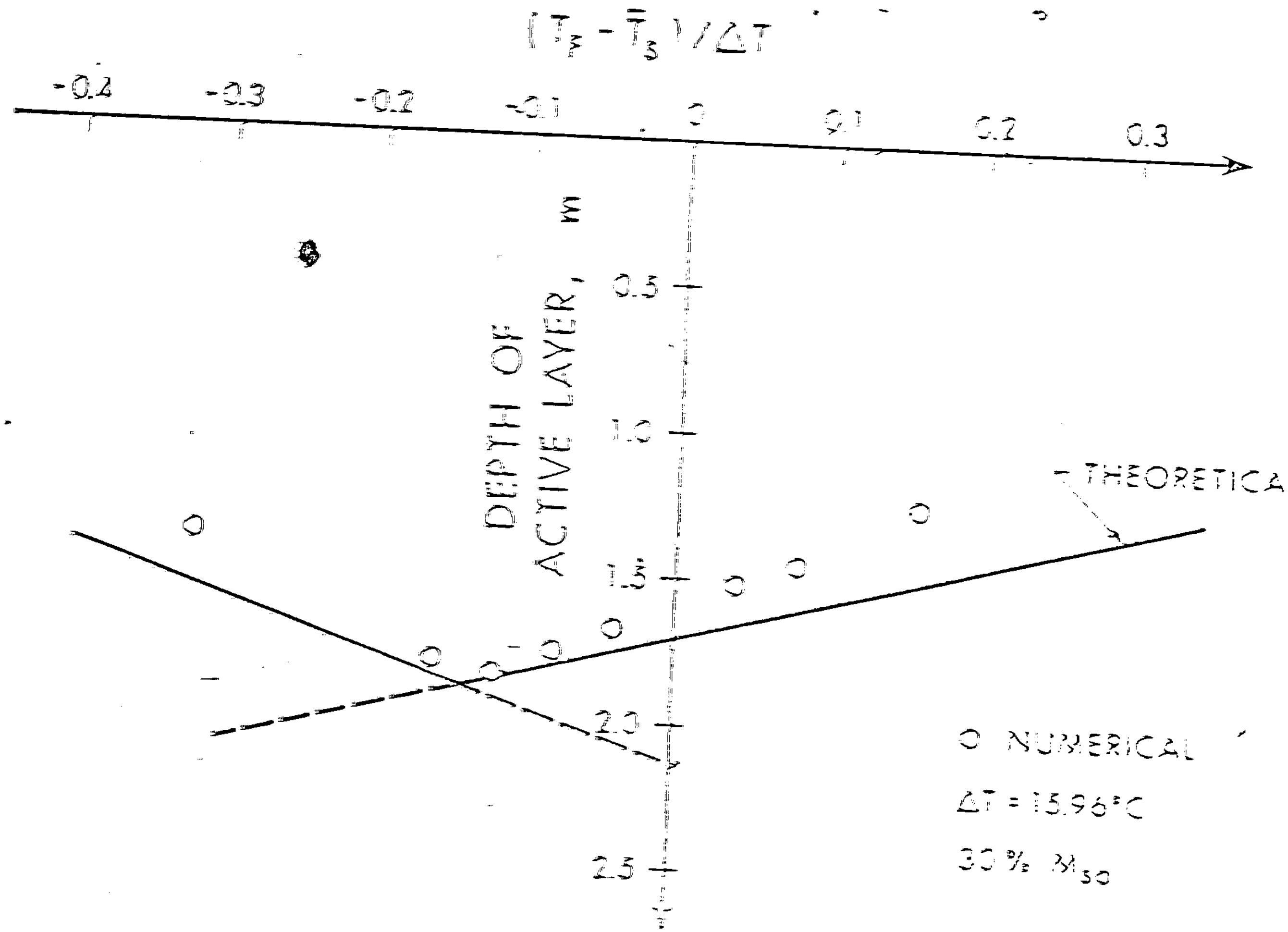

FIGURE 12 — Variation of $(T_F - T_S)/\Delta T$ with depth of active layer

maximum depth occurring when the value of $(T_F - T_a)/\Delta T = -0.14$. For a conductivity ratio k_{uf}/k_f of 0.647, which corresponds to a fine grained soil with 30% moisture content, the maximum depth of the active layer is 1.85 meters about 6.1 feet.

Again the effects of the latent heat of fusion and the conductivities of the frozen and the unfrozen soil will be examined separately and than in combination as they are related to the moisture content of the soil.

For both the naturally permafrost location and the non permafrost location, the depth of thaw and frost penetration respectively decreases as the latent heat of fusion L_f increases, as indicated in Figure (13). For the Edmonton conditions, case B, the decrease in active layer depth closely follows the theoretical predictions of the analytic model. The decrease in depth is therefore proportional to $(L_f)^{-1/2}$. For the naturally permafrost conditions, case A, the numerically predicted active layer depth follows the same trend as predicted by the analytic model, however the actual values from the numerical calculations are 20 to 25% less than those predicted analytically. The accuracy of the analytical prediction is in general best, as shown in Figure (12), when the average ground temperature is near the freezing point. This is because in this condition the Stefan number is near zero - the condition for which the analytical model was developed.

The analytic model would predict that the depth of the active layer for the permafrost soil is dependent only on the conductivity of the unfrozen soil and that for the non-permafrost soils the depth would depend only on the conductivity of the frozen soil. In particular the

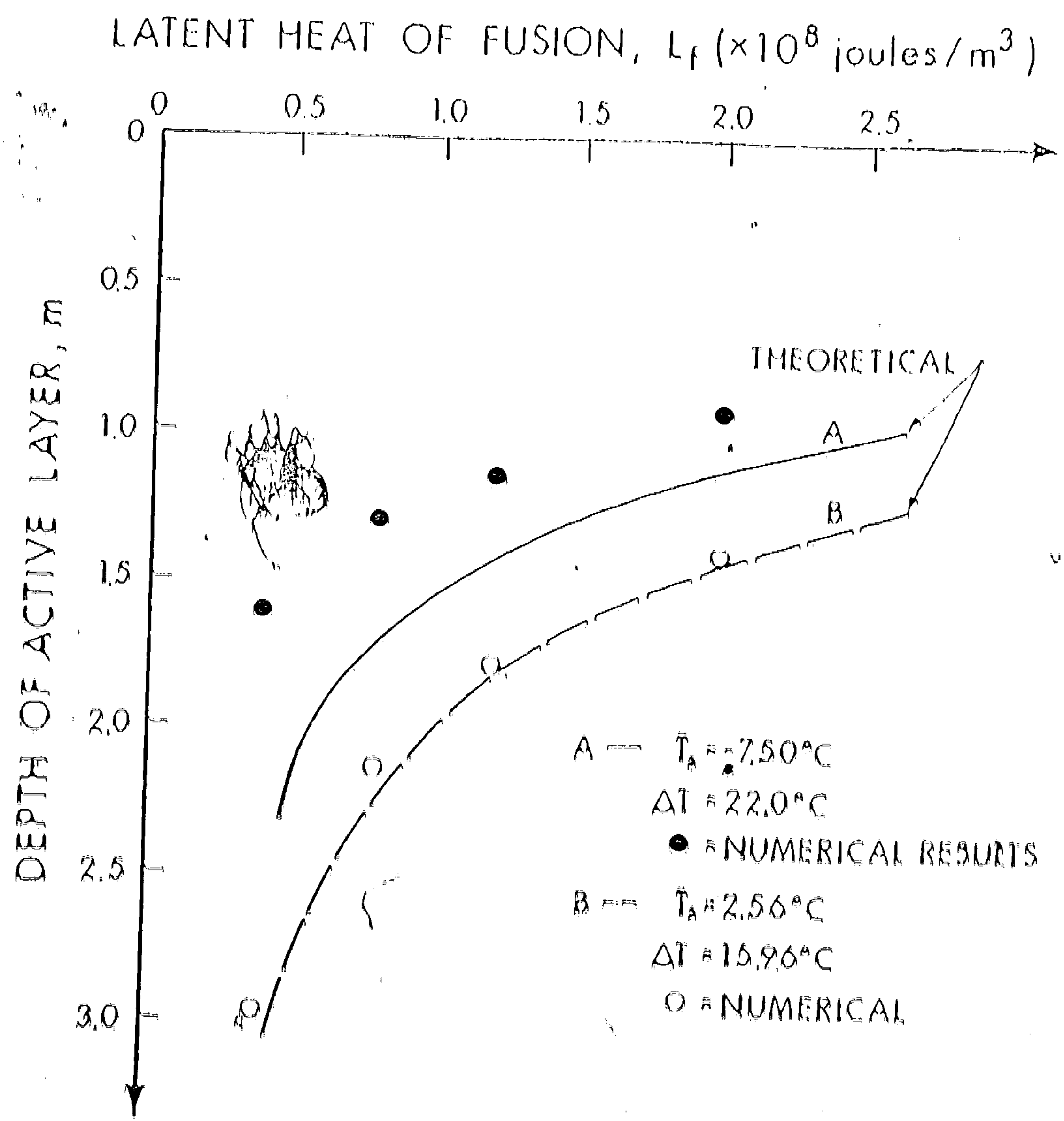

FIGURE 13 — The effects the latent heat of fusion L_f has on the depth of the active layer, for k_{uf}/k_f = 0.6471

depth in each case should be proportional to the square root of the appropriate conductivity. Figure (14) shows the results of the analytic and numerical models.

Figure (15) shows the relationship between the moisture content of the soil M_{so} and the depth of the active layer for the various locations. For the naturally permafrost locations such as Inuvik and Norman Wells, the depth of the active layer decreases as the moisture content increases. As for the Edmonton case (non-naturally permafrost) it is just the opposite, that is the depth of the active layer increases as the moisture content increases.

The results for Edmonton are interesting, in that just from a consideration of the latent heat which increases with moisture content one would expect the depth of the active layer to decrease. The increase in moisture content however also increases the conductivity of the frozen ground and this acts to produce the increase in the active layer depth observed. For the two permafrost locations however, the effect of the latent heat dominates the behavior of the active layer depth. That is as the latent heat increases the active layer depth decreases.

2.5 Conclusions

The analytic model developed, based on $S_f = 0$, gives results that are in close agreement with the numerically calculated results. The results obtained demonstrate that there exists a difference between the average ground surface temperature and the average temperature just below the active layer and that this difference is due to conductivity changes associated with phase changes. The difference between the two

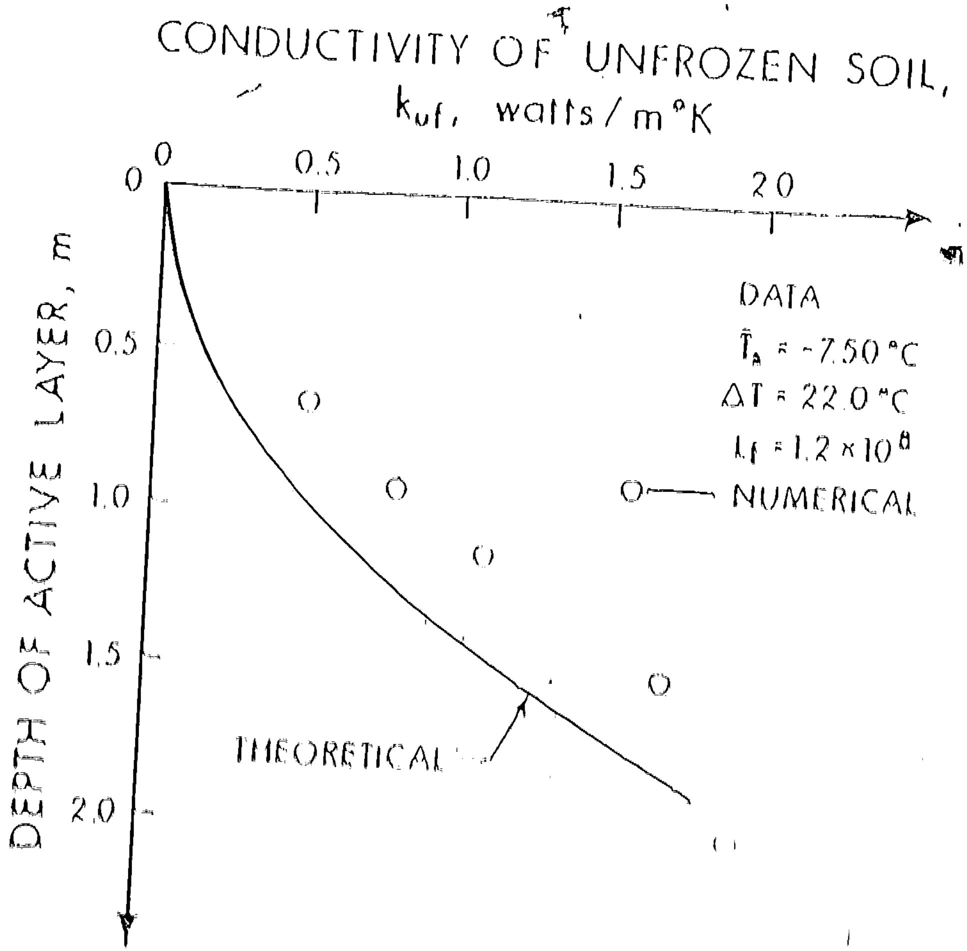

FIGURE 14 - Relationship between k_{uf} and depth of active layer in permafrost regions

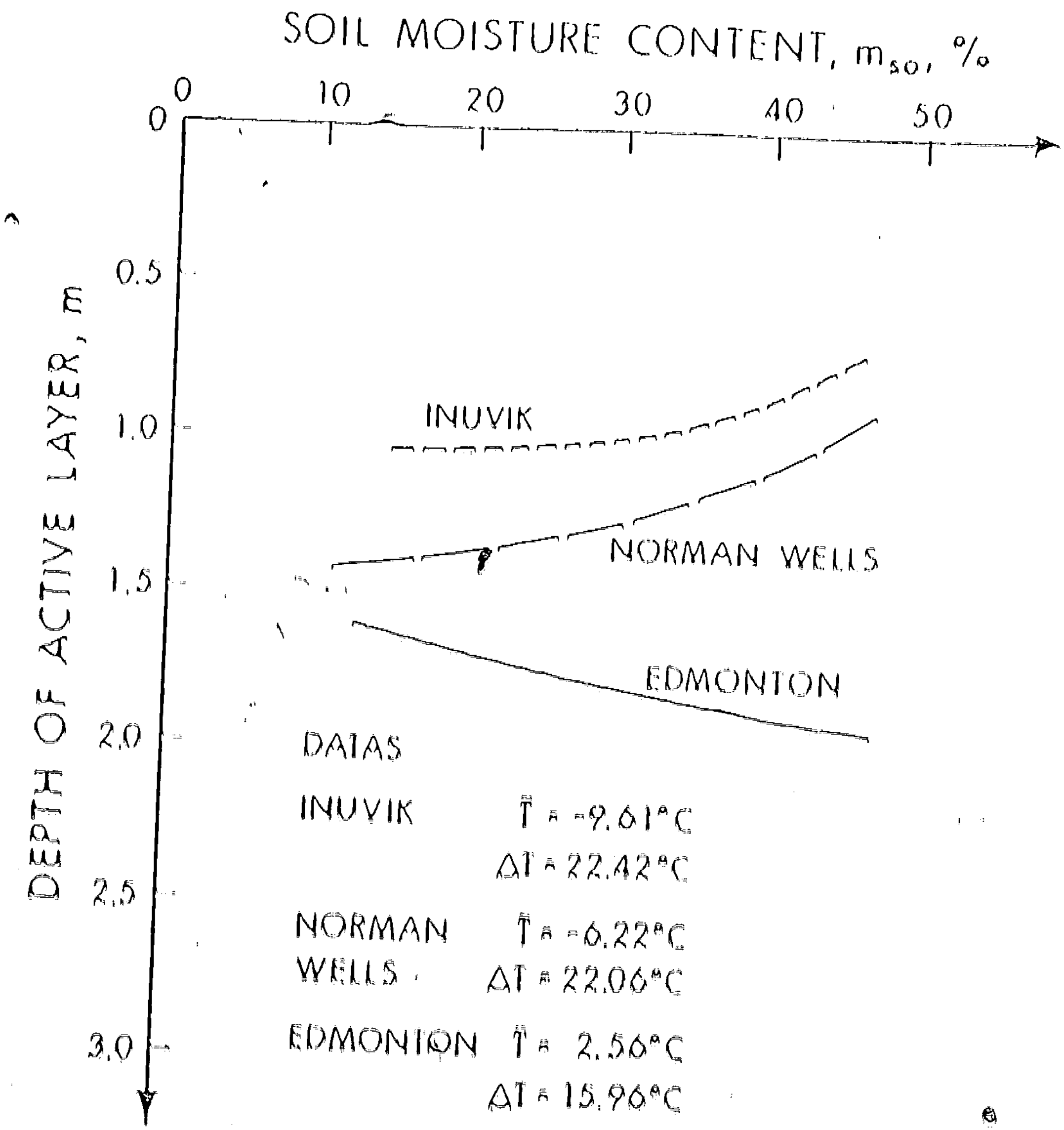

FIGURE 15 — Variation of M_{so} with depth of active layer

mentioned temperatures is largest for soil with large moisture content and in geographical locations where the average surface temperature is near freezing.

Interestingly enough, both the analytical and the numerical models show that the average ground temperature below the active layer is independent of the latent heat of fusion. The depth of the active layer is inversely proportional to the latent heat to the one half power as would be predicted from the classical Stefan problem.

PART III

WITH AN INSULATING LAYER OF VARYING U FACTOR

3.1 Introduction

Normally, instead of the imposed surface temperature situation discussed in the last section the actual ground surface has an insulating cover (vegetation cover in the summer and snow in the winter). This insulating cover will have a major effect on the ground temperature. This section of this thesis will examine the effects of this insulating cover on the ground temperature.

The analytical model presented will neglect the effects of the latent heat of fusion on the average ground temperature and will concentrate on the effects of the insulating layer. In the numerical model all the factors will be included and then a collation will be made between the two models.

3.2 Formulation of a ground temperature model with an insulating layer of varying U-factor

3.2.1 Analytical Model

Assume that the infinite ground mass can be replaced by a plate of some effective heat capacity ρc_s. This plate is then assumed to be at the temperature of the ground surface and that no heat flows into or out of it from the bottom. The effective heat capacity of the plate should be chosen so that the plate will have the same thermal response as the ground [illegible] Choosing an actual value for ρc_s will be discussed [illegible]oximation however neglects the storage of energy in latent heat which will affect the results as will be observed.

The model consists of a layer of insulation overlaying a plate of finite heat capacity, Figure (16).

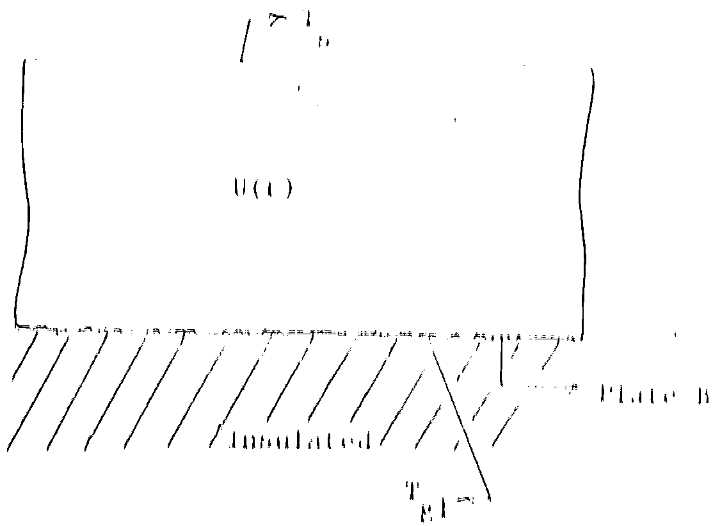

FIGURE 16

T_s = surface temperature

$= \bar{T}_s + \Delta T \sin\omega t$

U(t) = U factor of the insulating cover

$= k/d$

U(t) will be assumed to be of the form $\bar{U} + \Delta U \sin(\omega t + \phi_u)$.

The phase angle ϕ_u is the difference in phase between the variation of the U-factor and the surface temperature. A value of $\phi_u = 0$ means that U(t) is in phase with the surface temperature, that is the snow cover in winter is a better insulator than the vegetation cover in the summer. The normal case one would expect would be ϕ_u near zero. When $\phi_u = \pi$

U(t) is 180° out of phase with the surface temperature, implying that the summer vegetation cover is a better insulator than the snow in winter. This case would not be as likely, however it could possibly occur if the ground were covered with a thick layer of moss which became very dry during the summer months.

3.2.2. Solutions

For this model the governing equation for the ground surface temperature T_{g1} is

$$\rho c_e (dT_{g1}/dt) = U(t)[T_a(t) - T_{g1}] \quad (3.1)$$

where $$T_a(t) = \bar{T}_a + \Delta T \sin\omega t \quad (3.2)$$

$$U(t) = \bar{U} + \Delta U \sin(\omega t + \phi_u) \quad (3.3)$$

and T_{g1} is a function of time, t.

Let

$$\theta = T_{g1} - T_a(t)$$

$$\therefore d\theta/dt = dT_{g1}/dt - dT_a/dt$$

hence $$dT_{g1}/dt = d\theta/dt + dT_a/dt$$

but $$dT_a/dt = \omega\Delta T \cos\omega t$$

which means that

$$dT_{g1}/dt = d\theta/dt + \omega\Delta T_a \cos\omega t \quad (3.4)$$

Substituting equation (3.4) into equation (3.1), it gives,

$$rc_o(d\theta/dt) + \text{[illegible]} = U(t)\,\text{[illegible]}$$

or

$$d\theta/dt + U(t)\theta/rc_o = \text{[illegible]} \cos t \qquad (3.5)$$

From equation (3.3)

$$U(t) = U + \Delta U \sin(\omega t + \phi_o)$$

$$= U + \Delta U \sin\omega t \cos\phi_o + \Delta U \cos\omega t \sin\phi_o \qquad (3.6)$$

let

$$U/rc_o = A$$

$$\Delta U\cos\phi_o/rc_o = B \qquad (3.7)$$

$$\Delta U\sin\phi_o/rc_o = C$$

Equation (3.5) will now become

$$d\theta/dt + (A + B\sin\omega t + C\cos\omega t)\theta = m\Delta T\cos\omega t \qquad (3.8)$$

Assume

$$\theta = a_0 + \sum_{n=1}^{m} [a_n \sin(n\omega t) + b_n \cos(n\omega t)] \qquad (3.9)$$

$$\therefore d\theta/dt = \sum_{n=1}^{m} [a_n n\omega \cos(n\omega t) - b_n n\omega \sin(n\omega t)] \qquad (3.10)$$

Substituting equations (3.9) and (3.10) into equation (3.3), the expression becomes

$$\sum_{n=1}^{\infty} [a_n n\omega \cos(n\omega t) - b_n n\omega \sin(n\omega t)] + [a_0 + \sum_{n=1}^{\infty} (a_n \sin(n\omega t)$$

$$+ b_n \cos(n\omega t))] \times (A + B\sin\omega t + C\cos\omega t) = \omega\Delta T \cos\omega t \qquad (3.11)$$

Multiplying out the second term on the right hand side and then regrouping the common terms, equation (3.11) becomes

$$Aa_0 + Ba_0 \sin\omega t + Ca_0 \cos\omega t + \sum_{n=1}^{\infty} [(Aa_n - n\omega b_n) \sin(n)\omega t$$

$$+ (Ab_n + n\omega a_n) \cos(n)\omega t + 1/2(a_n C - b_n B) \sin(n-1)\omega t$$

$$+ 1/2(a_n B + b_n C) \cos(n-1)\omega t + 1/2(b_n B + a_n C) \sin(n+1)\omega t$$

$$+ 1/2(b_n C - a_n B) \cos(n+1)\omega t] = \omega\Delta T \cos\omega t \qquad (3.12)$$

or simplifying further by letting

$n = 1, 2 \ldots . N \ldots .$

Constant term

$$Aa_0 + 1/2\ (Ba_1 + Cb_1) = 0$$

sinωt term

$$Ba_0 + (Aa_1 - \omega b_1) + 1/2(Ca_2 - Bb_2) = 0$$

cos ωt term

$$Ca_0 + (Ab_1 + \omega a_1) + 1/2(Ba_2 + Cb_2) = \omega\Delta T$$

sin 2ωt term

$$1/2(Bb_1 + Ca_1) + (Aa_2 - 2\omega b_2) + 1/2(Ca_3 - Bb_3) = 0$$

cos 2ωt term

$$1/2(Cb_1 - Ba_1) + (Ab_2 + 2\omega a_2) + 1/2(Ba_3 + Cb_3) = 0$$

sin(N)ωt term

$$1/2(Bb_{N-1} + Ca_{N-1}) + (Aa_N - N\omega b_N) + 1/2(Ca_{N+1} - Bb_{N+1}) = 0$$

cos(N)ωt term

$$1/2(Cb_{N-1} - Ba_{N-1}) + (Ab_N + N\omega a_N) + 1/2(Ba_{N+1} + Cb_{N+1}) = 0 \qquad (3.13)$$

Writing these in the matrix form:

$$\begin{bmatrix} A & B/2 & C/2 & \cdots & & & & 0 \\ B & A & -\omega & C/2 & -B/2 & & & 0 \\ C & \omega & A & B/2 & C/2 & & & 0 \\ 0 & C/2 & B/2 & A & -2\omega & C/2 & -B/2 & 0 \\ 0 & B/2 & C/2 & 2\omega & A & B/2 & C/2 & 0 \\ & & & & & & & \\ 0 & & & & & & & \end{bmatrix} \begin{bmatrix} a_0 \\ a_1 \\ b_1 \\ a_2 \\ b_2 \\ a_3 \\ b_3 \\ \vdots \\ a_N \\ b_N \end{bmatrix} = \begin{bmatrix} 0 \\ 0 \\ \omega\Delta T \\ 0 \\ \vdots \\ 0 \end{bmatrix} \qquad (3.14)$$

The matrix in equation (3.14) is of infinite dimensions and thus exact values of the coefficients cannot be obtained in this way. However, under certain conditions the matrix may be approximated by truncating it at a certain value of N. In particular it was found by expansion of the first few terms, that if $U/r\omega_e$ and T/P are small parameters, the coefficients of 'a' and 'b' become small for large values of N. The approximation obtained by setting a_n and $b_n = 0$ for $n \geq 2$ will be obtained here. The matrix will be reduced to

$$\begin{vmatrix} A & B/2 & C/2 \\ B & A & -\omega \\ C & \omega & A \end{vmatrix} \begin{vmatrix} a_0 \\ a_1 \\ b_1 \end{vmatrix} = \begin{vmatrix} 0 \\ 0 \\ \omega AT \end{vmatrix} \qquad (3.15)$$

Solving for a_0, a_1 and b_1

$$a_0 = \frac{\begin{vmatrix} 0 & B/2 & C/2 \\ 0 & A & -\omega \\ -\omega AT & \omega & A \end{vmatrix}}{\begin{vmatrix} A & B/2 & C/2 \\ B & A & -\omega \\ C & \omega & A \end{vmatrix}}$$

$$\therefore a_0 = \frac{-\omega AT(-\omega B/2 - CA/2)}{A(A^2+\omega^2) - B/2(AB+C\omega) + C/2(B\omega - CA)}$$

$$= AT\,B/2A\,\{1 + CA/B\omega - 1/\omega^2(A^2 + B^2/2 + C^2/2)\}$$

hence

$$a_0 = 2U/(\ \ AT\cos\phi_u/2)\ [1 + \frac{U}{\rho c_e \omega}\frac{\sin\phi_u}{\cos\phi_u} - \frac{U^2}{(\rho c_e \omega)^2} + \frac{2U^2}{2(\rho c_e \omega)^2}] \tag{3.16}$$

Similarly

$$a_1 = \frac{\begin{vmatrix} A & 0 & C/2 \\ B & 0 & -\omega \\ C & -\omega AT & A \end{vmatrix}}{\begin{vmatrix} A & B/2 & C/2 \\ B & A & -\omega \\ C & \omega & A \end{vmatrix}} \tag{3.17}$$

$$\therefore a_1 = \frac{A(\ \ \omega^2 AT) + \frac{C}{2}(\ \ B\omega AT)}{A(A^2+\omega^2) - \frac{B}{2}(AB+C\omega) + \frac{C}{2}(B\omega\ \ CA)}$$

$$= \ \ AT\ (1 + \frac{CB}{2A\omega} - \frac{1}{\omega^2}(A^2 - \frac{B^2}{2} - \frac{C^2}{2}))$$

hence

$$a_1 = \ \ AT + AT\ \frac{U}{\rho c_e \omega}\ (\frac{U}{\rho c_e \omega} + \frac{U}{2\rho c_e \omega}\ (\frac{AU}{U})^2$$

$$- \frac{1}{4}(\frac{AU}{U})^2 \sin 2\phi_u) \tag{3.18}$$

and finally

$$b_1 = \frac{\begin{vmatrix} A & B/2 & 0 \\ B & A & 0 \\ C & \omega & -\omega AT \end{vmatrix}}{\begin{vmatrix} A & B/2 & C/2 \\ B & A & -\omega \\ C & \omega & A \end{vmatrix}} \tag{3.19}$$

$$\therefore b_1 = \frac{A(A\omega\Delta T_s) - \frac{B}{2}(B\omega\Delta T_s)}{\omega^2 A\left(1 + \frac{1}{\omega^2}\left(A^2 - \frac{B^2}{2} - \frac{C^2}{2}\right)\right)}$$

$$= \frac{\Delta T\,B^2}{2\omega A}\left(\left(1 - \frac{2A^2}{B^2}\right) \times \left(1 - \frac{1}{\omega^2}\left(A^2 - \frac{B^2}{2} - \frac{C^2}{2}\right)\right)\right)$$

Neglecting all the higher terms, i.e. terms with $(U/\rho c_g\omega)^3$ or higher

$$\therefore b_1 = \frac{\Delta T\,B^2}{2\omega A}\left(1 - \frac{2A^2}{B^2}\right)$$

or

$$b_1 = \Delta T\left(\frac{U}{\rho c_g\omega}\right)^2\left((-1) + \frac{1}{4}\left(\frac{\Delta U}{U}\right)^2 + \frac{1}{4}\left(\frac{\Delta U}{U}\right)^2\cos 2\phi_u\right) \qquad (3.20)$$

From equation (3.9)

$$\theta = a_0 + \sum_{n=1}^{\infty}\left(a_n\sin(n\omega t) + b_n\cos(n\omega t)\right)$$

$$= a_0 + a_1\sin\omega t + b_1\cos\omega t + \ldots\ldots\ldots\ldots\ldots\ldots\ldots \qquad (3.21)$$

Substituting equations (3.16), (3.18) and (3.20) into equation (3.21), the following expression follows:

$$\theta = \frac{\Delta U}{U}\,\Delta T\,\frac{\cos\phi_u}{2}\left(1 + \frac{U}{\rho c_g\omega}\,\frac{\sin\phi_u}{\cos\phi_u} - \frac{U^2}{(\rho c_g\omega)^2} + \frac{\Delta U^2}{2(\rho c_g\omega)^2}\right)$$

$$+ \left((-\Delta T) + \Delta T\,\frac{U}{\rho c_g\omega}\left(\frac{U}{\rho c_g\omega} + \frac{U}{2\rho c_g\omega}\left(\frac{\Delta U}{U}\right)^2\right.\right.$$

$$\left.\left. - \frac{1}{4}\left(\frac{\Delta U}{U}\right)^2\sin 2\phi_u\right)\right)\sin\omega t$$

$$+ ((\Delta T_o) \frac{U}{\rho c_g \omega} (1 + \frac{1}{4} (\frac{\Delta U}{U})^2 + \frac{1}{4} (\frac{\Delta U}{U})^2 \cos 2\phi_u) \times \text{const} \tag{3.22}$$

To obtain the difference between the average temperature $(\bar{T}_{gi} - \bar{T}_a)$, equation (3.22) may be integrated over a time cycle. The sin t term and the const term will drop out, leaving the following expression:

$$\int_0^{2\pi/\omega} \theta \, dt = \int_0^{2\pi/\omega} \frac{\Delta U}{U} \Delta T \frac{\cos\phi_u}{2} (1 + \frac{U}{\rho c_g \omega} \frac{\sin\phi_u}{\cos\phi_u}$$

$$- \frac{U^2}{(\rho c_g \omega)^2} + \frac{\Delta U^2}{2(\rho c_g \omega)^2}) \, dt$$

but

$$\int_0^{2\pi/\omega} \theta \, dt = \bar{\theta}(2\pi/\omega)$$

hence

$$\bar{\theta} = \frac{\Delta U}{U} \Delta T \frac{\cos\phi_u}{2} (1 + \frac{U}{\rho c_g \omega} \frac{\sin\phi_u}{\cos\phi_u} - \frac{U^2}{(\rho c_g \omega)^2} + \frac{\Delta U^2}{2(\rho c_g \omega)^2}) \tag{3.23}$$

In the limit $U/\rho c_g \omega \to 0$, noting that ΔU must by definition be less than U, equation (3.23) gives

$$(\bar{T}_{gi} - \bar{T}_a)/\Delta T = (\Delta U/U)(\cos\phi_u/2) \tag{3.24}$$

Also note that from equation (3.22), that this limiting situation implies that the ground temperature variations with time are negligible. In this case the temperature difference $(\bar{T}_{gi} - \bar{T}_a)$ varies linearly with $\Delta U/U$ and as the cosine of the phase angle, ϕ_u. This implies that for $\phi_u = 0$, that is for a snow cover of good insulating value, the average ground surface temperature T_{g1} is greater than the average surface temperature T_s. For $\phi_u = 180°$, that is the summer vegetation cover is a better insulator, the average ground surface temperature T_{g1} is less than the average surface temperature T_s. There is no difference between T_{g1} and T_s if however $\phi_u = 90°$. If $U/\rho c_e \omega$ is not zero, that is if the fluctuations of the ground temperature are accounted for, equation (3.24) shows that a difference between T_{g1} and T_s exists at $\phi_u = 90°$. The amount of the difference is

$$(T_{g1} - T_s) = (\Delta U \times \Delta T)/2\rho c_e \omega \quad . \tag{3.25}$$

For larger values of $U/\rho c_e \omega$ and $\Delta U/U$, higher order terms become more significant and equation (3.24) is not a good approximation.

3.3 Numerical Model

The method adopted here will be similar to that developed for the imposed surface temperature except for a slight modification at the soil surface level.

3.3.1 The difference between this and the previous model

(a) At the ground surface with imposed surface temperature

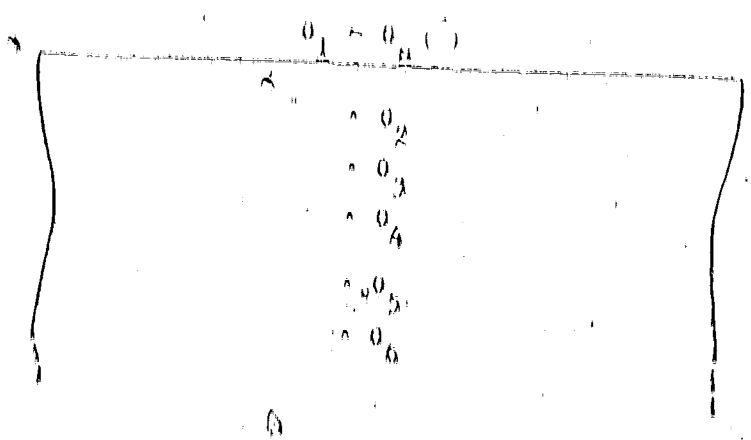

FIGURE 17(a)

Temperature

$$\theta_1 = \theta_a$$

Enthalpy

$$\phi_1 = L + S_{ul}\theta \qquad \text{if } \theta > 0$$

$$= S_l\theta \qquad \text{if } \theta < 0$$

(b) With an insulating layer

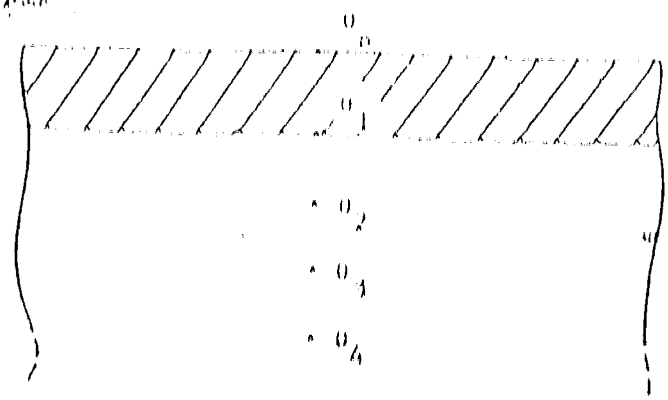

FIGURE 17(b)

At the soil surface

$$dh_1/\rho L = (U(T_a - T_1) - (T_1 - T_2)k/\Delta x)\ \Delta t/\Delta x \times 2 \times 1/\rho L \qquad (3.26)$$

or

$$\Delta\phi_1 = (U\Delta T/\rho L\ (\theta_a - \theta_1)\Delta x - k\Delta T/\rho L\ (\theta_1 - \theta_2))\ 2\Delta t/\Delta x^2$$

$$= (U\Delta T t_c/\rho L x_c\ (\theta_a - \theta_1)\Delta\zeta - k'(\theta_1 - \theta_2))\ 2\Delta\tau/\Delta\zeta^2$$

$$= (FUS(\theta_a - \theta_1)\Delta\zeta - k'(\theta_1 - \theta_2))\ 2\Delta\tau/\Delta\zeta^2 \qquad (3.27)$$

where $FUS = U\Delta T t_c/\rho L x_c$

but since

$$x_c^2 = k_1 t_c \Delta T/\rho L$$

$$\therefore FUS = \rho x_c/k_1 \qquad (3.28)$$

Initially the ground temperature were all assumed to be equalled to T_a or $\theta_1 = \theta_2 = \ldots \theta_n = \theta_a$.

Enthalpy

$$\Delta\phi_1 = \{FUS(\theta_a - \theta_1)2\Delta\zeta \times RTF - (\theta_1 - \theta_2)2 \times RT\} \qquad (3.29)$$

where $\quad RTF = \Delta t/\Delta\zeta^2 \qquad (3.30)$

and

$$RT = \Delta t/\Delta\zeta^2 \quad \text{if } \theta_1 + \theta_2 < 0$$

$$= (k_{u1}/k_1)\,\Delta t/\Delta\zeta^2 \quad \text{if } \theta_1 + \theta_2 > 0 \qquad (3.31)$$

$$\phi_1^{m+1} = \phi_1^m + \Delta\phi_1^m$$

Temperature

$$\theta_1^{m+1} = \phi_1^{m+1}/S_1 \quad \text{if } \phi_1^{m+1} < 0$$

$$= (\phi_1^{m+1}-1)/S_{u1} \quad \text{if } \phi_1^{m+1} > 0 \qquad (3.32)$$

The main difference between the two problems is, instead of setting the ground surface temperature equal to the air temperature, the ground surface temperature will now be varying. This is caused by the introduction of a varying insulating layer which separates the atmosphere from the ground surface. The temperature on the surface of the insulating layer is now assumed to be equalled to the air temperature.

So, except for these modifications at the ground surface level, all the procedures and parameters remain unchanged. The varying insulating layer is approximated by a harmonic function which may or may not be in phase with the air temperatures. Again temperature conditions of Edmonton, Inuvik and Norman Wells were used as the basic cases.

3.4 Results of the Numerical Calculations

3.4.1 Effects the insulating layer haveon the various temperatures.

The temperature profile, as illustrated in Figure 18, display similar characteristics as those for the imposed surface temperature, except that the insulating layer decreases the amplitude of the temperature variation at the ground surface. The amplitude of surface and ground surface temperature variations for the three cases, together with the soil and insulating properties are listed in Table 1. The properties of the insulating layer chosen for the three cases are rather arbitrary as there is very little data available on the insulating values of the various surface covers. Some rational range of values used is given in Appendix III. In all cases the phase angle ϕ_M is 0.0, that is the situation in which the winter snow cover is better insulator than the summer vegetation cover.

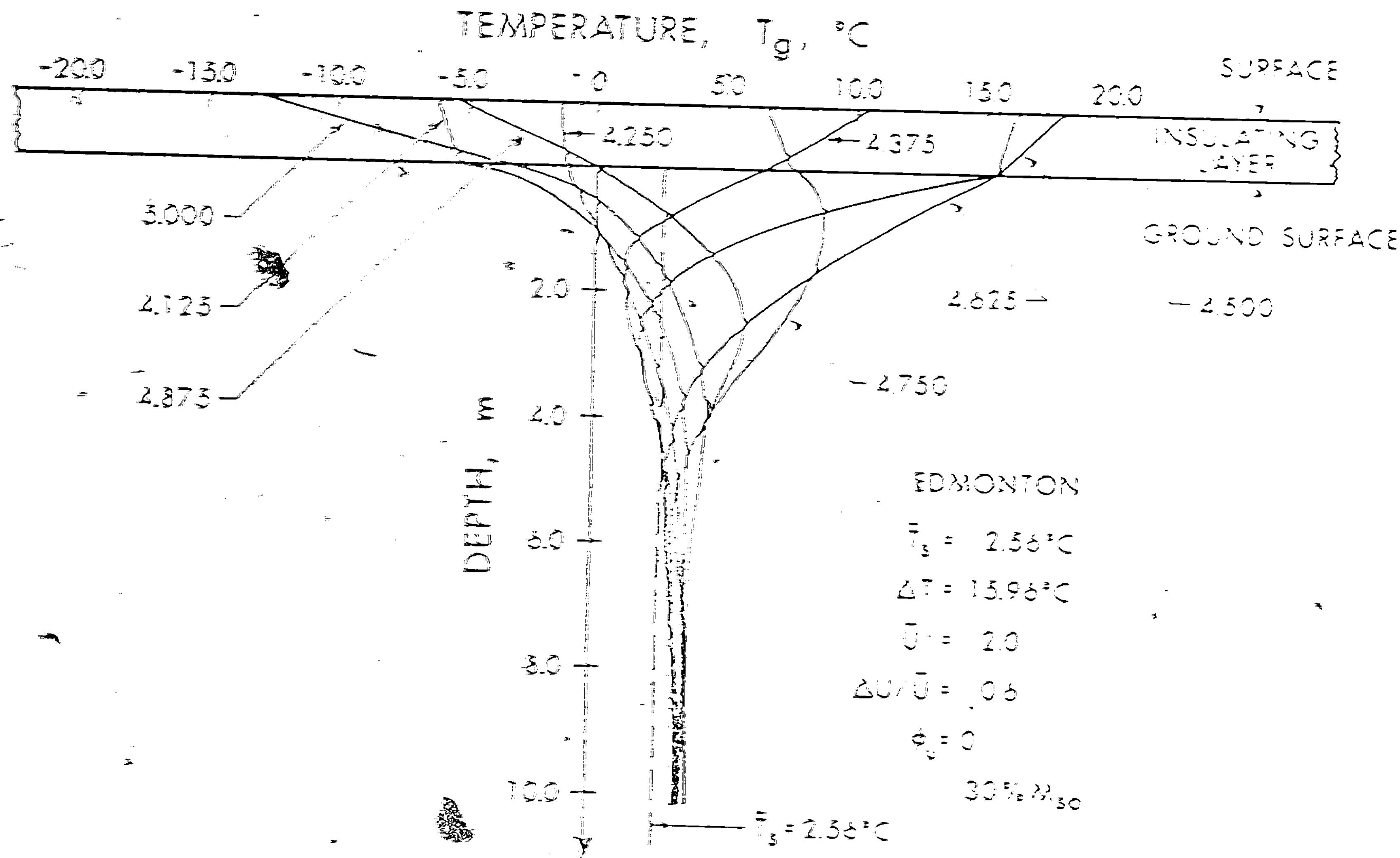

FIGURE 18 — Temperature distributions at Edmonton with imposed surface temperature

TABLE 1. Amplitude of Temperature Variation

Locations, soil and insulating properties	Amplitude of surface temperature variations (°C)	Amplitude of ground surface temperature variations (°C)
Edmonton.		
T_s = 2.56°C, ΔT = 15.96°C; U = 2.0, ΔU/U = 0.6; ϕ_0 = 0.0, H_{so} = [illegible]	18.1°C to 12.8°C	[illegible] to 5.1°C
Norman Wells:		
T_s = -6.22°C, ΔT = 22.06°C; U = 0.75, ΔU/U = 0.8; ϕ_0 = 0.0, H_{so} = 30%	15.1°C to 27.6°C	6.1°C to 2.5°C
Inuvik:		
T_s = -9.61°C, ΔT = 22.42°C; U = 0.75, ΔU/U = 0.8; ϕ_0 = 0.0, H_{so} = 30%	12.0°C to 31.3°C	3.0°C to 10.7°C

The amplitude of temperature variation at Norman Wells decreases the most because its average ground temperature is closer to 0°C, the temperature where the phase changes occur. As indicated by Figure (10), the temperature deep in the ground is greater than the average surface temperature T_s. This is true for all the three cases. Hence with the introduction of an insulating layer in phase with the air temperature, the ground temperature become warmer. This is the result predicted by the analytical model.

Figure (3.9) shows the variation of the average ground temperature with depth, with an insulating layer in place with the air temperatures. The temperature profiles show that the average temperatures deep in the ground are less than the average ground surface temperatures. These results are in agreement with and have been dealt with in the previous section where the surface temperatures were imposed. The temperature profiles also show that the average ground surface temperatures T_{gl} are greater than the average surface temperatures T_s. These results are predicted by the analytical model. The differences between the two average temperatures T_{gl} and T_s are very significant for both the Norman Wells and Inuvik cases, both of which are in the naturally permafrost locations. Also indicated are that the differences between T_s and T_{gl} are very much greater than that between T_{gl} and T_g, implying that the effects of the insulating layer are much greater than the effects of the thermal properties of the soil.

3.4.2 Effects the insulating layer have on $(T_s - T_{gl})$

This section will deal mainly with the effects the insulating layer has on the difference between the average top surface temperature T_s and the average ground surface temperature T_{gl}. The main parameters of the insulating layer U are, the average insulating cover $\bar{U}$, the amplitude of variation ΔU and the phase angle ϕ_u. It should be noted that the theory used in the figures would only be the "simple theory" or equation (3.24), which is the dominant term of the more complicated theory or equation (3.23).

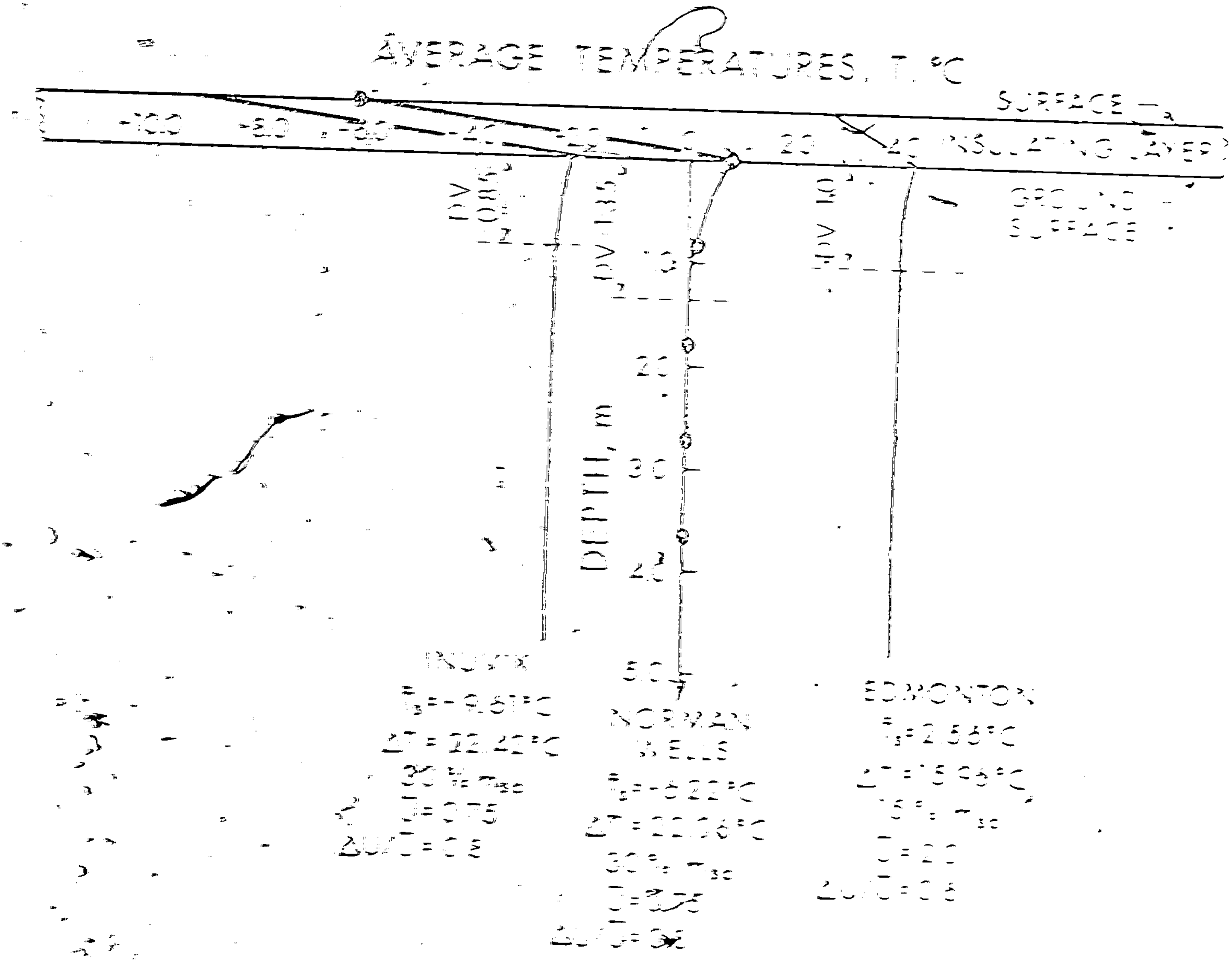

FIGURE 19 — Profiles of average temperature with imposed surface temperature and [illegible] = 0.0

Equation (3.[illegible]) of the "simple theory" where [illegible] (3.[illegible])

[illegible]

Also, [illegible] in the simple theory [illegible] ϕ_{a1} [illegible]. In the numerical model, the [illegible] the more complicated theory of equation (3.23) was not used [illegible] the standard theory was because of the difficulty in predicting the value of the effective heat capacity of the soil, that is, the effective heat capacity c_e varies as any one of the controlling parameters varies. Attempts were made to obtain a suitable average value of c_e and substituting it into the more complicated one to obtain a theoretical curve that would match the numerical results more closely. This was not possible in general because of the sensitivity of c_e to the other parameters of the problem.

The effects the ratio $\Delta U/U$ has on $(T_{gl} - T_a)/\Delta T$ are shown in Figure (20) for two cases, one when the insulating layer is in phase (ϕ_{ii} = 0.0), while the other when the insulating layer is 180° out of phase (ϕ_{ii} = 0.5) with the air temperature. For the case when ϕ_{ii} = 0.0, $(T_{gl} - T_a)/\Delta T$ increases almost linearly as $\Delta U/U$ increases and the numerical result is about 45% less than the results of the simple theory, that is neglecting the terms in $U/\rho c_a \omega$. When ϕ_{ii} = 0.5, $(T_{gl} - T_a)/\Delta T$ decreases as $\Delta U/U$ increases. The numerical results here are about 35% more than the results of the simple theory. The big difference between the simple theory results and the numerical results is mainly because of the assumption in the simple theory that $U/\rho c_a \omega$ = 0.0. An inspection of the more complicated theory, equation (3.23), indicates

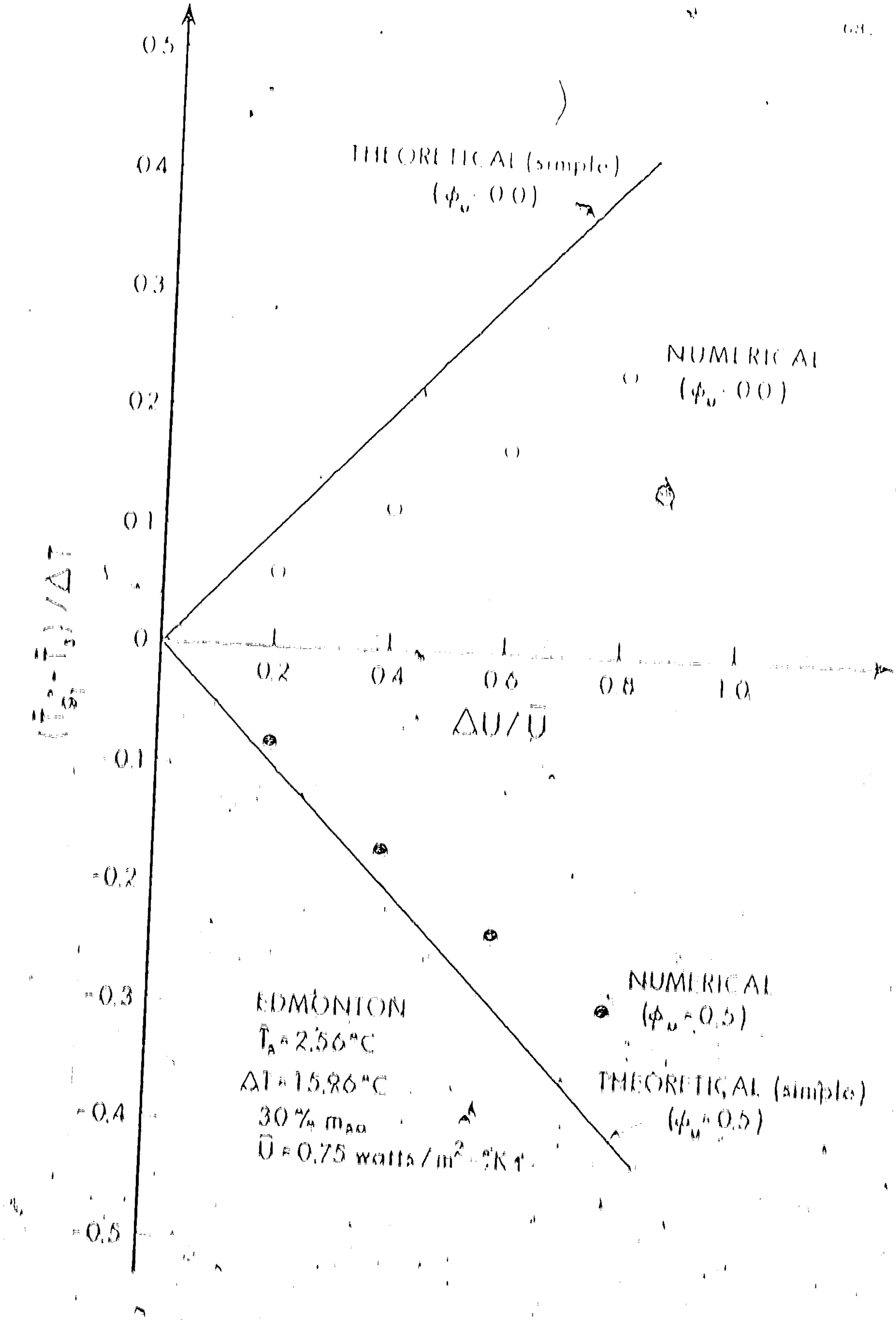

FIGURE 20 Variation of ΔU/Ū with ($\bar{T}_{B_i}$ − $\bar{T}_A$)/ΔT.

that any finite value in $k_2 c_e$ would decrease the absolute value of $(T_{gl}-T_s)/\Delta T$, being closer to the numerical results.

Figure (21) shows the relationship between $(T_{gl}-T_s)/\Delta T$ and B for a given value of 0.6. This insulating layer model will approach that of the imposed surface temperature model when B approaches infinity. Analytically, the simple theory indicates that $(T_{gl}-T_s)/\Delta T$ is independent of B but however the more complicated theory qualitatively shows a decrease in $(T_{gl}-T_s)/\Delta T$ as B increases. The numerical results confirm this behavior. They also show that the decrease in $(T_{gl}-T_s)/\Delta T$ is greater at 15% moisture content than at 30 moisture content. This could be attributed to the fact that the effective heat capacity (ρc_e) is greater in the 30% case.

Figure (22) shows the relationship between $(T_{gl}-T_s)/\Delta T$ and the insulating layer phase constant ϕ_s, for the various moisture content at Inuvik and Edmonton. When phase constant $\phi_s = 0.0$, the value of $(T_{gl}-T_s)/\Delta T$ is positive and it increases with moisture content. For phase constant $\phi_s = 0.5$, the value of $(T_{gl}-T_s)/\Delta T$ is negative and it decreases with moisture content. However, when the phase constant $\phi_s = 0.25$, the simple theory indicates a zero value for $(T_{gl}-T_s)/\Delta T$, but the numerical results shows that the value of $(T_{gl}-T_s)/\Delta T$ is positive and it decreases as the moisture content increases. On the other hand the more complicated theoretical solution predicts a positive value of $(T_{gl}-T_s)/\Delta T$ when $\phi_s = 0.25$. The above observations are true for both Inuvik and Edmonton cases. Generally the values of $(T_{gl}-T_s)/\Delta T$ for Inuvik case are greater than those for Edmonton at all phase constants.

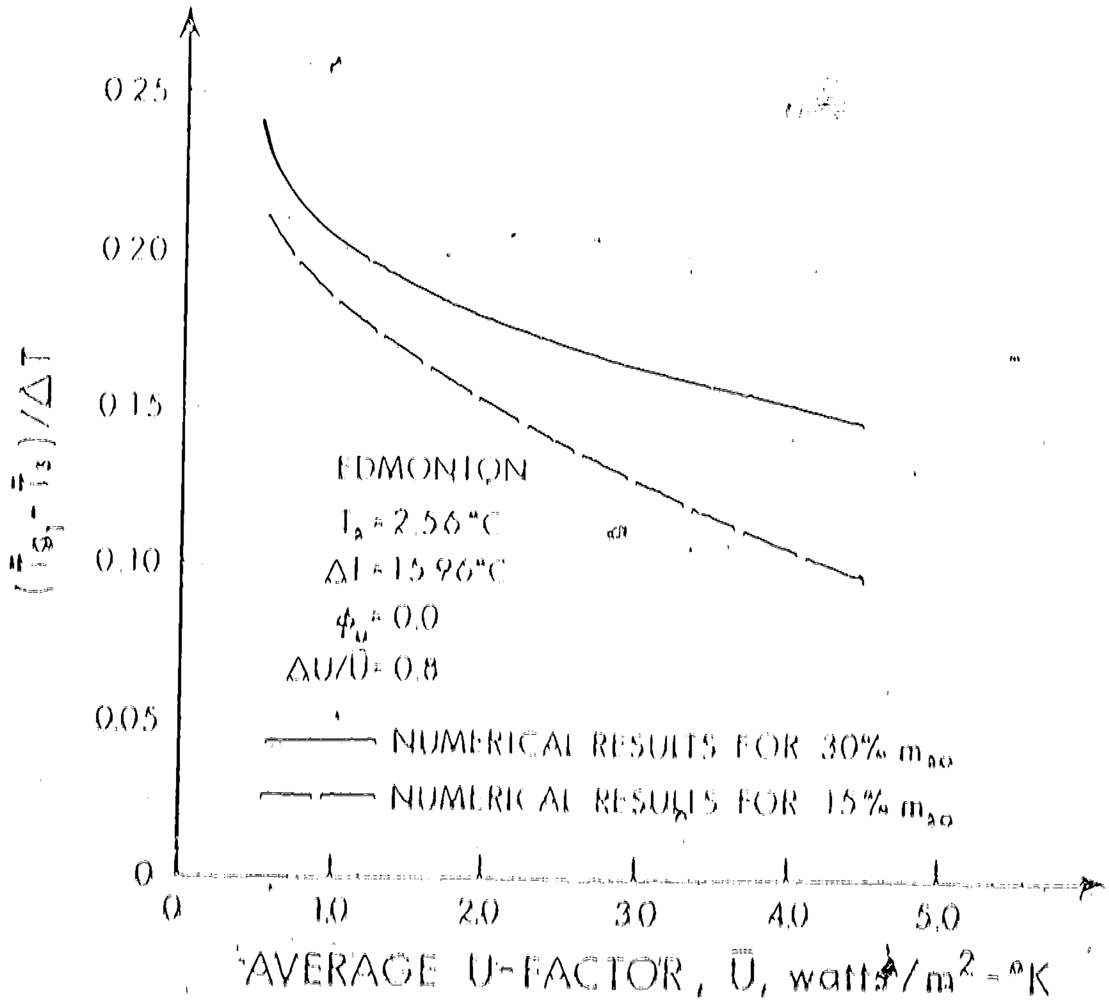

FIGURE 21 - Variation of $\bar{U}$ with $(\bar{T}_{g_1} - \bar{T}_a)/\Delta T$

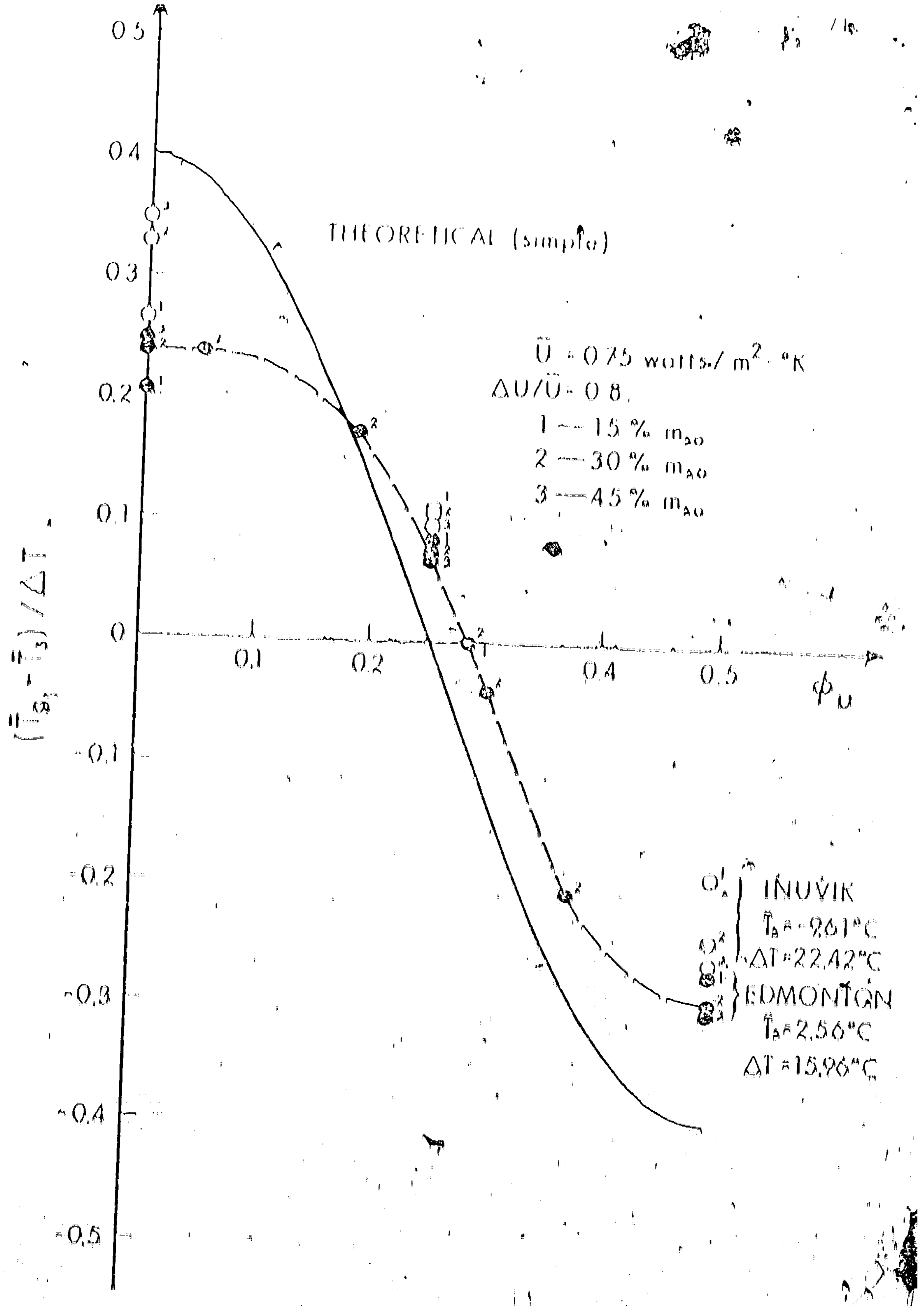

THEORETICAL (simple)
Ū = 0.75 watts/m² · °K
ΔU/Ū = 0.8
1 — 15 % m_Ao
2 — 30 % m_Ao
3 — 45 % m_Ao
INUVIK
T_A = -9.61°C
ΔT = 22.42°C
EDMONTON
T_A = 2.56°C
ΔT = 15.96°C
φ_u
(T_s - T_3) / ΔT
0.5
0.4
0.3
0.2
0.1
0
-0.1
-0.2
-0.3
-0.4
-0.5
0.1
0.2
0.4
0.5

and that the moisture content effects the values of $(T_{gl} - T_s)/T$ at Inuvik significantly more than those at Edmonton.

3.5 Depth of the active layer

3.5.1 Depth of frost or thaw penetration

Shown in figure (23) is the typical thaw penetration for Norman Wells. Depth of maximum thaw or frost penetration for the three locations under consideration are listed in table 2. Listed also are the soil and insulating properties. The method of obtaining the depth of frost or thaw penetration is similar to the one discussed earlier in Section (2.4.1), for the imposed temperature case.

TABLE 2. Depth of frost or thaw penetration with imposed surface temperature

Locations, soil and insulating properties		Depth of thaw or frost penetration (meters)
Edmonton:	T_s = 2.56°C, ΔT = 15.96°C	
	U = 2.0, $\Delta U/U$ = 0.6	0.925 m. (= 3 feet)
	ϕ_u = 0.0, M_{ao} = 15%	
Norman Wells:	T_s = -6.22, ΔT = 22.06°C	
	U = 0.75, $\Delta U/U$ = 0.8	0.825 m. (= 2.7 feet)
	ϕ_u = 0.0, M_{ao} = 30%	
Inuvik:	T_s = -9.61°C, ΔT = 22.42°C	
	U = 0.75, $\Delta U/U$ = 0.8	0.425 m. (= 1.4 feet)
	ϕ_u = 0.0, M_{ao} = 30%	

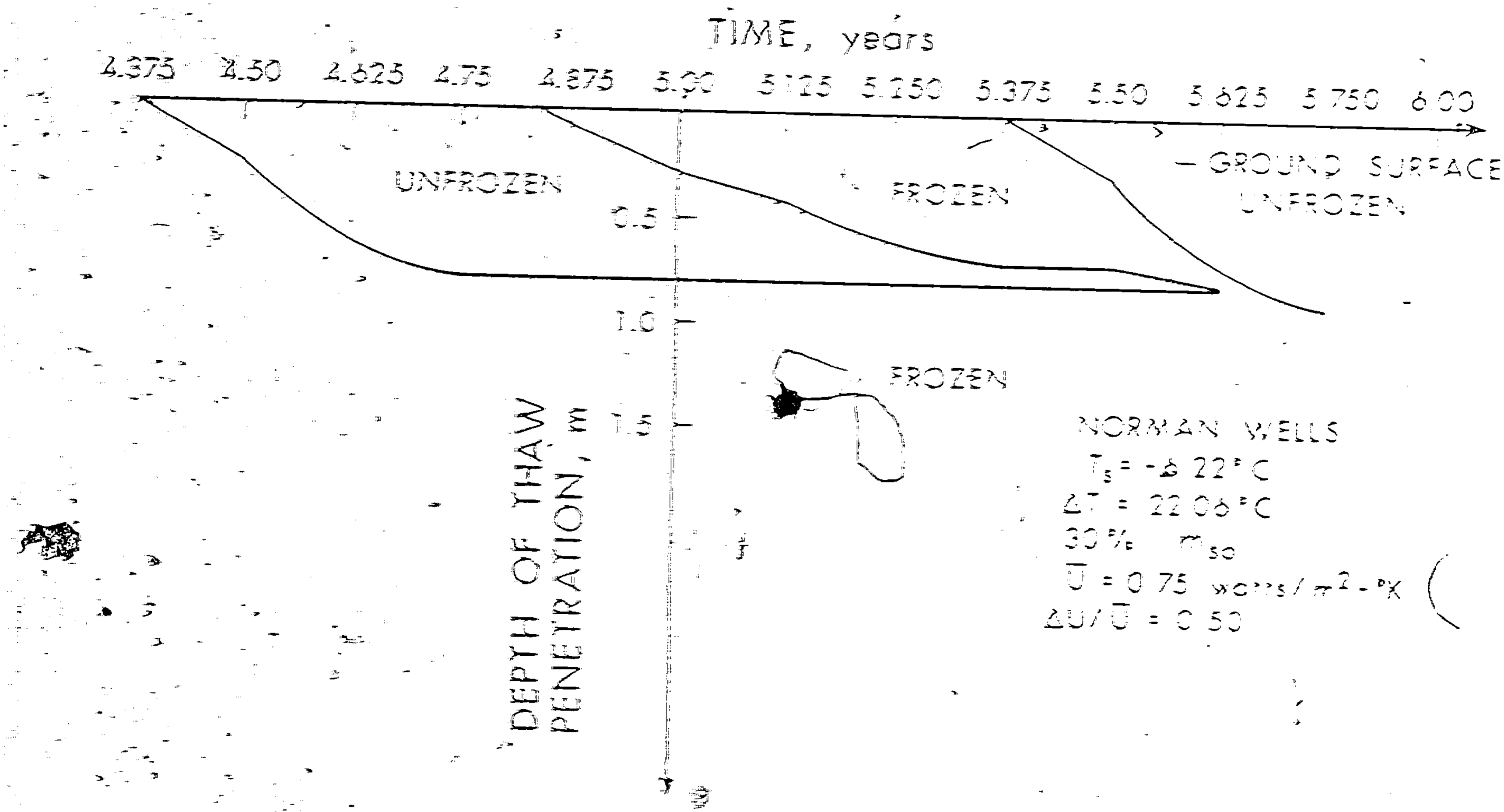

FIGURE 23 — Depth of thaw penetration in Norman Wells with the insulating layer in phase (c_u = 0.0) with the air temperature

3.5.2 Effects of the insulating layer on the active layer

Figures (24) and (25) show the relationship between the average insulating layer U and the depth of active layer for Edmonton case, with various phase constant ϕ_u and moisture content M_{so}. Generally, if all the parameters remain unchanged, an increase in U will cause an increase in the depth of the active layer for the Edmonton case of the non naturally permafrost location as indicated by both the figures. Specifically for a given U and moisture content M_{so}, the depth of the active layer increases as the phase constant ϕ_u increases and for a given U and phase constant ϕ_u, the depth increases as the moisture content decreases.

For Edmonton with 30% moisture content, $U = 0.75$ and phase constant $\phi_u = 0.0$, the depth of the active layer decreases as $\Delta U/U$ increases as indicated by Figure (26). However, if the phase constant $\phi_u = 0.5$, the depth of the active layer increases at first gradually and then rapidly as $\Delta U/U$ increases.

Figure (27) shows the relationship between the moisture content M_{so} and the depth of the active layer for both Inuvik and Edmonton at the various phase content ϕ_u. Figure (27) indicates that for the Edmonton case (non-naturally permafrost location), at a given U-factor, the depth of active layer increases as ϕ_u increases and decreases as the moisture content M_{so} increases, the result obtained in Figures (24) and (25). For Inuvik, a naturally permafrost location, for a given U-factor and phase constant ϕ_u, the depth of the active layer decreases as the moisture content increases, similar to that for Edmonton but the depth decreases as the phase constant ϕ_u increases, opposite to

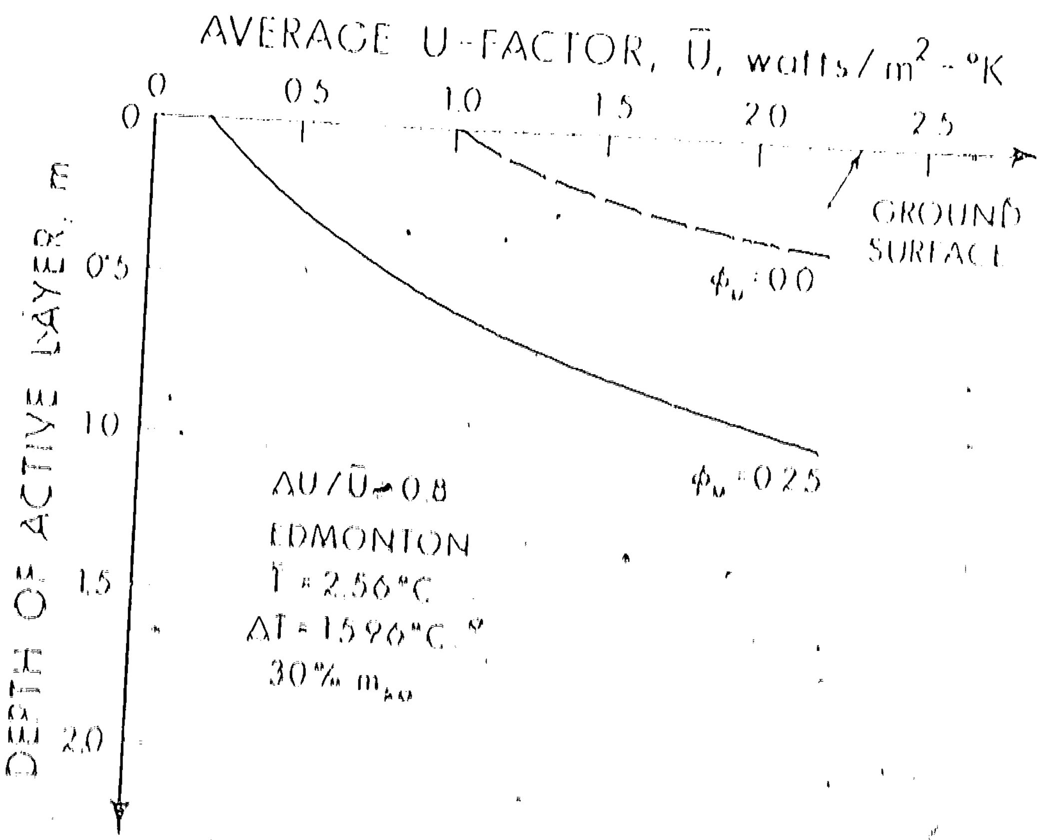

FIGURE 24 — Variation of Ū and ϕ_u with depth of active layer

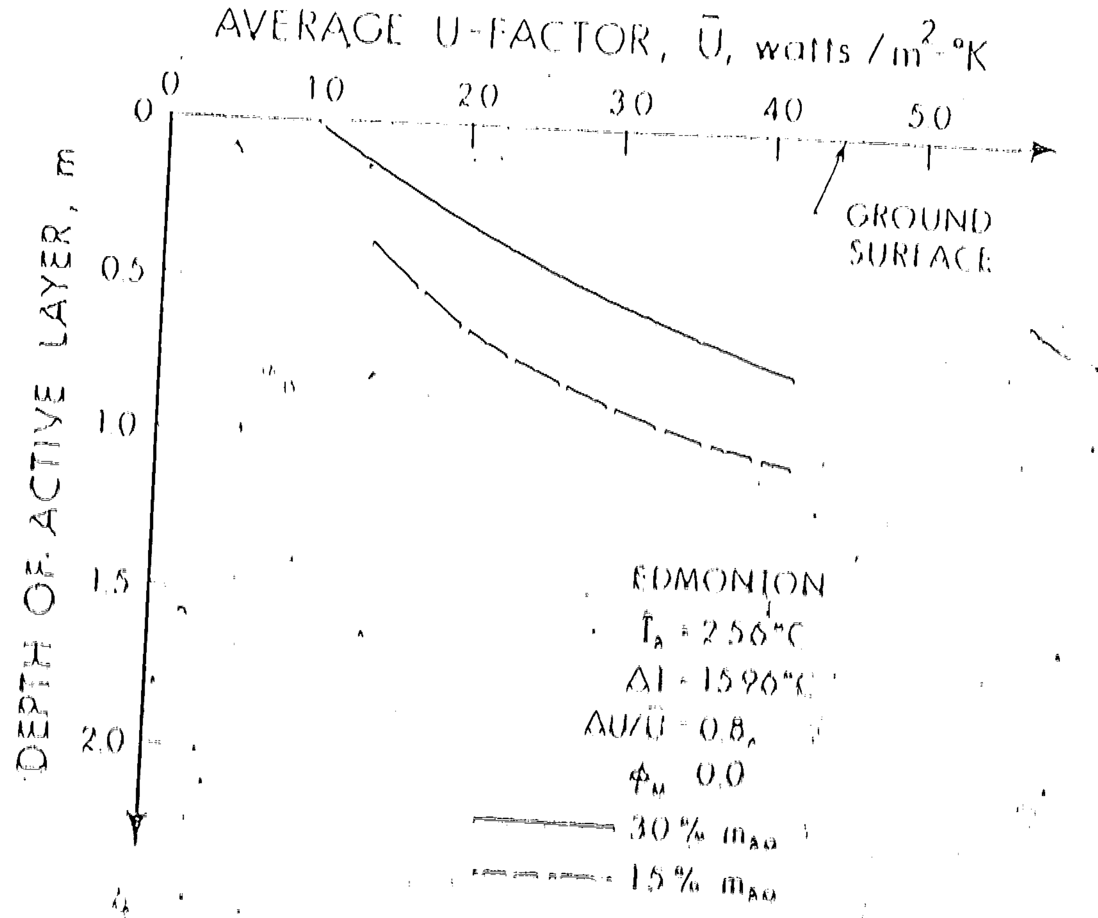

FIGURE 25 Variation of $\bar{U}$ and M_{AO} with depth of active layer

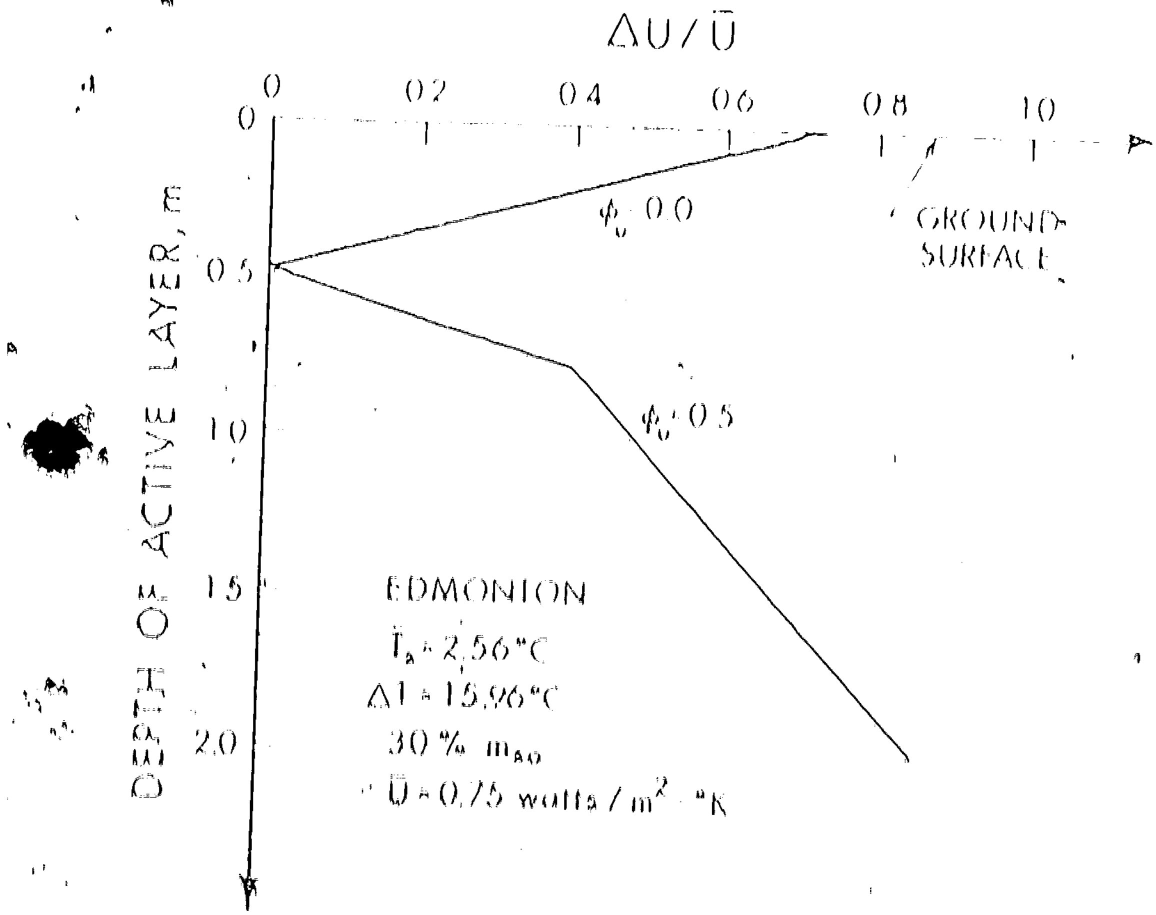

FIGURE 26 Variation of ΔU/Ū with depth of active layer

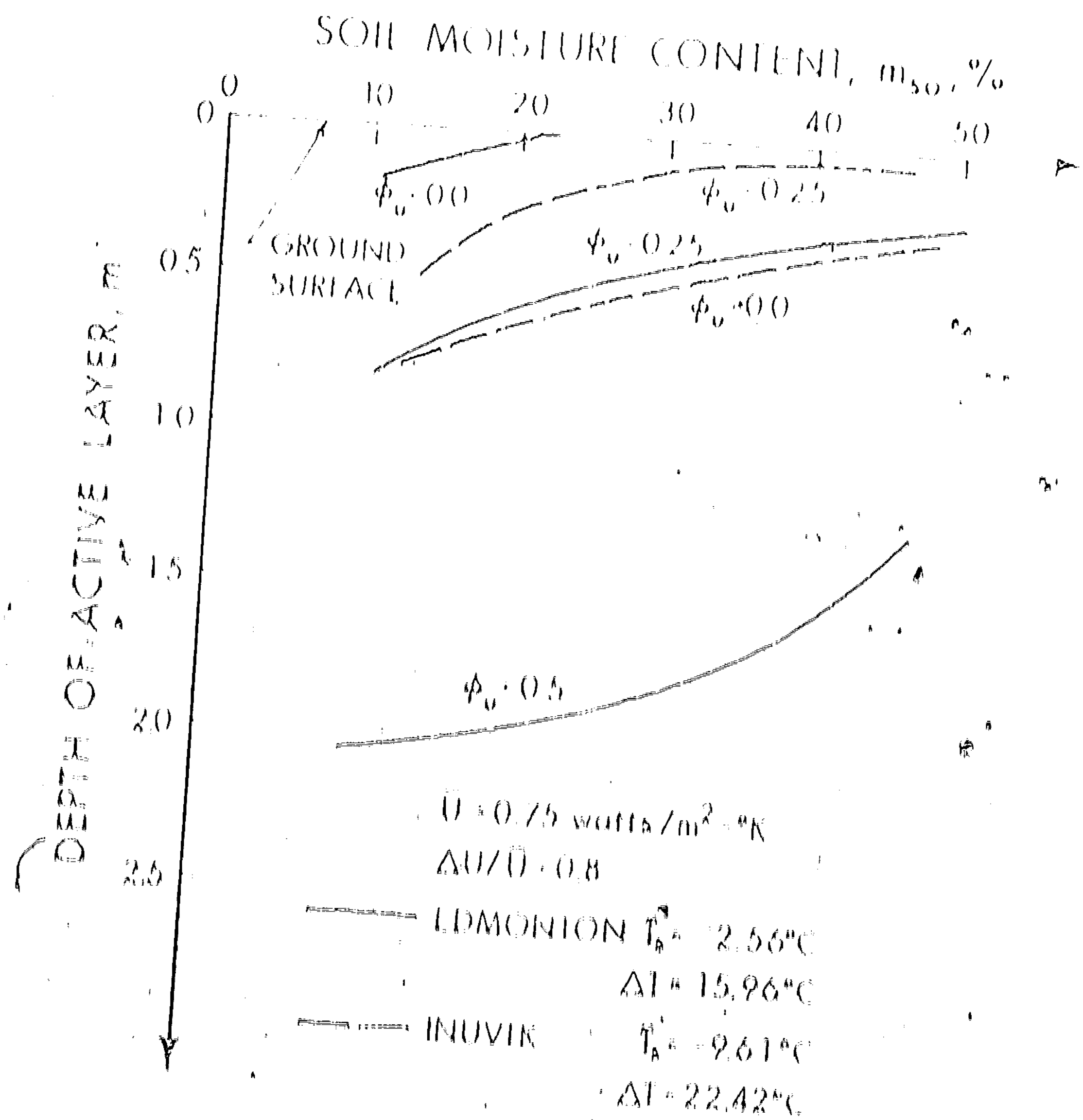

FIGURE 27 - Variation of M_{50} and ϕ_u with depth of active layer Λ

[illegible]

5.6 Conclusions

With the addition of an insulating layer, the amplitude of temperature variation at the ground surface is smaller; the greatest change occurs when the mean ground temperature is close to 0°C. Except for the smaller amplitude of temperature variation, the profiles of the ground temperatures are the same as those for the imposed ground surface temperature cases. An insulating layer in place with the air temperature would cause the average ground temperature to be warmer than the average air temperature. As [illegible] increases, that is approaching the imposed ground surface temperature condition, the effect of the insulating layer on the ground temperature decreases. The effect of the insulating layer is largest for high moisture content soils.

For both Edmonton (non-permafrost location) and Inuvik (naturally permafrost location) cases, an increase in moisture content H_{m} would cause the active layer depth to decrease. However, for a given H_{m}, an increase in ϕ_{u} would cause the active layer depth in Edmonton to increase whereas that in Inuvik to decrease.

PART IV

UNSTEADY HEAT CONDUCTION WITH CHANGE OF PHASE AND VARYING HEAT FLUX AT OUTER BOUNDARY

4.1 INTRODUCTION

In this section, instead of assuming T_s equals the air temperature T_a, T_s here will be calculated from a balance of heat fluxes at the surface. It is reasonable to assume that the calculated T_s^* will be different from the air temperature T_a because of the various complex heat fluxes.

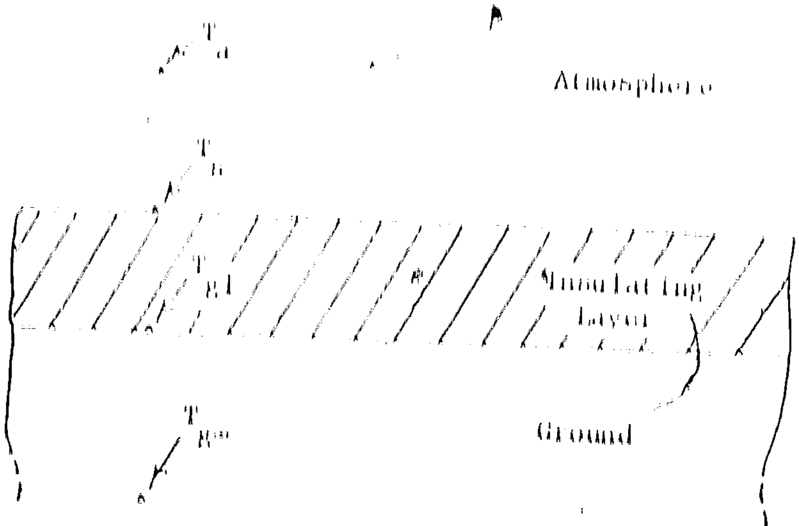

FIGURE 28

Figure (28) shows the various major average temperatures in the ground-atmosphere system,

briefly, $T_{g\infty} \neq T_{sl}$: because of the freezing and thawing

$T_{sl} \neq T_s$: because of the insulating layer

$T_s \neq T_a$: because of the heat fluxes

4.2 Disposition of Solar Radiation

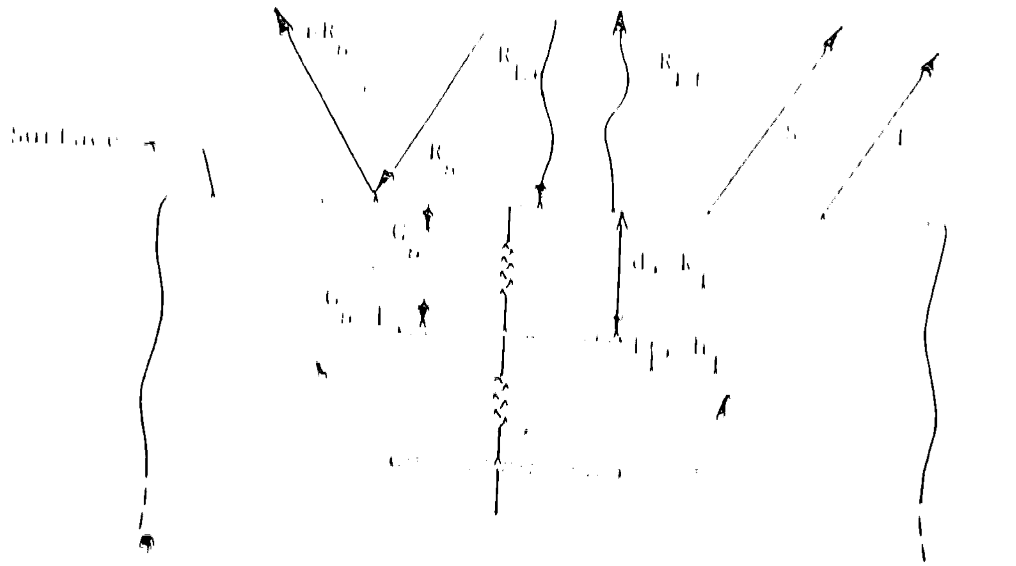

FIGURE 29

Figure (29) shows the major components of the disposition of solar radiation in the earth-atmosphere system. The components are:

i) R_s, incoming solar radiation

ii) rR_s, amount of R_s reflected

iii) $R_{L\downarrow}$, long-wave radiation down from the sky

iv) $R_{L\uparrow}$, long-wave radiation (infrared radiation) from the ground

v) S, sensible heat flux

vi) L, latent heat flux

vii) G_s, heat flux conducted through the insulating surface into the ground.

All of these components will be individually discussed later in this section.

4.2 The air temperature T_a will be assumed to vary as a pure harmonic function of time around an average value (Appendix I). Considering only the case for Norman Wells, the average air temperature $\bar{T}_a$ is $-6.2°C$ and its amplitude of oscillation A_a is 22.06°C.

$$T_a = \bar{T}_a + A_a \sin(\omega t_1)$$

The differentiation between summer and winter conditions will be determined by whether the air temperature T_a is above or below the freezing temperature 0°C. With reference to Appendix I, for Norman Wells

when $0.42 < t_n < 0.83$ (summer conditions)

$0.42 > t_n > 0.83$ (winter conditions)

Heat Fluxes

4.2.1 Incoming Solar Radiation (R_s)

This value of R_s is usually the measured value and is independent of the nature of the ground surface. The incoming solar radiation is made up of diffuse and direct radiation and is the total solar radiation that reaches the earth surface. On the average about half of the solar radiation intercepted by the earth eventually reaches the surface. The rest is either reflected and scattered back to space by clouds and atmospheric constituents or is absorbed by clouds and atmospheric constituents. Appendix IV shows the range of short wave radiation (R_s) for a latitude of 65°N. This data was recorded from 1943-1957.

these values are assumed to be those of Norman Wells (65° 17' N) and that the terms are assumed to vary sinusoidally about an average value.

$$R_s = \bar{R}_s + \Delta R_s \sin(\omega t_R) \qquad (6.1)$$

4.2.2 . Reflected Short Wave Radiation (rR_s)

All solar radiation incident on the earth surfaces is not absorbed there, a certain portion of that is reflected and is lost to space. The amount reflected depends primarily on the color, moisture content, texture and the composition of the surface. In general, a wet or dark surface has a lower reflectivity than the dry or light surface.

TABLE 3. Albedo of Natural Surfaces (1)

Type of Surface	Reflectivity, r
Fresh snow cover	0.75 - 0.95
Dense cloud cover	0.60 - 0.90
Old snow cover	0.40 - 0.70
Clean firm snow	0.50 - 0.65
Light sand dunes, surf	0.30 - 0.60
Clean glacier ice	0.30 - 0.46
Dirty firm snow	0.20 - 0.50
Dirty glacier ice	0.20 - 0.30
Sandy soils	0.15 - 0.40
Meadow and fields	0.12 - 0.30
Densely built-up areas	0.15 - 0.25
Woods	0.05 - 0.20
Dark cultivated soil	0.07 - 0.10
Water surface, sea	0.03 - 0.10

The values given in Table 3 are obtained from Geiger (45). Observing the values given in the table, shows that the albedo of different natural surfaces vary from about 3 to 30%. This is because the albedo varies with the moisture content of the soil and also varies both with the wavelength and the angle of incidence of the solar rays. The values of the last two cases are given in Sellers (43). In the case of cultivated soil, albedo depends strongly on the moisture content of the soil, an increase in soil moisture decreases the albedo. For the standard data set used in the calculations, the reflectivity was assumed to have an average winter and summer values, r_w and r_s. These values were chosen to be representative of vegetation in summer and snow cover in winter, $r_s = 0.16$ and $r_w = 0.60$.

4.2.3 Long wave emission from the earth's surfaces (R_{LE})

The surface of the earth, as any other body, radiates energy. Because of the earth's temperature most of the emission lies in the invisible infrared region of the spectrum. The earth is commonly assumed to emit and absorb energy as a gray body in the infrared region. The formula for the earth's surface emission may thus be written as

$$R_{LE} = \varepsilon_s \, \sigma (T_s + 273)^4 \qquad (4.2)$$

according to Stefan-Boltzman law

where σ is the Stefan Boltzmann constant

$= 5.67 \times 10^{-8}$ Watts/m^2 °K^4

T_s is the temperature of the surface in °C and ε_s is the infrared emissivity of the surface. The emissivity of a black body is unity. Typical infrared emissivities, expressed in percent for the various surfaces are given in Table 4. The data are from Sellers (43).

TABLE 4. Infrared Emissivities (ϵ_s)

(Per cent)

Surface	ϵ_s
Water	92 - 96
Snow, fresh	82 - 99.5
Snow, ice granules	89
Ice	96
Soil, frozen	93 - 94
Sand, dry	84 - 90
Sand, wet	95
Gravel, coarse	91 - 92
Ground, moist, bare	95 - 98
Ground, dry, plowed	90
Grass, high dry	90
Field and shrubs	90
Pine forest	90

As indicated in Table 4 the values of ϵ_s for the various surfaces vary from 82 to 99.5%.

4.2.4 Long-wave counter-radiation from the atmosphere (R_{Lt})

Although the atmosphere is nearly transparent to short-wave radiation, it readily absorbs the terrestrial radiation. The principal absorbers being water vapor, atmospheric gases and clouds.

As a result only about 9 per cent of the terrestrial radiation escapes directly to space. The atmosphere in turn reradiates the absorbed terrestrial radiation, partly to space and partly back to the surface (counter radiation). The counter radiation which is absorbed by the surface R_{LI}, for clear skies is

$$R_{LI} = \epsilon_s \epsilon_a \sigma (T_a + 273)^4 \qquad (4.3)$$

where ϵ_a is the effective emissivity of the air and has been approximated by

$$\epsilon_a = a - b e^{-c e_a}$$

a, b and c are empirical constants and e_a is the vapor pressure in millibars.

Geiger (45) uses

$a = 0.82$

$b = 0.25$

$c = 0.094$

The vapor pressure e_a has further been approximated by (Appendix IV)

$$e_a = W e^{23.4 - 5900/(T_a + 273)} \qquad (4.4)$$

where W is the relative humidity (Appendix V).

The counter-radiation R_{LI} from a cloudy sky is expressed in terms of the value for a clear sky (45) by the equation

$$\epsilon_{a(corr)} = (1 + Bw_c)\, \epsilon_a \qquad (4.5)$$

where M is a constant and w_c is the extent of cloud cover (Appendix VI), which for overcast skies is 1.0 and for clear skies is 0.0. Radiation from the clouds, as indicated in equation (4.5), does not increase linearly with w_c, but almost as a quadratic function. Other than depending on the extent of the cloud cover, counter radiation also depends on the height of the cloud, as indicated by the values of M in Table 5. In general, the higher and thinner the clouds the less they will contribute to the counter radiation reaching the ground. Typical values for M are listed in Table 5 (45).

TABLE 5. Values of M

Cloud Type	Height (m)	M
Cirrus	12,200	0.04
Cirrostratus	8,390	0.08
Altocumulus	3,660	0.17
Altostratus	2,140	0.20
Stratocumulus	1,220	0.20
Stratus	460	0.24

4.2.5 Sensible Heat Flux (S) and Latent Heat Flux (L)

The temperature of the earth surface is usually different from the temperature of the lower layer of the atmosphere. Consequently, a vertical heat flux exists between the underlying surface and the atmosphere affected by the turbulent heat exchange in the air layer near the ground. The determination of these vertical turbulent heat fluxes usually presents the greatest difficulties in any heat balance problem. Because of the complexities involved in developing suitable equations for these two fluxes, detailed descriptions will not be presented here, however they are available in Sellers (61), Budyko (44), Geiger (45) and Matveev (47). The most common method for obtaining the formula for the vertical turbulent heat fluxes in the air layer near the ground is to assume that the process of turbulent diffusion is similar to that of molecular diffusion.

Hence for sensible heat flux S, the equation is

$$S = -\rho c_p K_h (\Delta T/\Delta z) \quad (4.6)$$

and for latent heat flux L, the equation is

$$L = -\rho L_a K_w (\Delta q/\Delta z) \quad (4.7)$$

K_h and K_w are the corresponding eddy diffusivities and q, T and z are the specific humidity, temperature and height. Assuming S and L do not vary within the air layer thickness of one or two meters above the underlying surface, equations (4.6) and (4.7) can then be integrated from the surface to a height z, one or two meters above the ground to give

$$S = \rho c_p D_h (T_s - T_a) \quad (4.8)$$

and

$$L = \rho L_a D_w (q_s - q_a). \quad (4.9)$$

or

$$L = (0.622 L_e D_w)(e_s - e_a)/P \qquad (4.10)$$

Further, if it is assumed that the diffusion of heat takes place by the same mechanism as the diffusion of water vapor, $D_h = D_w$, hence equations (4.8) and (4.10) can be written as

$$S = A(T_s - T_a) \qquad (4.8)$$

and

$$L = B(e_s - e_a) \qquad (4.10)$$

where

$$A = \rho c_p D$$

$$B = (0.622 \rho L_e D)/P$$

D, e_s, e_a and P are the diffusivity coefficient, surface vapor pressure, air vapor pressure and the total pressure.

From Appendix V, the saturated surface vapor pressure e_{ss} is given by

$$e_{ss} = e^{23.4} e^{-5900/(T_s+273)} \qquad (4.11)$$

and that for the air vapor pressure is

$$e_a = w e^{23.4} e^{-5900/(T_a+273)} \qquad (4.12)$$

For the top surface with a certain moisture content M_s, the surface vapor pressure e_s is

$$e_s = M_s e^{23.4 - 5900/(T_s + 273)} + (1 - M_s) e_a$$

$$= M_s e_{ss} + (1 - M_s) e_a \qquad (4.13)$$

D, the diffusivity coefficient for heat and moisture in the air layer near the ground are presented in various forms by different authors (41, 44). The principal properties of the diffusivity coefficient are that it changes considerably with the wind velocity, increases as the surface roughness increases and that the coefficient is higher in dry region. It also will depend on the stability of the air layer. From Sellers (41), the diffusivity coefficient is given by

$$D = f + gu^2 \qquad (4.14)$$

where D is in m./sec, g is a constant with values around 0.002, u is the wind velocity in m./sec and the coefficient f is extremely variable with values ranging from 0.0045 m./sec to 0.0007 m./sec, depending on the type of surface. The coefficient f increases as the surface roughness increases.

Values used in the calculations are

$f = 0.003$ m./sec,

$g = 0.002$

$u = 4.5$ m./sec

4.2.6 Heat Flux to the Ground (G_s)

The insulating layer lying over the ground was assumed to have no heat capacity, therefore, with reference to Figure (29),

$G_s = G_{s-1}$

$$T_s = T_1 + (d/k_1)\, G_s \qquad (4.15)$$

or

$$G_s = (k_1/d)(T_s - T_1)$$

4.2.7 The Insulating Layer (U Factor)

The layer was assigned a U factor, k_1/d, having an average winter and summer values, U_w and U_s.

$$d/k_1 = d_s/k_s \qquad 0.42 < t_n < 0.83$$

$$= d_w/k_w \qquad 0.42 > t_n > 0.83$$

4.2.8 Energy Balance

Net heat flux to the ground surface is

$$F = (1-r)\, R_s + R_{Ld} - R_{Lt} - S - LE \qquad (4.16)$$

For energy balance at the surface, F is also equal to G_s, the heat flux to the ground.

4.3 The Input Variables Required for the Solution to Equation (42) are:

(a) Radiation Parameters:

R_s, ΔR, ϕ_R, t_R, a, b, c

(b) Relative Humidity:

W_h

(c) Cloud Cover:

W_c, N

(d) Sensible and Latent Heat Parameters:

r_s, L_e, P, L, ρ, u, c_p

(e) Air Temperature Parameters:

T_a, ΔT_a, ϕ_T

(f) Surface Conditions:

t_s, t_w, d_s, d_w, t_1, t_2, k_s, k_w, M_s

(g) Ground Parameters:

k_f, k_{uf}, ρc_f, ρc_{uf}, ρL_f, M_{oo}

4.4 Standard Input Data Set (Norman Wells)

i) Radiation Parameters:

R_s = 100 watts/m^2

ΔR_s = 100 watts/m^2

ϕ_R = 0.273

ϵ_s = 0.90

a = 0.82

b = 0.25

c = 0.094 1/mb

σ = 5.67 x 10^{-8} watts/m^2 °K^4

ii) Relative Humidity:

ω = 0.65

iii) Cloud cover.

W_c = 0.63

N = 0.2

iv) Sensible and Latent Heat Parameters:

ρ = 1.20 kg/m^3

L_e = 2.41 x 10^6 Joules/kg

P = 1018 mb

f = 0.003 m/sec

B = 0.002

u = 4.50 m/sec

c_p = 1.0 x 10^3 Joules/kg °C

v) Air Temperature Parameters:

T_a = 6.22 °C

ΔT_a = 22.06 °C

ϕ_T = 0.29

vi) Surface Conditions:

M_s = 0.30 (surface moisture content)

ϵ_s = 0.16

ϵ_w = 0.60

d_s = 0.[illegible]5 m.

d_w = 0.38 m.

k_s = 0.30 watts/m°C

k_w = 0.17 watts/m°C

ϵ_1 = 0.42

ϵ_2 = 0.84

VIII) Ground Parameters.

M_{so} = 0.30 (soil moisture content)

k_f 1.70 watts/m°C

k_{uf} 1.10 watts/m°C

ρc_f 1.60 x 10^6 joules/m^3 °C

ρc_{uf} 2.40 x 10^6 joules/m^3 °C

L_f 1.20 x 10^8 joules/m^2 °C

4.5 Introduction of the Analytical Section

For a given set of input variables, equation (4.16) along with the equations of heat transfer in the ground (Part III) can be solved for the ground temperature variation throughout the year. This will be done numerically in the following section. However, because of the large number of input variables involved and the uncertainties in some of the empirical expressions for the heat flux, the absolute determination of the ground or surface temperatures may be questionable. One can however predict the changes in the ground and the surface temperatures that would result from changes in any one of the controlling parameters. This approach which is essentially a 'sensitivity analysis' will be taken with the model presented. First this will be done analytically. The analytic calculation will require the neglect of the interaction of the ground and the surface heat fluxes.

4.5.1 Analytical Section

The main objectives of this section are to obtain analytic estimates of the effects of the various heat fluxes acting on the surface of the ground cover. These effects will be expressed in terms of an effective surface temperature, an effective "heat transfer coefficient", and an average influence coefficient. The values of these parameters will be compared to the values obtained numerically.

4.5.2 Effective surface temperature and effective "heat transfer coefficient"

A linear approximation to equation (4.16) can be obtained by expanding it in a Taylor series about some temperature $T_s^{\wedge}$. Thus

$$F(T_s) = F(T_s^{\wedge}) + \partial F/\partial T_s\Big|_{T_s^{\wedge}} (T_s - T_s^{\wedge}) + \ldots \qquad (4.17)$$

where terms in a higher order in the temperature difference $(T_s - T_s^{\wedge})$ have been neglected.

If $T_s^{\wedge}$ is chosen such that $F(T_s^{\wedge}) = 0$, then equation (4.17) becomes

$$F(T_s) = \partial F/\partial T_s\Big|_{T_s^{\wedge}} (T_s - T_s^{\wedge}) \qquad (4.18)$$

The term $\partial F/\partial T_s\Big|_{T_s^{\wedge}}$ in equation (4.18) is essentially an effective heat transfer coefficient which could be called h_{eff}, thus giving

$$F(T_s) = h_{eff} (T_s - T_s^{\wedge}) \qquad (4.19)$$

The temperature $T_s^{\wedge}$ is the temperature the surface would have if there was no heat flux to the ground. It will therefore be close to the true surface temperature when there is a thick insulating layer of snow or vegetation on the ground. More specifically one would expect equation (4.19) to be a good approximation when $h_{eff} \gg U$, where U is the U factor or conductance of the surface insulating layer. This approximation will be checked in a latter section. A temperature similar to T_s^* when used in heat transfer literature on human comfort or other similar topics is often called an effective or radiation temperature. The former term will be used in this thesis.

To find T_s^*, equation (4.16) is set equal to zero and may be rewritten in the form

$$Y = A_0 - A_1 Y^4 - A_2 e^{-5900/Y} \tag{4.20}$$

where $Y = T_s^* + 273$ and A_0, A_1 and A_2 are known constants.

$$A_0 = 1/\rho c_p D \times (R_s(1-r) + \epsilon_s \epsilon_{a(corr)} \sigma (T_a + 273)^4$$

$$+ (0.622\ \rho L_s D/P)\ H_s e_a + \rho c_p D (T_a + 273))$$

$$A_1 = 1/\rho c_p D \times (\epsilon_s \sigma)$$

$$A_2 = 1/\rho c_p D \times ((0.622 \rho L_s D/P)\ H_s e^{23.4})$$

Defining the functions

$$f(Y) = Y - A_0 + A_1 Y^4 + A_2\ e^{-5900/Y} \tag{4.21}$$

$$f'(Y) = 1.0 + 4A_1 Y^3 + (5900\ A_2/Y^2)\ e^{-5900/Y} \tag{4.22}$$

Equation (4.20) can be solved by first assuming an initial approximation to a root, then generating successive approximations from the iteration

$$Y_{i+1} = Y_i - f(Y_i)/f'(Y_i) \qquad \text{(Newton's Method)}$$

$T_B\hat{}$ for the entire year for the standard data, given in section (4.4) was then obtained as tabulated in Table 6 along with the values of air temperature, T_a.

TABLE 6. Values of $T_B\hat{}$ for the entire Year

Time, t (year)	$T_B\hat{}$ (°C)	T_a (°C)
0.000	−31.37	−27.41
0.125	−28.22	−25.21
0.250	−13.77	−11.71
0.375	3.76	5.01
0.500	16.97	15.15
0.625	13.58	12.77
0.750	− 2.03	− 0.73
0.875	−21.31	−17.45
1.000	−31.37	−27.41

$\overline{T_B\hat{}} = -7.78°C$, $\overline{T_a} = -6.22°C$

It will be noted that $\hat{T}_s$ is lower than T_a in winter and higher than T_a in summer. This difference may be attributed to the fact that the value of the reflectivity of summer vegetation is very much lower than the reflectivity of winter snow cover, the respective values being 0.16 and 0.6. The greatest difference between $\hat{T}_s$ and T_a occurs in the winter when the additional heat flux due to solar radiation is minimum.

To find the effective "heat transfer coefficient", equation (4.16) must be differentiated with respect to T_s. This gives

$$\partial F/\partial T_s = 4\,\varepsilon_s\,\sigma(T_s+273)^3 + \rho c_p D$$

$$+ (0.622\,\rho L_v D/P)\,H_s e^{23.4}(5900/(T_s+273)^2)\,e^{-5900/(T_s+273)}.$$

$$h_{eff} = \partial F/\partial T_s\Big|_{\hat{T}_s} \qquad (4.23)$$

The effective "heat transfer coefficient" h_{eff} is thus the sum of the terms due to radiation, sensible heat and latent heat. These terms are labelled h_r, h_s and h_L respectively and values are given for various times during the year in Table 7. It will be noted that h_r and h_L are time dependent while h_s is not. The effective "heat transfer coefficient" h_{eff} that results, ranges from a low of 18.48 watts/m^2-°K in winter to a high of 30.0 watts/m^2-°K in summer. Its average value for the entire year is 22.51 watts/m^2-°K. Values of h_{eff} obtained from William (51) for latitude 40°N to 60°N indicates that for average conditions of exposure, the coefficient varies between 19.39 to 29.09 watts/m^2°K (16.68 to 25.02 kcal/m^{2}h °K). This analytical value of effective "heat transfer coefficient" h_{eff}, will be later compared to the value of h_{eff} obtained numerically.

TABLE 7. Values of h's for the Entire Year

Time, t (year)	h_r (Lw radiation)	h_s (Sensible)	h_L (Latent)	h_{eff} watts/m^2°K
0.000	2.88	15.36	0.24	18.48
0.125	2.99	15.36	0.32	18.67
0.250	3.56	15.36	1.08	20.00
0.375	4.33	15.36	4.01	23.70
0.500	4.98	15.36	9.66	30.00
0.625	4.80	15.36	7.78	27.94
0.750	4.06	15.36	2.06	22.08
0.875	3.25	15.36	0.58	19.19
1.00	2.88	15.36	0.24	18.48

4.5.3 Analytical average influence coefficient for the standard data set

The main objective here is to find the change in T_s caused by a change in x_i where x_i is one of the controlling input parameters. If the net heat flux to the ground is zero, then equation (4.16) becomes

$$0 = R_s(1-r) - \epsilon_s \sigma(T_s+273)^4 + \epsilon_s' \epsilon_{a(corr)} \sigma(T_a+273)^4$$

$$- \rho c_p D(T_s - T_a) - (0.622\ \rho L_e D/P)(e_s - e_a)$$

which implies that

$$f(T_s,\ x_i) = 0 \tag{4.24}$$

Taking the total derivative of equation (4.24) with respect to the independent parameters x_i, gives

$$df/dx_i = 0 = \partial f/\partial T_s\ \ dT_s/dx_i + \partial f/\partial x_i$$

implying

$$dT_s/dx_i = -(\partial f/\partial x_i / \partial f/\partial T_s) \tag{4.25}$$

$\partial f/\partial T_s$ was obtained previously in finding the effective heat transfer coefficient. The average influence coefficient is

$$dT_s/dx_i$$

which is equated to

$$\int_0^1 dT_s/dx_i\ dt \tag{4.26}$$

In integrating equation (4.26), the nominal values of T_s is assumed to be T_s^0, the value which gives $f = 0$. Taking the partial derivative of f with respect to the independent variable x_i, $\partial f/\partial x_i$:

i) $\partial f/\partial R_s = (1-r)$

but

$$R_s = \bar{R}_s(1+\Delta R/\bar{R}_s\ \sin(\omega t+\phi_R))$$

$$\partial R_n/\partial R_n = 1$$

$$\partial R_n/\partial(\Delta R/R_n) = R_n \sin(\omega t+\phi_R)$$

$$\therefore \partial I/\partial R_n = (1-r)$$

and

$$\partial I/\partial(\Delta R/R_n) = (1-r)\, R_n \sin(\omega t+\phi_R)$$

ii) $\partial I/\partial r = -R_n$

iii) $\partial I/\partial \varepsilon_n = -\sigma(T_n+273)^4 + \varepsilon_{a_{corr}}\, \sigma(T_a+273)^4$

iv) $\partial I/\partial u = -\rho c_p D(T_n-T_a) - (0.622\rho L_v D/P)(e_n-e_a)$

v) $\partial I/\partial w_e = 2\varepsilon_n\, \sigma\, M\, w_e\, \varepsilon_a(T_a+273)^4$

vi) $\partial I/\partial M_a = -(0.622\rho L_v D/P)(e_{sa}-e_a)$

vii) $\partial I/\partial w = \varepsilon_n\, \sigma(T_a+273)^4(1+Mw_e^2)(b e e_{sa}\, e^{-ce_a}) \ldots$

$$+ (0.622\rho L_v D/P)\, M_a\, e_{sa}$$

viii) $\partial I/\partial T_a = 4\varepsilon_n\, \varepsilon_{a_{corr}}(T_a+273)^3 + \varepsilon_n\, \sigma(1+Mw_e^2)(T_a+273)^4 \times$

$$(b e\, e_a 5900\, e^{-ce_a})/(T_a+273)^2 + \rho c_p D + (0.622\rho L_v D/P)\, M_a \times$$

$$(b e\, e_a 5900)\, e^{-ce_a}/(T_a+273)^2$$

but

$$T_a = \bar{T}_a(1+\Delta T/\bar{T}_a \sin(\omega t+\phi_T))$$

$$\partial T_a / \partial T_a = 1$$

$$\partial T_a / \partial(\Delta T / T_a) = T_a \sin(\omega t + \phi_T)$$

$$\therefore \partial f / \partial T_a = \partial f / \partial T_a \times dT_a / T_a$$

and

$$\partial f / \partial(\Delta T / T_a) = \partial f / \partial T_a \times \partial T_a / \partial(\Delta T / T_a)$$

(x) $\partial f / \partial T_s = -4\varepsilon_s \sigma (T_s + 273)^3 - \rho c_p D - 0.622 \rho L_e D / P \times$

$$M_s e_{ss} 5400 / (T_s + 273)^2$$

As stated earlier dT_s/dx_i can be determined by using the chain rule

$$dT_s/dx_i = -(\partial f/\partial x_i / \partial f/\partial T_s)$$

The average

$$\overline{dT_s/dx_i} = \int_0^1 dT_s/dx_i \, dt$$

where it is assumed that $\overline{T_s} = T_s^*$.

The integration of dT_s/dx_i over the entire year was done by trapezoidal rule.

Define the influence coefficient to be the change in temperature T_s or T_s^* caused by a percentage change in the input parameters. Note, parameters r, ε_s, w, M_s and ν which represent ratios, will be expressed as percentage, 1 to 100, for the purpose of uniformity in the definition of the influence coefficients. That is for instance, the standard [illegible] used is 0.9 which will be 90% for use in calculating the influence coefficients. The one exception is the air temperature. Its influence coefficient will be expressed in terms of a temperature change in °C of T_s or T_g for a given temperature change in °C of T_a.

The influence coefficients will be used later to determine which are the most important parameters in so far as their effects on the ground temperature are concerned and also they will be used to estimate changes in ground temperature that would result from given changes in the input parameters. Ideally, to be of practical use, the influence coefficient for a particular parameter should be a constant over the range of that parameter and be unaffected by changes in other parameters. That is the effects of a parameter should be linear and uncoupled. As can be seen from the equations in this section (4.5.3), for the various influence coefficients, this cannot be exactly true for any variations of the input parameter; however, it may still be a reasonable approximation for small changes in the parameters.

To get some estimate of the likely values of the influence coefficients and the range of their values, Table 8 gives the average coefficients for the two data sets. One is the standard data set from section (4.4) and the other is a modified data set obtained by changing selected parameters within the limit of their reasonable ranges. It can be seen that most of the influence coefficients are the same for both data sets, however, some do vary. In particular the coefficient for $(\Delta u)/u$ changed very significantly between the two data sets. This is because it depends on the temperature difference, $(T_A - T_M)$, which is turn is affected by all the other parameters. The effect of the average wind velocity u, is thus strongly coupled. The influence coefficient for M_B changed by about 30% between the data sets. This could be attributed primarily to strong nonlinear dependence of vapor pressure on temperature.

TABLE 8. Analytical Values of the Average Influence Coefficients

Input Parameters	Average Influence Coefficients: Standard Data Set T_B	Average Influence Coefficients: Modified Standard Data Set[4] T_B
$(\Delta R_B)/R_B$	0.024	0.025
Δa_R[1]	0.090	0.070
$\Delta(t)$	-0.051	-0.045
$\Delta(t_B)$	-0.047	-0.047
$(\Delta u)/u$	-0.028	-0.043
$\Delta(R_H)$[2]	0.018	0.017
$\Delta(w_c)$	0.027	0.026
$\Delta(M_B)$[3]	-0.017	-0.023
(ΔT_A^*)	(0.819)	(0.812)

(1) $a_R = \Delta R/R_B$

(2) $R_H = w$

(3) $M_B = XMB$

(4) some of the parameters of the standard data set are modified within their limits from their individual nominal values.

4.6 Numerical Model

Basically the numerical model to be presented is similar to the numerical model presented in Part II of this thesis, except for the different boundary conditions and changes in the definition of the various dimensionless variables. The problem now has, instead of an imposed temperature boundary condition, a varying heat flux at one boundary. The changes in the definition of the various dimensionless variables are necessary so as to accommodate the new parameters.

The varying heat fluxes are those discussed in the early sections of this part (Part IV). The insulating layer is assumed to have negligible heat capacities and values of the insulating values are from Appendix III. The parameters in the ground remain unchanged.

4.6.1 Formulation

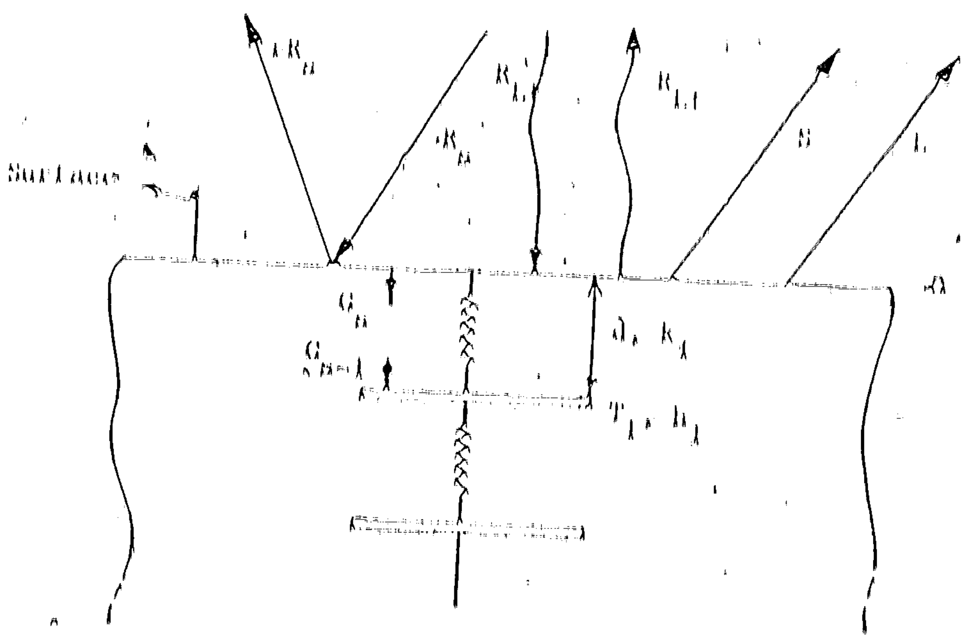

Governing Equations

$$G_s = (1 - r) R_s + R_{li} - R_{lo} \ldots \qquad (4.27)$$

$$G_{s,1} = G_s$$

$$T_s = T_1 + d_1 G_s / k_1$$

$$\Delta x \, dh_1/dt = G_{s,1} - G_{1,2}$$

$$\Delta x \, dh_i/dt = G_{i-1,i} - G_{i,i+1}$$

$$h = \rho c_f T \qquad T \le T_f$$

$$h = \rho c_u T + \rho L_f \qquad T > T_f$$

$$G_{i,j} = k(T_i - T_j)/\Delta x$$

where $k = k_f \qquad T \le T_f$

$= k_u \qquad T > T_f$

4.6.2 Normalization

Defining the various dimensionless variables.

Writing,

$$x_e = R_s t_e / \rho L_f \qquad \text{where } t_e = 1 \text{ year.}$$

$$\Delta T = R_s x_e / k_f$$

$$\theta = (T - T_f)/\Delta T$$

$$\phi = h/\rho L_f$$

S_1 = [illegible]

S_{u1} = [illegible]

$\zeta = x/x_c$

$t = t/t_c$

$G_n' = G_n/R_n$

$R_n' = R_n/R_n$

$R_{L,i}' = R_{L,i}/R_n$

$R_{L,l}' = R_{L,l}/R_n$

$S' = S/R_n$

$L' = L/R_n$

$k' = k/k_{u1}$

$k_r = k_{u1}/k_1$

The governing equations become

$$G_n' = (1-t)\, R_n' + R_{L,i}' - R_{L,l}' - S' - L' \qquad (4.28)$$

$$G_{n-1}' = G_n'$$

$$\theta_n = \theta_1 + (R_n d/k_1 \Delta T)\, G_n'$$

[illegible] $G'_{n} \ldots R\,T(\theta_{1} - \theta_{2})/x_{c}$

$\Delta\phi_{1} = (G' \ldots k'(\theta_{1} - \theta_{2})) \ldots /\ldots^{2}$ [illegible] $i=1$

$\Delta\phi_{i} = (k'(\theta_{i-1} - \theta_{i}) - k'(\theta_{i} - \theta_{i+1})) \ldots /\ldots^{2}$ $i/1$

$\phi = S_{1}\ \theta$ $\theta > 0$ $i=1,2,3\ldots$

$\phi = S_{u1}\ \theta + 1$ $\theta < 0$ $i=1,2,3\ldots$

$k' = k_{1}$ $\theta_{i+1} + \theta_{i} > 0$

$= 1$ $\theta_{i+1} + \theta_{i} < 0$

$R_{n}' = 1 + (\Delta R/R_{n}) \sin 2\pi(t + \phi_{R})$

$R_{L}' = \epsilon_{n}' \epsilon_{corr}\ \sigma(T_{a}+273)^{4}/R_{n}$

$R_{L}' = \epsilon_{n}\ \sigma(T_{n}+273)^{4}/R_{n}$

$H' = A(T_{n} - T_{a})/R_{n}$

$L' = B(e_{n} - e_{a})/R_{n}$

$e_{nn} = e^{23.4} e^{-5900/(T_{n}+273)}$

$$e_{sa} = e^{23.4}\, e^{-5900/(T_a+273)}$$

$$e_a = w e_{sa}$$

$$e_s = N_s e_{sa} + (1 - N_s)\, e_a$$

$$\epsilon_a = a - b e^{-c e_a}$$

$$\epsilon_{a_{corr}} = \epsilon_a (1 + f w_c^2)$$

$$A = \rho c_p D$$

$$B = 0.622\, \rho L_v D/P$$

$$D = 1 + g u^2$$

$$T_a = \bar{T}\,(1 + \Delta T/\bar{T}\, \sin 2\pi(t + \phi_T))$$

$$k = k_s \qquad t_1 < t \leq t_2$$

$$= k_w \qquad t \leq t_1,\ t_2 < t$$

$$d/k = d_s/k_s \qquad t_1 < t \leq t_2$$

$$= d_w/k_w \qquad t \leq t_1,\ t_2 < t$$

Rewriting the governing equations in the normalized form

$$R_n' = 1 + \Delta R/R_n \sin 2\pi(t+t_R) \qquad (4.29)$$

$$R_{Li}' = \epsilon_a \epsilon_{a\,corr}\, \sigma (T_a+273)^4/R_n \qquad (4.30)$$

$$R_{Lo}' = \epsilon_n\, \sigma (T_n+273)^4/R_n \qquad (4.31)$$

$$S' = A(T_n - T_a)/R_n \qquad (4.32)$$

$$L' = B(e_n - e_a)/R_n \qquad (4.33)$$

$$G_n' = (1-r)\,R_n' + R_{Li}' - R_{Lo}' - S' - L' \qquad (4.34)$$

$$\theta_n = \theta_1 + (R_n d/k_1 \Delta T)\, G_n' \qquad (4.35)$$

$$\Delta\phi_i^m = [G_n' \Delta z - (\theta_1 - \theta_2)]\, \Delta t\, 2/\Delta z^2 \qquad i = 1 \qquad (4.36)$$

$$\Delta\phi_i^m = [(\theta_{i-1} - \theta_i) + (\theta_{i+1} - \theta_i)]\, \Delta t/\Delta z^2 \qquad i \neq 1 \qquad (4.37)$$

$$\phi_i^{m+1} = \phi_i^m + \Delta\phi_i^m \qquad (4.38)$$

$$\left.\begin{array}{ll} \theta_i^{m+1} = \phi_i^{m+1}/s_i & \phi_i < 0 \\ \theta_i^{m+1} = (\phi_i^{m+1} - 1)/s_{ui} & \phi_i > 0 \end{array}\right\} \qquad (4.39)$$

4.6.3 Method of Solution

(a) Initially, set all the ground temperatures equal to an approximate initial temperature, θI (ie. $\theta_n = \theta I$).
The initial enthalpies are then calculated.

$$\phi_n = S_{uf}\,\theta_n + L \qquad \text{if } \theta_n > 0$$

$$= S_f\,\theta_n \qquad \text{if } \theta_n < 0$$

(b) Using equations (4.29) and (4.30) to compute R_s' and $R_{L\downarrow}'$ respectively.

$$R_s' = 1 + \Delta R/\bar{R}_s \sin 2\pi(t + \phi_R) \tag{4.29}$$

$$R_{L\downarrow}' = \epsilon_a' \epsilon_{a(corr)}\, \sigma (T_a + 273)^4/\bar{R}_s \tag{4.30}$$

(c) To solve for T_s

In equation (4.34), only $R_{L\uparrow}'$, S' and L' are functions of T_s. On substituting these expressions into equation (4.34), the resulting expression is

$$G_s' = (1-r)\,R_s' + R_{L\downarrow}' - (\epsilon_s \sigma/\bar{R}_s)(T_s + 273)^4 -$$

$$(A/\bar{R}_s)(T_s - T_a) - (B/\bar{R}_s)(M_s\, e^{23.4})(e^{-5900/(T_s+273)} -$$

$$W e^{-5900/(T_a+273)})$$

Then substitute G_s' into equation (4.35)

$$\theta_s = \theta_1 + (R_s d/k_1 \Delta T)\, G_s' \qquad (4.35)$$

and writing $\theta_s = (T_s - T_F)/\Delta T$, equation (4.35) becomes

$$Y = A_0 - A_1 Y^4 - A_2\, e^{-5900/Y} \qquad (4.40)$$

where $Y = T_s + 273$ and A_0, A_1, A_2 are known constants.

$$A_0 = [(1-r)\, R_s + \epsilon_s \epsilon_{a\,corr}\, \sigma(T_a + 273)^4 + \rho c_p D(T_a + 273)$$

$$+ (\Delta T\, (\theta_1 + 273))/d/k_1 + BM_s e_a \;/ (\rho c_p DH/d/k_1)$$

$$A_1 = \epsilon_s \sigma/(\rho c_p DH/d/k_1)$$

$$A_2 = BM_s e^{23.4}/(\rho c_p DH/d/k_1)$$

$$f(Y) = Y - A_0 + A_1 Y^4 + A_2\, e^{-5900/Y} \qquad (4.41)$$

$$f'(Y) = 1.0 + 4A_1 Y^3 + 5900 A_2/Y^2\, e^{-5900/Y} \qquad (4.42)$$

Equation (4.40) is solved by first approximating a root, then by means of successive approximations from the interation

$$Y_{i+1} = Y_i - f(Y)/f'(Y) \qquad (4.43)$$

$$T_s = Y - 273$$

(d) With the above T_n, values for $R_{L\uparrow}'$, S' and L' are obtained from equations (4.31), (4.32) and (4.33) respectively.

$$R_{L\uparrow}' = \epsilon_n \sigma (T_n + 273)^4 / R_n \qquad (4.31)$$

$$S' = A(T_n - T_a)/R_n \qquad (4.32)$$

$$L' = B(e_n - e_a)/R_n \qquad (4.33)$$

(e) Then compute G_n' using equation (4.34)

$$G_n' = (1-r)\, R_n' + R_{L\downarrow}' - R_{L\uparrow}' - S' - L' \qquad (4.34)$$

(f) Compute the enthalpy changes at each nodal point, using equation (4.36) for the top layer and equation (4.37) for all the remaining layers.

$$\Delta\phi_i^m = [G_n'\Delta z - (\theta_1 - \theta_2)]\, \Delta t \times 2/\Delta z^2 \qquad i=1 \qquad (4.36)$$

$$\Delta\phi_i^m = [(\theta_{i-1} - \theta_i) + (\theta_{i+1} - \theta_i)]\, \Delta t/\Delta z^2 \qquad i \neq 1 \qquad (4.37)$$

Then using enthalpies from the last time step and plus these enthalpy changes, new values of enthalpies at each nodal point are calculated by using equation (4.38).

$$\phi_i^{m+1} = \phi_i^m + \Delta\phi_i^m \qquad i=1,2,3\ldots \qquad (4.38)$$

(g) The enthalpy ϕ_i^{m+1} is then used to calculated θ_i^{m+1} by using equation (4.39)

$$\theta_i^{m+1} = \phi_i^{m+1}/S_l \qquad \phi_i < 0$$

$$= (\phi_i^{m+1} - 1)/S_u \qquad \phi_i > 0 \tag{4.39}$$

ϕ_i^{m+1} and θ_i^{m+1} are the new enthalpies and temperatures one time step ahead of ϕ_i^{m} and θ_i^{m} respectively.

(h) Proceed as before, as the time step advances, the initial enthalpies and temperatures are those just computer, ϕ_i^{m+1} and θ_i^{m+1} respectively. The computation is over when the temperature distribution for an entire year approaches a steady state.

4.7 Results of the Numerical Calculations

As stated in Part II of this thesis only the steady periodic solution will be of interest, the transient behavior produced by starting from a constant temperature will not be considered. Usually it was necess ary to carry out the calculations through only five yearly cycles of temperature variation in order to obtain the steady periodic condition (refer to Part II).

4.7.1 Heat Fluxes

Figure (30) shows the values of the various Heat Fluxes and also the Net Heat Flux to the ground surface during the fourth to the fifth year. As indicated, all the heat fluxes peak at about the same

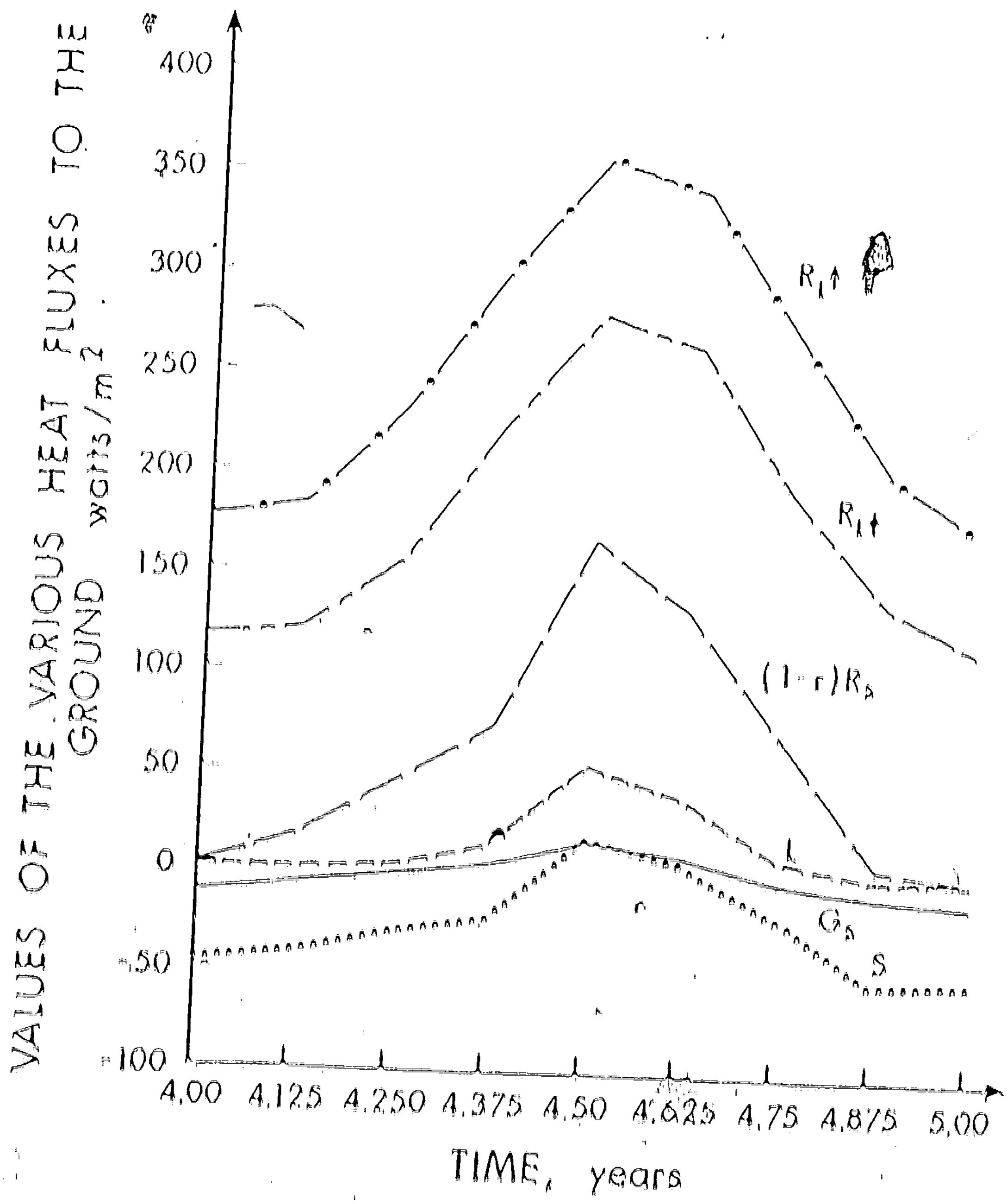

FIGURE 30 : Values of the various heat fluxes to the ground

time of the year, that is, when the air and surface temperatures are maximum and correspondingly as the air and surface temperatures are minimum. The net incoming Solar Radiation $(1-r)\cdot R_s$, which is not directly temperature dependent, however peaks during the summer months and has a minimum value during the winter. All the component heat fluxes have positive values, that is they are in the direction defined as Figure (29), throughout the entire year except for the Sensible Heat Flux, which varies from a minimum negative value to a maximum positive value. This is because during the winter, the surface temperature T_s is lower than the air temperature T_a and in summer, T_s is greater than T_a. The empirical equation for S is

$$S = \rho c_p D(T_s - T_a),$$

as such S is negative in winter and positive in summer.

The net heat flux to the ground G_s also varies from a minimum of -12 watts/m^2 to a maximum of 15 watts/m^2. The empirical expression for G_s is

$$G_s = (1-r)\, R_s + R_{L\downarrow} - R_{L\uparrow} - S - L.$$

The negative values of G_s during the winter months indicate that heat is given off by the ground during the winter, and similarly positive values of G_s indicate that heat is absorbed.

TABLE 9. Comparing the Various Heat Fluxes from Various Sources for Norman Wells (65°N)

Data Source	Net Radiation R_{net} watts/m²	Latent Heat L watts/m²	Sensible Heat S watts/m²
1. Sellers (41)			
Mean values for 60-70°N	26.0	18.2	7.8
2. Hare (52)	22.1	-	-
3. Standard Data Set	6.9	15.4	-22.4
4. Modified Standard Data Set	22.7	20.1	2.6

As indicate[illegible] 9 the values of the various heat fluxes depends very much on [illegible]uon of the input parameters. The values from Modified Stand[illegible]ata Set agree favourably to those obtained from Sellers, wherea[illegible] those values from the Standard Set are significantly different. The [illegible]odified set are just the values of the standard set with some varia[illegible]ons in some of the controlling parameters such as T_a, R_a, ΔR_a, ϵ_a, Spring, Fall, d_s and d_w. The variations are however within the range of variations of each of the individual parameter.

4.7.2 Temperatures Distributions

Figure (31) shows the values of the various temperatures, namely, T_a (air temperature), T_s (surface temperature), T_{gl} (ground surface temperature) and T_{gm} (temperature at below the active layer) during the fourth to fifth years. The graph [illegible]ows that in winter the

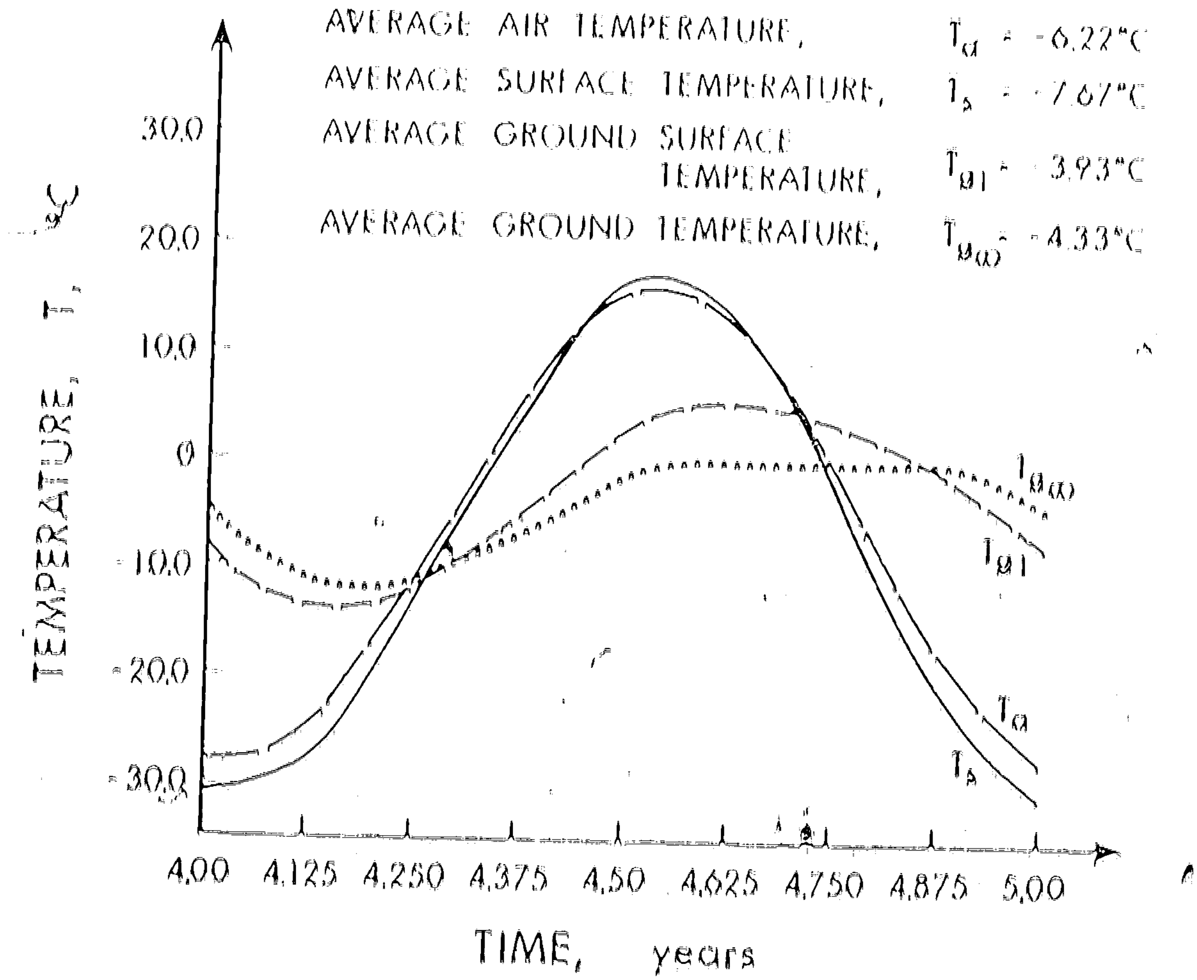

FIGURE 31 Profiles of temperature distributions with varying heat fluxes at the surface. $\bar{U}$ = 0.76 watts/m^2 - °K, $(U_A - U_W)/\bar{U}$ = 1.0 and ϕ_M' = 0.0

temperature deep in the ground $T_{g\infty}$ is warmer than the ground surface temperature T_{gl} which in turn is warmer than the surface temperature T_s. The air temperature T_a is cooler than the ground surface temperature T_{gl} but is warmer than surface temperature T_s. During the summer months the reverse is true, that is $T_{g\infty}$ is cooler than T_{gl} which in turn is cooler than T_s. The air temperature T_a is warmer than T_{gl} but is cooler than T_s. It also will be noted that the averages of these temperatures over the year are not the same. The differences in the average temperatures between the various levels is due to non-linearities in the equations.

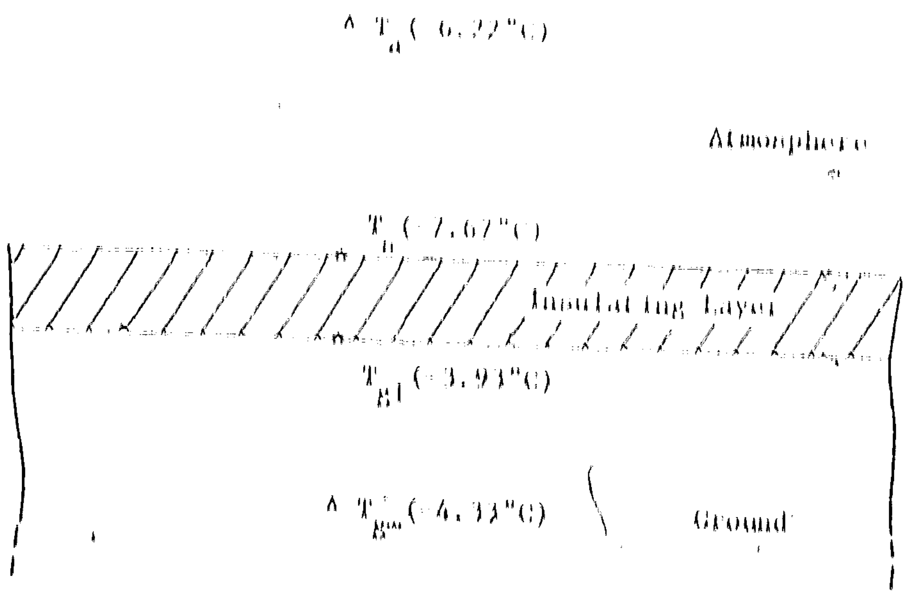

FIGURE 32

The difference in $(T_{gl}-T_{g\infty})$ was studied in Part II and the difference in (T_s-T_{gl}) in Part III. The difference in T_a-T_s arises in this section because of the non-linear nature of the heat flux equations. As indicated in Figure (32), the average temperatures are $T_a = -6.22°C$,

T_s – 7.67°C, T_{gl} – 3.93°C and $T_{g\infty}$ – 5.11°C. Note that $(T_s - T_{gl})$ is by far the largest of these differences indicating the importance of the insulating layer in the determination of the net difference between the ground temperature and the air temperature. Measured values obtained by Brown (29) for the difference between the average air temperature T_a and the average ground temperature $T_{g\infty}$ (50 to 100 feet deep) varies from 2.7 to 4.5°C (or 5 to 8°F). However in one of his other papers Brown (50) obtained another set of values of $T_a - T_{g\infty}$ (12" deep) for Norman Wells which ranges from 0.7 to 11°C. The measurements were made under different conditions at different sites. The computed values for $(T_a - T_{g\infty})$ is 1.9°C. These large variations in the value of $(T_a - T_{g\infty})$ are mainly due to large number of varying influential parameters which the value of $(T_a - T_{g\infty})$ are dependent on. Factors that are particularly influential are net radiation, vegetation, snow cover and ground thermal properties.

4.7.3 Depth of Thaw Penetration

The depth of thaw penetration in Norman Wells is about 0.625 m (approximately 2 feet), as indicated in Figure (33). The result compares favorably with those obtained by Gold (33).

4.7.4 Average Influence Coefficients

Earlier in section (4.5.3) the analytical model for finding the average influence coefficients was developed by assuming that there was no interaction between the ground and the surface heat fluxes. The values for the standard data set were presented in Table 8.

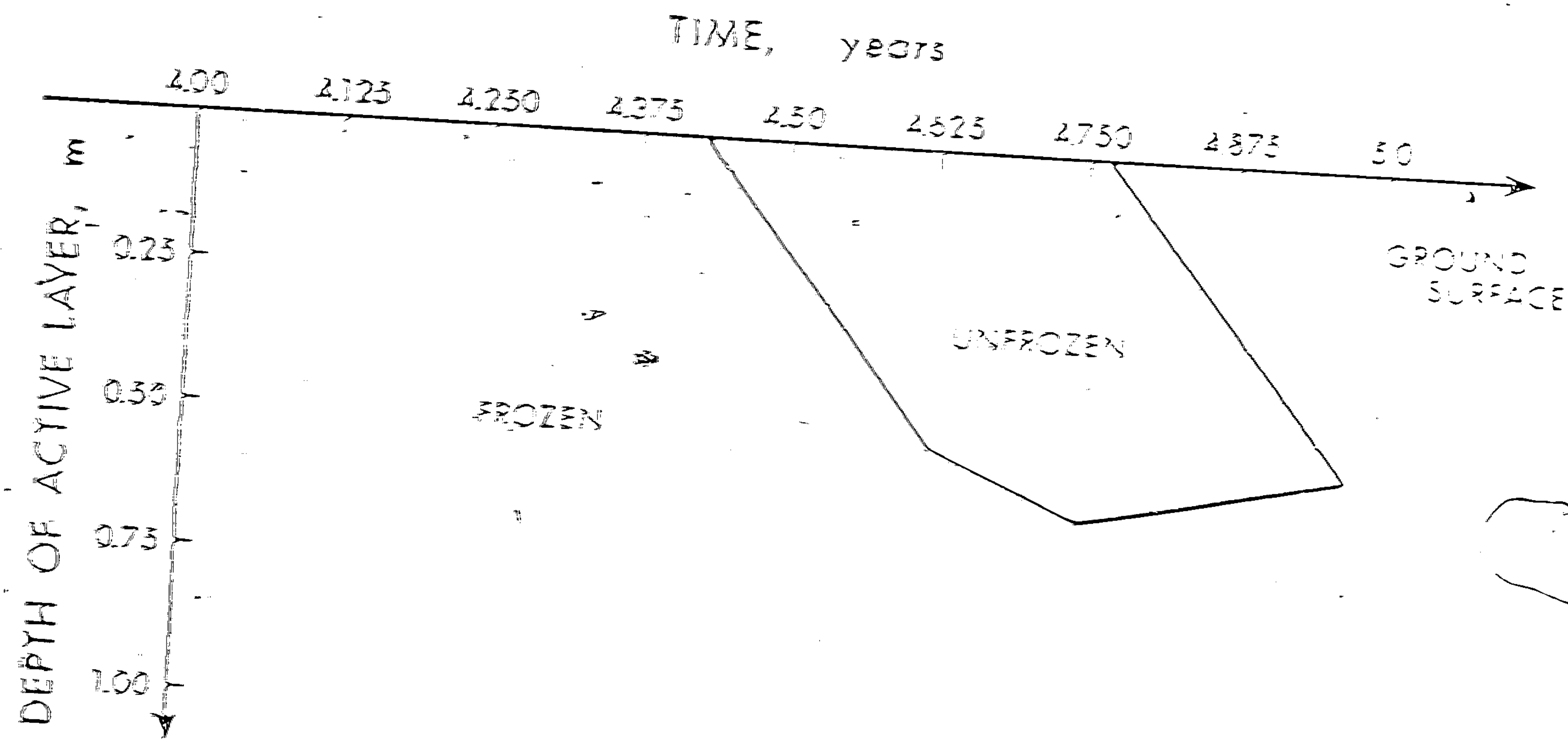

FIGURE 33 – Depth of thaw penetration at Norman Wells with varying heat fluxes at the surface

In this section the values of the average influence coefficients are obtained numerically and the interactions between the ground and the surface fluxes are taken into account. The values are obtained by varying a single parameter at a time and then divide the change in the average surface temperatures (T_s) and the change in the average ground temperatures (T_{gs}) by the change in the varying parameter. The range of variation for each individual parameter is a carefully chosen range within the realistic climatic conditions of the location under study.

The values of the average influence coefficient for the standard data set are presented in Table 10. The table also shows that the set of values obtained analytically compares favourably with those obtained numerically. From these coefficients and an estimate of the possible range of each parameter (column 5) the magnitude of its effect on the ground temperature can be estimated (column 6). The order of importance of a parameter in determining the difference between T_{gs} and T_s or $(T_{gs}-T_s)$ for a given T_a will be indicated by the magnitude of ΔT_{gs} in column 6 of Table (10). That is to say the parameter inducing the largest ΔT_{gs} will be the most important and so on in descending order. The order of importance are $(\Delta U_w)/U_w$, $(\Delta U_s)/U_s$, M_{so}, $(\Delta V)/V$ and $(\Delta R_s)/R_s$ and is in rough agreement with the field observations summarized by Brown (53).

The range of T_{gs} possible for one air temperature is 16.77°C (sum of ΔT_{gs} in column 6). The range of (T_a-T_{gs})(12 inches deep) for Norman Wells obtained by Brown (50) is from 0.7 to 11°C. This can explain the occurrence of isolated pockets of permafrost in regions as far south

TABLE 10: Numerical Values of the Average Influence Coefficients

Input Parameters (1)	Average Influence Coefficients $\hat{T}_a$ (Analytical) (2)	T_a (3)	$T_{g''}$ (4)	Range of Input (5)	$\Delta T_{g''}$ (6)
$(\Delta R_n)/R_n$	0.024	0.025	0.030	40%	1.20
$\Delta(t_a)$	0.051	0.022	0.033	20	0.66
$\Delta(t_w)$		0.020	0.015	20	0.30
$\Delta(e_a)$	-0.047	-0.038	0.040	10	0.40
$\Delta(K_H)$	0.018	0.027	0.033	30	0.99
*$\Delta(M_a)$	-0.018	0.018	-0.024	20	0.48
$\Delta(w_c)$	-0.027	0.019	0.021	20	0.42
$(\Delta V)/V$	-0.028	-0.024	-0.042	30	1.26
$\Delta(\Delta U_a/U_a)$	--	0.0	0.036	100	3.60
$\Delta(\Delta U_w)/U_w$	--	0.0	-0.056	100	5.60
$(\Delta \dot{T}_a)$	(0.819)	(0.958)	(1.089)	(1.0°C)	3.27
$\Delta(\gamma_{soil})^{(1)}$	--	0.0	-0.020	30	0.60
*$\Delta(M_{so})^{(2)}$	--	0.0	0.042	30	1.26

(1) γ_{soil} = density of soil

(2) M_{so} = soil moisture

* non-linear

as Edmonton and isolated pockets of thawed soil as far north as Fort McPherson (67°N).

Most influence coefficients were found to be constant within 20% over the range of the input parameters. Typical results for the non-linear cases are shown in Figure (34) and Figure (35). The application of these influence coefficients will be discussed later in section (4.7.7).

4.7.5 Effective 'heat transfer coefficient'

In section 4.5.2 the analytical value for the effective 'heat transfer coefficient' was determined by differentiating equation (4.42) with respect to the T_s to give equation (4.23).

$$h_{eff} = \partial F/\partial T_s \Big|_{T_s^\wedge} \qquad (4.23)$$

The value of h_{eff} was then determined by assuming the nominal value of T_s to be $T_s^\wedge$, the value which gives $F = 0$.

In the numerical model, the effective 'heat transfer coefficient' h_{eff} is determined by dividing the change in the heat flux to the ground Q_s by the corresponding change in the average surface temperature T_s. These changes can be brought about by gradually increasing the heat flux from deep in the ground.

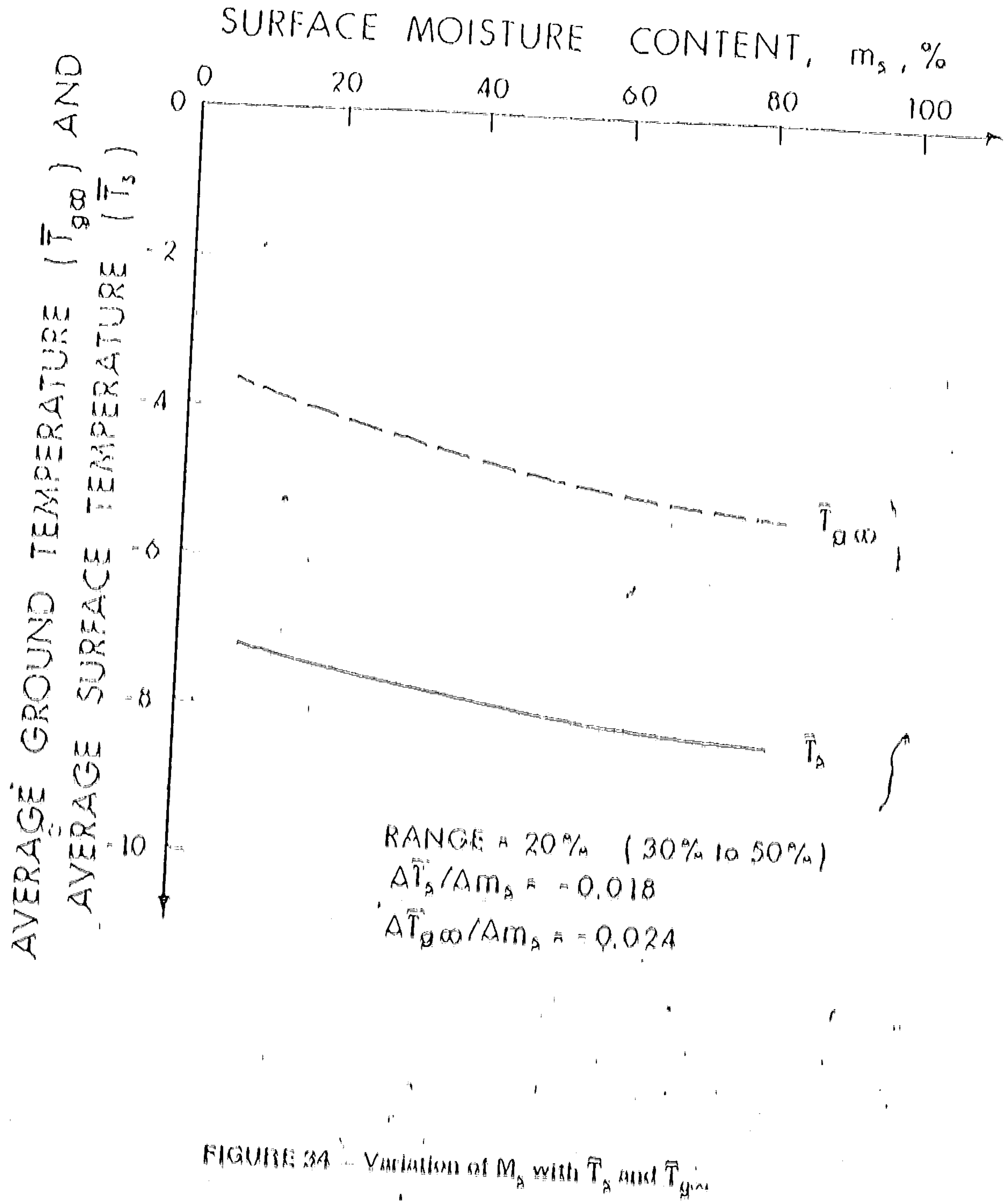

FIGURE 34 – Variation of M_s with $\bar{T}_s$ and $\bar{T}_{g\infty}$

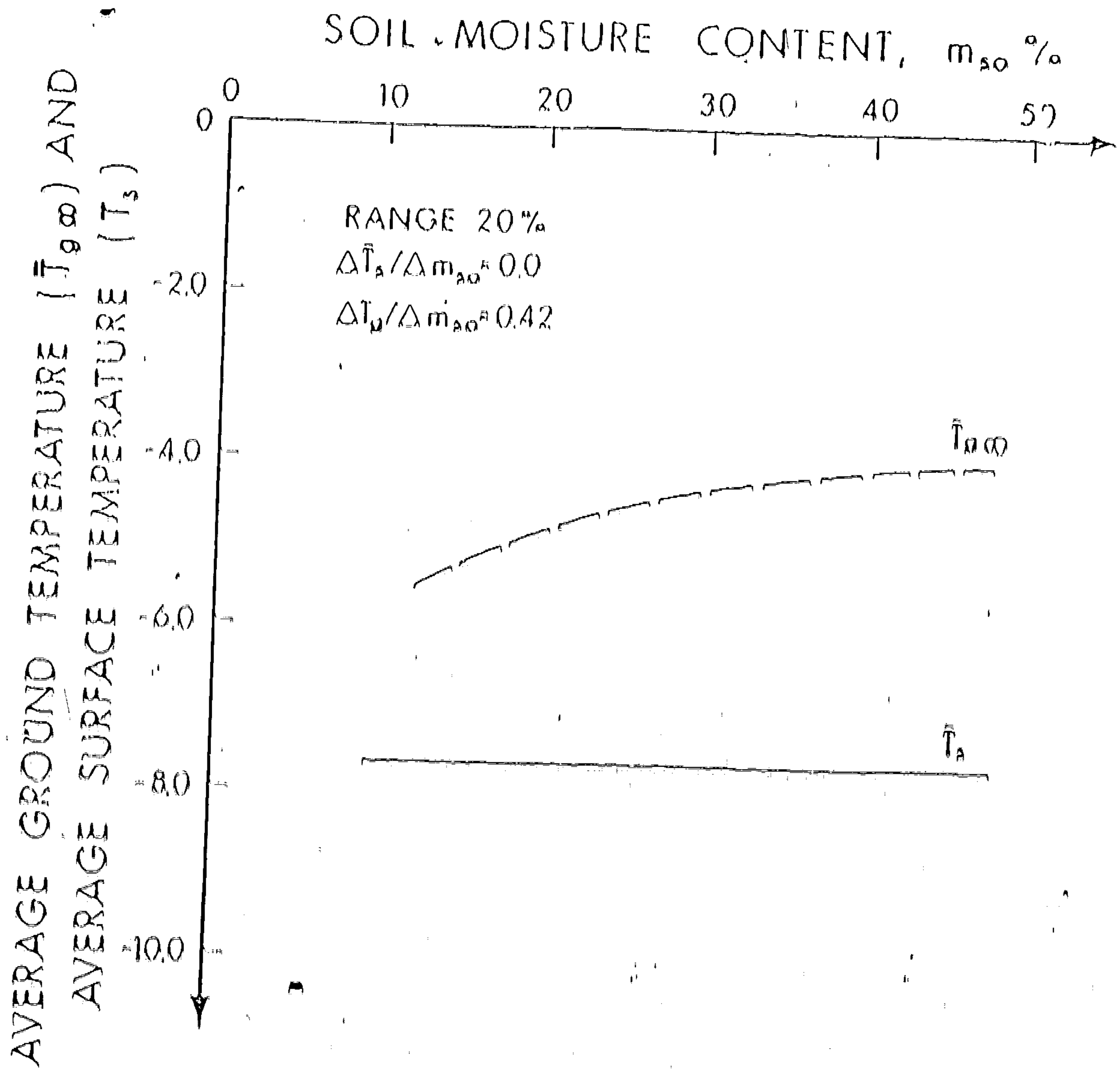

FIGURE 35 – Variation of M_{so} with $\bar{T}_A$ and $\bar{T}_{g\infty}$

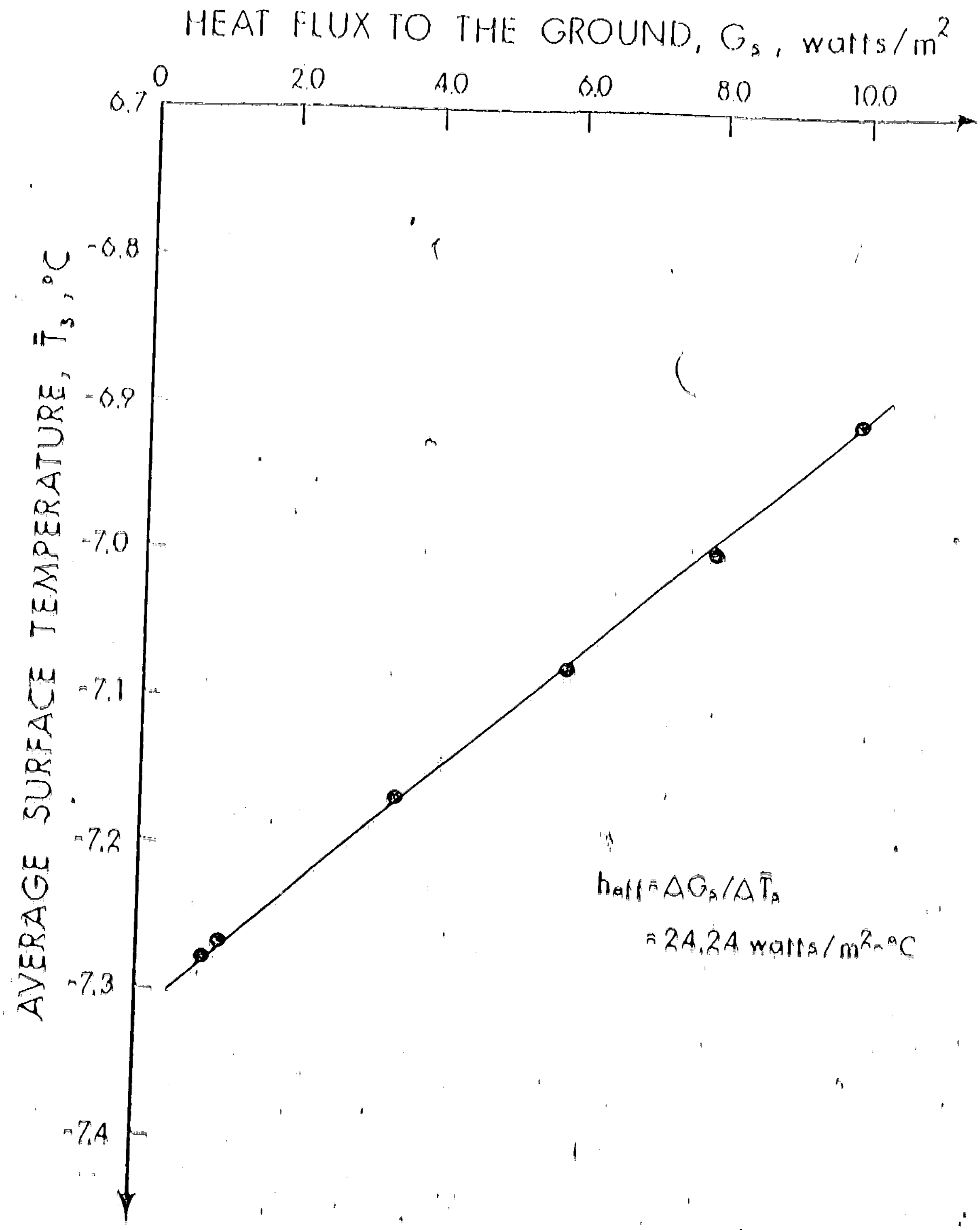

FIGURE 36 – Relationship between the heat fluxes to the ground and the average surface temperature

Empirically the model can be written as

$$G_s = h_{eff} \, (T_s - \hat{T}_s) \tag{4.44}$$

$$\partial G_s / \partial T_s = h_{eff}$$

$$\therefore h_{eff} = \Delta G_s / \Delta T_s$$

From Figure (36) the value of h_{eff} obtained by this numerical method is 24.24 watts/m^2-°C, which is slightly higher than the value of h_{eff} (22.51 watts/m^2 °C) obtained analytically. However both the values are well within the range of 19.39 to 29.09 watts/m^2-°K obtained by Williams (51) for latitude 40° to 60°N. This also indicates that the analytical method used is good for a rough approximation, provide the nominal value of T_s is nearly equal to $\hat{T}_s$.

4.7.6 Coupling between Air and Ground Temperatures

Figure (37) shows the various temperatures at the various time intervals during the fourth year. Unlike the case in Figure (31) where the average U-factor $\bar{U}$ was 0.76, the $\bar{U}$ in this case is relatively large, about 6.0. Comparing the two graphs show that except for the ground surface temperature T_{g1}, all the other temperatures namely, air temperature T_a, surface temperature T_s and ground temperature T_{gm}, exhibits the same behaviors. T_{g1} for this case closely follows T_a whereas in Figure (31), $\hat{T}_{g1}$ closely follows T_{gm}. This means that for $\bar{U} = 0.76$ the major thermal resistance between the air and the ground is the insulating cover and for $\bar{U} = 6.0$ the major resistance is provided

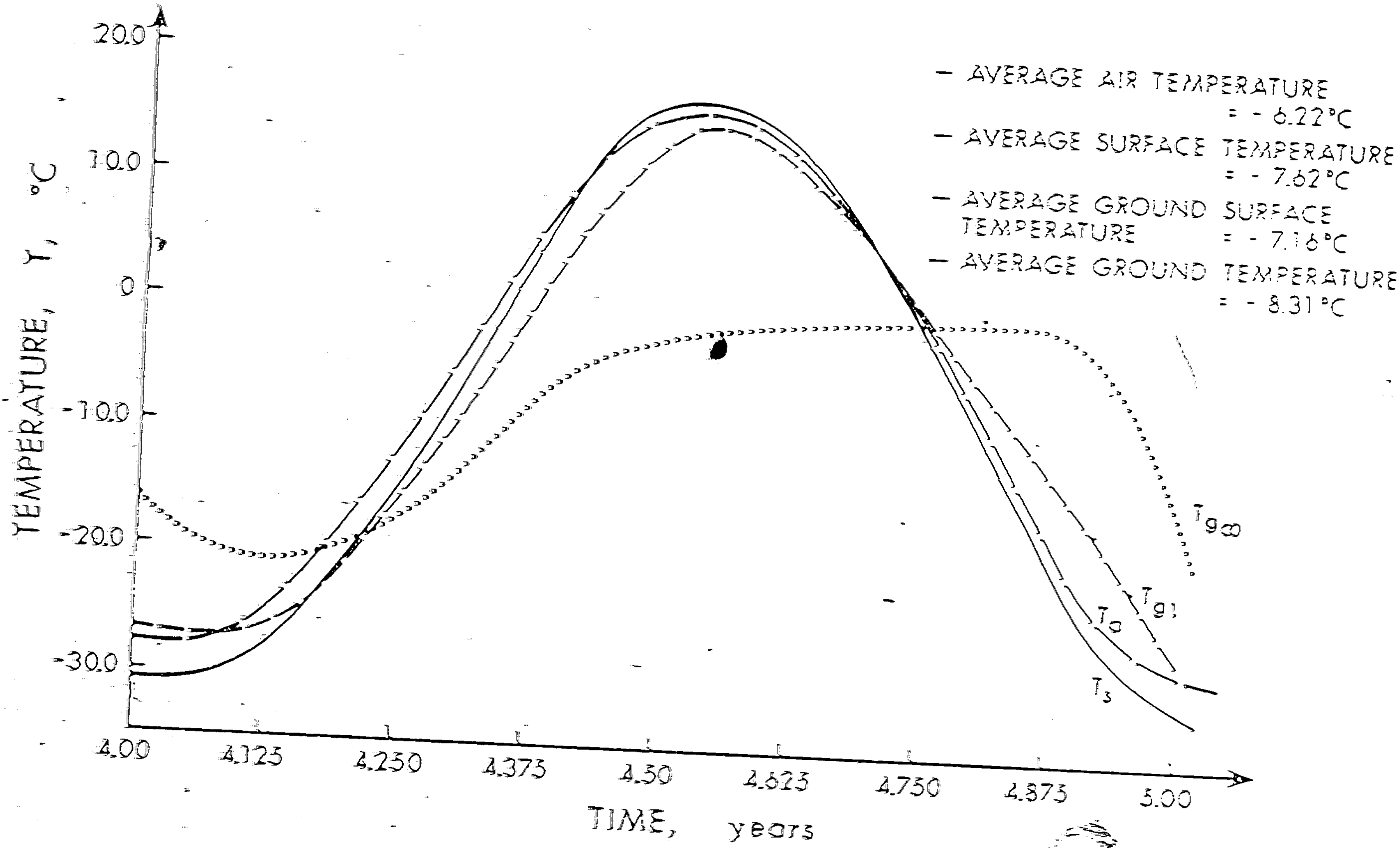

FIGURE 37 — Profiles of temperature distributions with varying heat fluxes at the surface. $\overline{U}$ = 6.0 watts/m² — °K, ($U_s - U_{sy}$)/$\overline{U}$ = 1.0 and [illegible] = 0.0

by the ground itself. The average surface temperature T_s remains unaffected by the change in U, however the average ground temperatures above and below the active layer, T_{gl} and $T_{g\infty}$ become colder, from -3.9°C and 4.33°C to -7.16°C and 8.31°C respectively.

Figure (38) shows more clearly the effect U has on the average temperatures of the surface and the ground. For small U-factor, thus high thermal resistance between the surface and the ground, the two ground temperatures T_{gl} and $T_{g\infty}$ are almost the same. This occurs because the amplitude of variation in temperature T_{gl} is small and thus no difference between T_{gl} and $T_{g\infty}$ can be created by the mechanisms discussed in Part II. In this case the ground temperature will be determined by the characteristics of the surface cover and the climate parameters and will be unaffected by the soil type or the moisture content. Also note that the average ground temperature is higher than the average air temperature in this situation. This is because of the differential heat valve effect of the insulating layer, as discussed in Part III. As U increases, that is as the insulating properties of the ground cover become poorer, the ground temperatures decrease and the difference between T_{gl} and $T_{g\infty}$ increases. Two factors cause this phenomenon. First, as U increases, the effectiveness of the insulating layer as a differential heat valve decreases. Thus the temperature difference $(T_s - T_{gl})$ decreases resulting in the lowering of the ground temperature. Secondly, as the U-factor increases, the amplitude of the temperature variation in T_{gl} will increase. This increases the effectiveness of the heat valve effect caused by freezing and thawing of the soil and generates the difference between T_{gl} and $T_{g\infty}$.

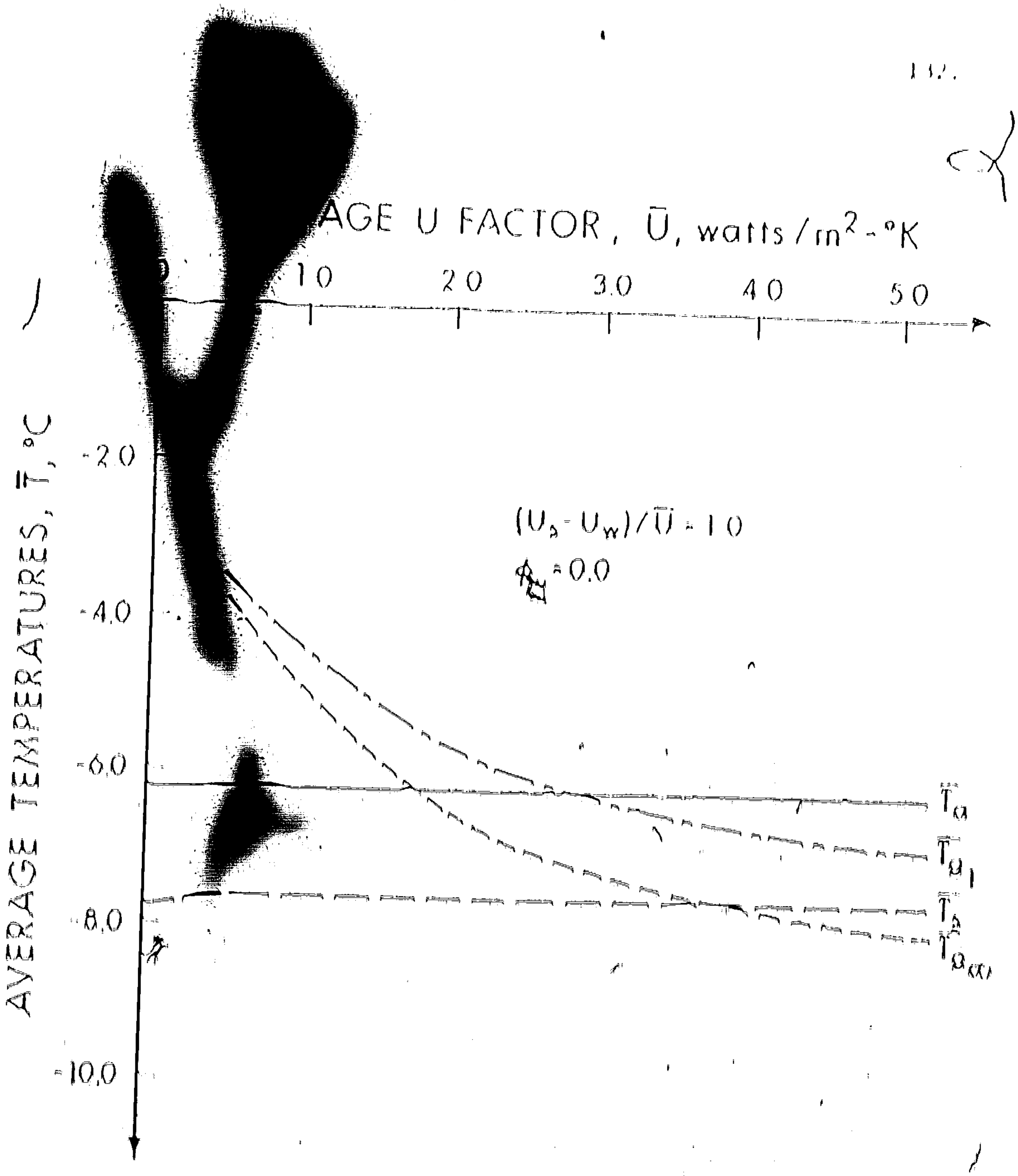

FIGURE 38 — Variation of Ū with T̄

An average U factor of six corresponds roughly to a surface with compacted snow, 10 cm deep in winter and a 5 cm of vegetation in the summer (Appendix III). For surfaces with less insulating value than this, the effects of the insulating cover on the average ground temperature will become negligible. In that case the ground temperature will be controlled by the soil properties and the climatic conditions.

Figure (39) shows the relationship between $(U_s - U_w)/U$ and the various average temperatures for a given U. The figure shows that the average surface temperature T_s is independent of $(U_s - U_w)/U$ but the average ground temperatures T_{g1} and $T_{g\infty}$ increase very significantly as $(U_s - U_w)/U$ increases. The difference between T_s and $T_{g\infty}$ is 4°C for $(U_s - U_w)/U = 1.0$. This indicates that variations in the U-factor of the surface cover are the major cause of difference between the average air and ground temperatures.

It will be noted from Figure (38) that the average surface temperature is relatively insensitive to the U-factor of the insulating layer. This implies that the surface temperature is controlled by the balance of the heat fluxes that occur to and from the air and that the heat flux to and from the ground is too small to have a major effect. This is basically the assumption used in deriving the analytic approximation in section (4.5.2). As stated in that section the requirement for application of that assumption is that $U \ll h_{eff}$. The value of U used is 6.0 watts/m^2-°K and the calculated value for h_{eff} is 24.24 watts/m^2-°K. Listed in Table 11 are the values of T_s and T_s^A for an entire year.

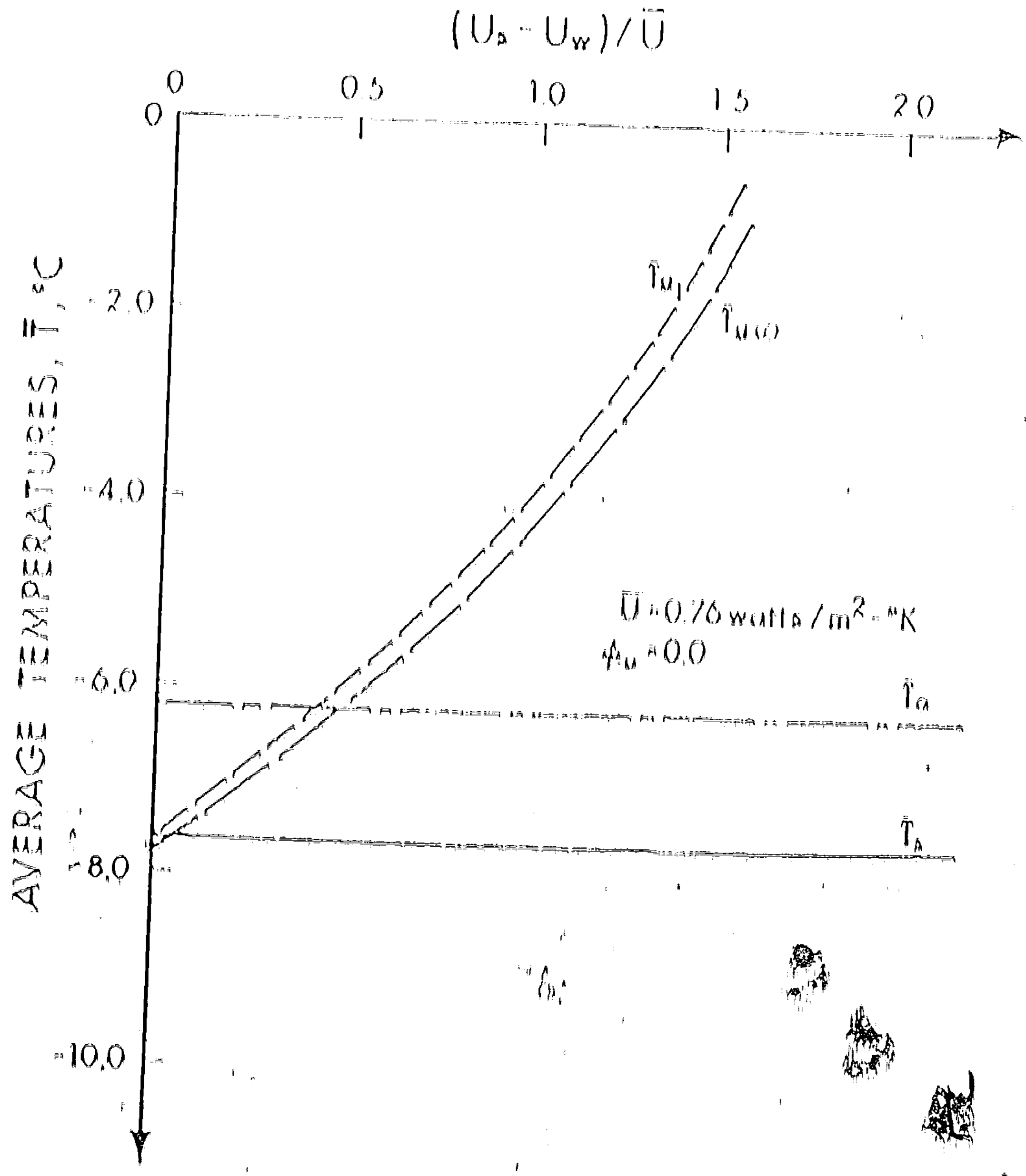

FIGURE 39 Variation of $(U_s - U_w)/\bar{U}$ with $\bar{T}$

TABLE 11. Value of T_s and T_s^ for the Standard Data Set

Time (Year)	T_s^ from Section (4.5.2)	T_s $U = 0.76$ $(U_s - U_w)/U = 1.0$	T_s $U = 6.0$ $(U_s - U_w)/U = 1.0$
0.000	31.37	30.82	30.51
0.125	28.22	27.89	27.88
0.250	13.74	13.73	-14.01
0.375	3.74	3.56	3.21
0.500	16.97	16.42	16.11
0.625	13.58	13.23	13.15
0.750	2.03	1.93	1.50
0.875	-21.31	-20.85	-19.96
1.000	31.37	30.81	30.51

Comparing T_s to T_s^ in Table 11 shows that the difference between the two is very small, even when $U = 6.0$. It also indicates that for problems with small heat fluxes to the ground, the problem of determining the surface balance becomes uncoupled from the problem of heat flow in the ground. Under these conditions, it may also be concluded that it is adequate to assume $T_s = T_a$ for most cases, however a better estimate would be $T_s = T_s$^. This is because by assuming $T_s = T_s$^ the effects of the heat fluxes are taken into account.

Even if U for surface cover is greater than h_{eff}, T_s may still be close to T_s^ because of the insulating value of the ground itself. A general test of the applicability of the approximation

$T_s - T_s^*$ is given by the equation,

$$T_s - T_s^* = q/h_{eff}$$

where q is the instantaneous value of the heat flux to the ground. If the maximum value of the heat flux q is less than 24 watts/m^2, the maximum difference of $(T_s - T_s^*)$ will be less than 1°C.

4.7.7 Applications of the Influence Coefficient

As indicated in table 10 the influence coefficients are relatively constant over the ranges indicated. Because they are uncoupled, the influence coefficients can be used to estimate the effects of the disturbances which simultaneously effect more than one parameter such as disturbances to the surface cover.

As an illustration of the application of the influence coefficients, the effects will be calculated for a disturbance to the surface cover which causes the following changes in the parameters:

a_s changes from 16% to 8%

ϵ changes from 90% to 97%

U_s changes from 1.2 to 2.4 (watts/m^2 °K)

and M_s changes from 30% to 80%

Keeping all other parameters constant, the values predicted for the changes in $\bar{T}_s$ and T_{gw} using the influence coefficients will be compared to the values obtained numerically. The changes in $\bar{T}_s$ and T_{gw} caused by the change in U_s and M_s will be obtained from the graphs indicated as their relationship are nonlinear.

Changes in T_s and $T_{g''}$ caused by the change in M_s.

M_s changes from 30 to 80

From Figure (34)

$\Delta T_s = -0.7°C$

$\Delta T_{g''} = -0.9°C$

Changes in T_s and $T_{g''}$ caused by the change in U_s.

U_s changes from 1.2 to 2.4

A change in U_s will cause a change in U and $(U_s - U_W)/U$. The change in U is from 0.76 to 1.25.

From Figure (38)

$\Delta T_s = 0$

$\Delta T_{g''} = -1.1°C$

The change in $(U_s - U_W)/U$ is from 1.0 to 1.56.

From Figure (39)

$\Delta T_s = 0$

$\Delta T_{g''} = +3.1°C$

TABLE 12. Changes in T_s and $T_{g''}$

Parameters	Original Values	New Values	Δ	ΔT_s	$\Delta T_{g''}$
t	90	97	+7	-0.2	-0.2
F_s	16	8	-8	+0.2	+0.3
U_s	1.2	2.4	ΔU	0.0	-1.1
			$\Delta(U_s - U_W)/U$	0.0	+3.1
M_s	30	80	50	-0.7	-0.9
			TOTAL	-0.7	+1.2

TABLE 13. Values of Computed T_s and $T_{g\infty}$

	Original Values (°C)	New Values (°C)	
		Numerically Computed	Computed by Using Influence Coeff.
T_s	7.7	8.4	~8.4
$T_{g\infty}$	4.4	3.5	~3.2

As indicated the values obtained for T_s and $T_{g\infty}$ by using the influence coefficients and graphs compare favourably with those actually computed.

4.8 Conclusions

The problem of periodic heat flow to the ground in a freeze-thaw is very complicated because it involves about 30 to 40 parameters. The values of the heat fluxes to and from the ground are very sensitive as demonstrated by their significant difference between the standard data set and the modified data set in Table 9. Thus the absolute determination of the ground temperature is open to doubt, however it is possible to predict the change in the ground temperature that would result from a change in any one of the controlling parameters. It is however impractical to solve the whole problem everytime there is a change in one of its parameters. A much more practical method is to make use of the influence coefficients presented in Table 10. From these coefficients and an estimate of the possible range of each parameter, the magnitude of its effect on the ground temperature can be estimated. The most important parameter is the parameter with the biggest effect. The order of importance of the parameters agrees with those obtained by Brown (53) from field observations. The most important parameter being the winter insulating layer, then follow the summer insulating layer, soil moisture content, wind velocity and so on. For instance the predicted quantitative effect of winter insulating layer on the ground temperature is +5.6°C whereas the effects caused by the winter reflectivity, r_w is +0.3°C.

Two sets of values of the influence coefficients were obtained, one was obtained by the analytical method where the heat flux to the ground was neglected while the other was obtained numerically. The values obtained analytically for most cases agree with those obtained numerically. These values of influence coefficients, as demonstrated in section (4.2.7), could be used to predict the changes in T_s and T_g, caused by simultaneous variations in some parameters.

The results suggested that various approximations to the surface boundary condition could be applied. First and the simplest would be to assume $T_s = T_a$. This is a common assumption in some calculations of thermal regime in the ground. For the standard data set used, it was found that the maximum value of $|T_s - T_a|$ was 3.4°C. The second approximation which would include the effects of radiation, sensible and latent heat fluxes would be to assume $T_s = T_s^\wedge$. $T_s^\wedge$ is the value that T_s would be if heat flow to the ground is neglected. This approximation uncouples the problem of determining the heat fluxes at the surface from that of heat flow in the ground. The sufficient criteria for using this approximation is that U-factor >> h_{eff}. The maximum value of $|T_s - \hat{T}_s|$ was less than 1°C for $U > 6.0$ watts/m^2-°K. The third approximation would be the assumption that instead of an imposed surface temperature, a Neumann boundary condition exists at the surface. That is that the surface temperature is related to the heat flow to the ground by the equation

$$q = h_{eff}(T_s - \hat{T}_s)$$

where both h_{eff} and $\hat{T}_s$ are time dependent. Both the analytical and the numerical value of the effective 'heat transfer coefficient', h_{eff} obtained agree favourably with the value obtained from field observations by Williams (51). In this approximation, the very complicated heat flux relationships at the ground surface have been simplified by a linear dependence. This last approximation would appear to have very general applicability.

BIBLIOGRAPHY

(1) Carslaw, H.S. and Jaeger, J.C., "Conduction of Heat in Solids", Clarendon Press, Oxford, London, 1959.

(2) Berggren, W.P., "Prediction of Temperature Distribution in Frozen Soil", Transactions, American Geophysical Union, Volume 24, Part 3, 1943.

(3) Stefan, J., "Über die Theorie der Eisbildung insbesondere über die Eisbildung in Polarmeere", Annalen der Physik und Chemie, Volume 42, 1891, pp. 269.

(4) Aldrich, H.P. and Paynter, H.M., "Analytical Studies of Freezing and Thawing of Soils", First Interim Report, Arctic Construction and Frost Effects Laboratory, Corps of Engineers, 1953.

(5) Moulton, L.K., "Prediction of the Depth of Frost Penetration", Report 5, Engineering Experiment Station, West Virginia University, 1969.

(6) Muehlbauer, J.C. and Sunderland, J.E., "Heat Conduction with Freezing and Thawing", Applied Mechanics Review, Volume 18, No. 12, 1965.

(7) Scott, R.F., "Heat Transfer in Soil Involving the Change in State", Geotechnique, Volume 11, 1961.

(8) Kersten, M.S., "Frost Penetration: Relationship to Air Temperatures and Other Factors", Bulletin 225, Highway Research Board, 1959.

(9) Carlson, H., "Calculation of Depth of Thaw in Frozen Ground", Special Report No. 2, Highway Research Board, 1952.

(10) Gunderson, J.R., "A Study of Heat Conduction with Phase Change", M.Sc. Thesis, University of Alberta, 1966.

(11) Lock, G.S.H., Gunderson, J.R., Quon, D. and etc., "A Study of one-dimensional Ice Formation with particular reference to Periodic Growth and Decay", Int. J. Heat Mass Transfer, Volume 12, 1969, pp. 1343-1352.

(12) Murray, W.D. and Landis, F., "Numerical and Machine Solution of Transient Heat-Conduction Problems Involving Melting and Freezing", Trans. ASME, Volume 81, 1959, pp. 106.

(13) Lachenbruch, A.H., "Some estimates of the Thermal Effects of a Heated Pipeline in Permafrost", U.S. Geol. Surv. Circ. 632, 1970.

(14) Doherty, P.C., Geological Survey Computer Contribution No. 4, "Hot Pipes", U.S. Geol. Surv., Computer Center Div., Washington, D.C., 1970.

(15) Fleming, A.K., "The Numerical Calculation of Freezing Processes", Presented at International Institute of Refrigeration Meeting, Washington, D.C., 1971.

(16) Hwang, C.T., Murray, D.W. and Brooker, E.W., "A Thermal Analysis for Structures on Permafrost", Can. Geotech. J. 9: 33-40, 1972.

(17) Charlwood, R.G. and Svec, O., "Northern Pipelines: An Application for Numerical Analysis, Part II", Symposium on applications of solid mechanics, University of Waterloo, Waterloo, Ontario 1972.

(18) Biot, M.A. and Daughaday, H., "Variational Analysis of Ablation", J. of Aerospace Sciences, Volume 29, 1962, pp. 227.

(19) Goodman, T.R., "The Heat-Balance Integral and Its Application to Problems Involving a Change of Phase", Trans. ASME, Volume 80, 1958, pp. 335.

(20) Goodman, T.R., "Application of Integral Methods to Transient Non-linear Heat Transfer", Advances in Heat Advances, Volume 1.

(21) Poots, G., "An Approximate Treatment of a Heat Conduction Problem Involving a Two-Dimensional Solidification Front", Int. J. Heat and Mass Transfer, Volume 5, 1962, pp. 339.

(22) Rubinshtein, L.I., "On Heat Conduction in a Multilayer Medium with Phase Transitions", Doklady Akademia Nauk Novaia Seriia, Volume 79, 1951, pp. 221.

(23) Weiner, J.H., "Transient Heat Conduction in Multiphase Media", Brit. J. of Applied Physics, Volume 6, 1955, pp. 361.

(24) Cochran, D.L., "Rate of Solidification, Application and Extension of Theory", Technical Report No. 24, Stanford University, Stanford, California, 1955.

(25) Otis, D.R., "Solving the Melting Problem using the Electric Analog to Heat Conduction", Heat Transfer and Fluid Mechanics Institute, Stanford University, Stanford, California, 1956.

(26) Forster, C.A., "Finite Difference Approach to some Heat Conduction Problems Involving Change of State", Report of English Electric Co., Luton, England.

(27) Tien, R.H. and Geiger, G.E., "A Heat Transfer Analysis of the Solidification of a Binary Eutectic System", J. Heat Transfer, 89, pp. 230-235, 1967.

(28) Lunardini, V.J., "The Thermal Properties of Permafrost", 23rd Canadian Geotechnical Conference, Nov. 1970, Banff, Alberta.

(29) Brown, R.J.E., "Relation between Mean Annual Air and Ground Temperatures in the Permafrost Region of Canada", Nat. Res. Coun., Canada, Div. Bldg. Res., Res. Paper No. 296, 1966.

(30) Burns, B.M., "The Climate of the Mackenzie Valley - Beaufort Sea, Volume I", Climatological Studies No. 24, 1973, Atmospheric Environmental Service - Canada.

(31) Annual Meteorological Summary for Edmonton, Alberta, 1972, Atmospheric Environmental Service - Canada.

(32) Jansson, L.E., "Ground Frost Penetration in Sweden", Nat. Res. Coun., Canada, Tech. Trans. 1532, 1972.

(33) Gold, L.W., Johnston, G.H. and Goodrich, L.E., "Thermal Effects in Permafrost", Nat. Res. Coun., Canada, Div. Bldg. Res., Tech. Paper No. 376, 1972.

(34) Wijk, W.R. Van, "Physics of Plant Environment", North Holland Publishing Company - Amsterdam, 1966.

(35) Carnahan, B., Luther, H.A. and Wilkes, J.O., "Applied Numerical Methods", John Wiley & Sons Inc., Toronto, 1969.

(36) Gold, L.W., "Influence of the Snow Cover on the Average Annual Ground Temperature at Ottawa, Canada", Nat. Res. Coun., Canada, Div. Bldg. Res., Paper No. 203.

(37) Potter, J.G., "Snow Cover", Climatological Studies, Number 3, Department of Transport, Meteorological Branch, Canada, 1965.

(38) Brown, R.J.E., "Occurrence of Permafrost in Canadian Peatlands", Nat. Res. Coun., Canada, Div. Bldg. Res., Res. Paper No. 432.

(39) MacFarlane, I.C., "Muskeg Engineering Handbook", University of Toronto Press, Toronto, 1969.

(40) Bader, H., "Review of the Properties of Snow and Ice", Corps of Engineers, U.S. Army, SIPRE Report No. 4, 1951.

(41) Mellor, M., "Properties of Snow", U.S. Army Material Command, CRREL, Hanover, New Hampshire.

(42) Gavrilova, M.K., "Radiatsionnyi klimat Arktiki (The Radiation Climate of the Arctic)", edited by M.I. Budyko, Gidrometeoizdat, 1963.

(43) Sellers, W.D., "Physical Climatology", The University of Chicago Press, Chicago, 1965.

(44) Budyko, M.I., "Teplovoi balans zemnoi poverkhnosti (Heat Balance of the Terrestrial Surface)", Gidrometeoizdat, Leningrad, 1956 - Translated by Stepanova, N.A., Office of Climatology, U.S. 1958.

(45) Geiger, R., "The Climate near the Ground", Havard University Press, Massachusetts, 1966.

(46) Hay, J.E., "Modelling the Radiation Climate of Canada", Canadian Association of Geographers Annual Conference, 1970.

(47) Matveev, L.T., "Fundamental of General Meteorology, Physics of the Atmosphere", Israel Program for Scientific Translations, Jerusalem, 1967.

(48) "Climate Normals", Volume 4, Humidity, Canada Department of Transport, Meteorological Branch, Toronto, 1968.

(49) "Climatic Normals", Volume 3, Canada Department of Transport, Meteorological Branch, Toronto, 1968.

(50) Brown, R.J.E., "Some observations of the Influence of Climatic and Terrain Features on the Permafrost at Norman Wells, N.W.T., Canada", Nat. Res. Coun., Canada, Div. Bldg. Res.

(51) Williams, G.P., "Heat Transfer Coefficients for Natural Water Surfaces", Nat. Res. Coun., Canada, Div. Bldg. Res., Res. Paper 202, 1963.

(52) Hare, F.K. and Hay, J.E., "Aspects of the Large Scale Annual Water Balance over Northern North America", Canadian Geographer, July, 1971.

(53) Brown, R.J.E., "Permafrost in Canada", University of Toronto Press, Toronto.

APPENDIX

Data used for the Air Temperatures.

Edmonton:

From Burns (30), the average air temperature and the amplitude of variation for Edmonton are:

$T_a = 2.56°C$

$\Delta T = 15.96°C$

The values for Edmonton are obtained from the Annual Meteological Summary for Edmonton (31). Adopting the same procedure, similar values were also obtained for Norman Wells and Inuvik and are those tabulated in Table 14.

TABLE 14. T_a and ΔT for Norman Wells and Inuvik

Locations	Average Temp. T_a (°C)	Amplitude of Variation ΔT(°C)
Norman Wells	-6.22	22.06
Inuvik	-9.61	22.42

The values for Norman Wells and Inuvik are from Burns (30).

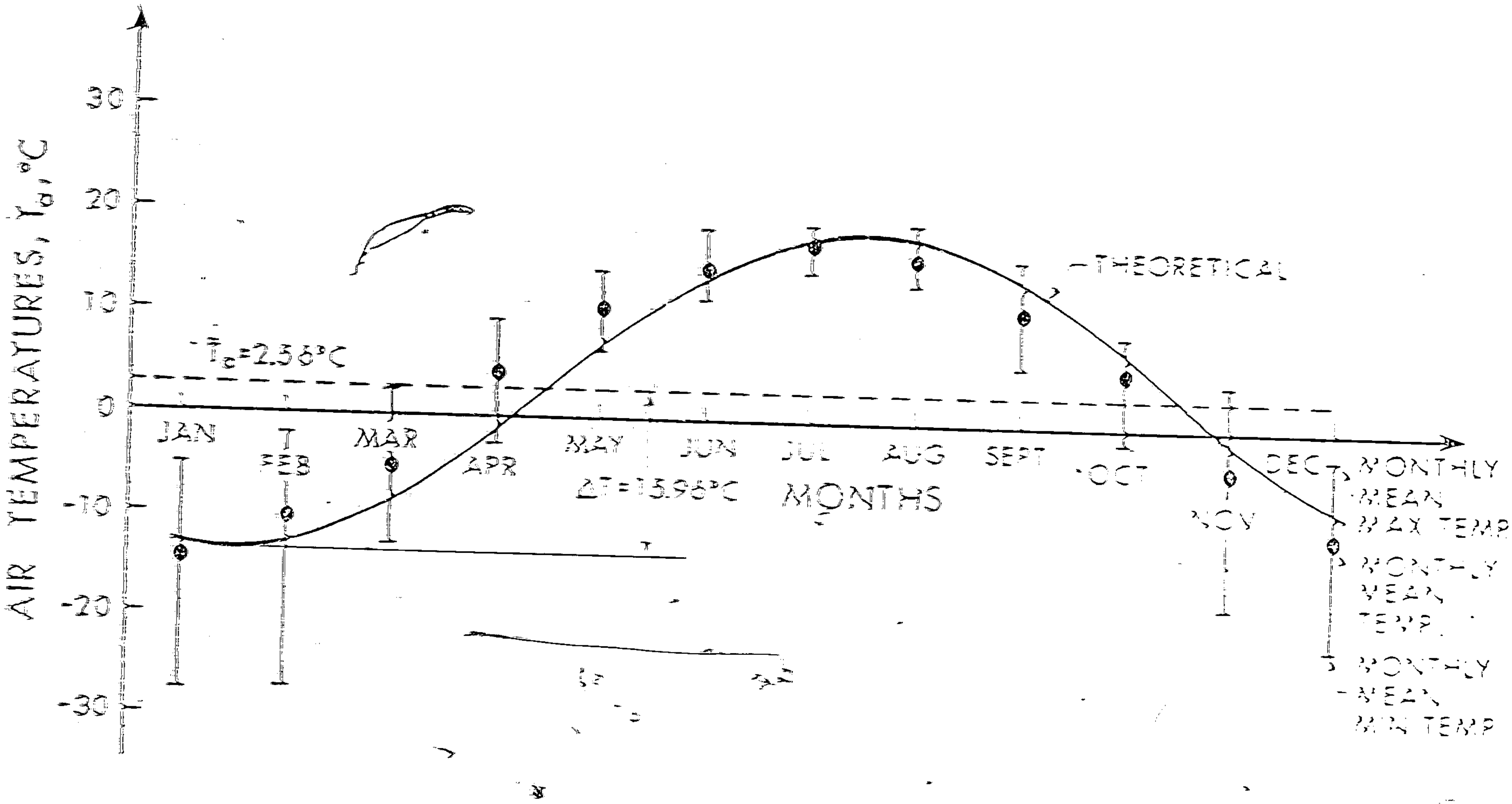

FIGURE 40 — Monthly mean temperature — Edmonton (1880 - 1972)
Source: Annual Meteological Summary for Edmonton

APPENDIX II

Soil Properties from "The Thermal Properties of Permafrost" by Virgil J. Lunardini (25).

Fine Grained Soil.

TABLE 15. Values of k_f and c_f for Frozen Soil, $T = -3.89°C$

Moisture Content, M_{wo} (% of dry wt.)	Thermal Conductivity, k_f (watts/m °K)	Heat Capacity, c_f (Joules/m^3 °K)
15	0.82	1.2×10^6
30	1.70	1.6×10^6
45	2.20	1.9×10^6

TABLE 16. Values of k_{uf} and c_{uf} for Unfrozen Soil, $T = 4.44°C$

Moisture Content, M_{wo} (% of dry wt.)	Thermal Conductivity, k_{uf} (watts/m °K)	Heat Capacity, c_{uf} (Joules/m^3 °K)
15	0.70	1.6×10^6
30	1.10	2.4×10^6
45	1.05	3.0×10^6

TABLE 17. Values of L_f

Moisture Content, M_{so} (% of dry wt.)	Heat of Fusion, L_f (Joules/m^3)
15	60×10^6
30	120×10^6
45	200×10^6

APPENDIX III

U Factor for snow cover

The average density of the snow cover is 250 kg/m³ and its average thermal conductivity is 0.13 watts/m °C (Gold, 1963).

TABLE 18. Snow Cover Depth for Norman Wells from Potter (37)

Year	Snow Depth (m.)		U Factor of Snow Cover U_{SN} (watts/m² °C)	
	Minimum Depth	Maximum Depth	U_{SN}(Min)	U_{SN}(Max)
0.0	0.28	0.71	0.46	0.18
0.083	0.28	0.76	0.46	0.17
0.167	0.46	1.02	0.28	0.13
0.250	0.48	0.97	0.27	0.13
0.333	0.0	0.61	∞	0.21
0.417	0.0	0.0	∞	∞
0.500	0.0	0.0	∞	∞
0.583	0.0	0.0	∞	∞
0.667	0.0	0.0	∞	∞
0.750	0.0	0.15	∞	0.87
0.833	0.0	0.31	∞	0.42
0.917	0.15	0.46	0.87	0.28
1.00	0.28	0.71	0.46	0.18

U Factor for Vegetation (Peat) Layer

TABLE 19. Values of k_{uf} and k_f for Peat

Dry Weight kg/m^3	Moisture Content % of dry wt.	Thermal conductivity watts/m°C k_{uf}	k_f
250	50	0.067	0.075
	150	0.20	0.33
	250	0.32	0.75
100	50	0.037	0.045
	150	0.058	0.077
	250	0.08	0.15

Values of the thermal conductivity were obtained from Lunardini (28).

Consider only the conditions that give the largest and the smallest values of k_{uf} and k_f for peat.

TABLE 20. Values of U_{uf} and U_i

Dry Weight kg/m^3	Moisture Content % of dry wt.	Depth of Peat (m)	U factors watts/m² °C U_{uf}	U_i
250	250	0.1	3.20	7.50
		0.2	1.60	3.75
		0.3	1.07	2.50
100	50	0.1	0.37	0.45
		0.2	0.18	0.22
		0.3	0.12	0.15

From the table, the conditions that best fit the values used in the numerical calculations are

Dry density = 250 kg/m^3

Moisture content = 250%

Depth of peat = 0.25 m

The corresponding U-factor values are

$$U_{uf} = 1.28 \text{ watt/m}^2\text{-}^\circ C$$

$$U_i = 3.0 \text{ watt/m}^2\text{-}^\circ C$$

U-factor in Summer and Winter

U-factor in summer, $U_s = U_{uf}$

U-factor in winter, $U_w = \dfrac{1}{\dfrac{1}{U_{SN}} + \dfrac{1}{U_i}}$

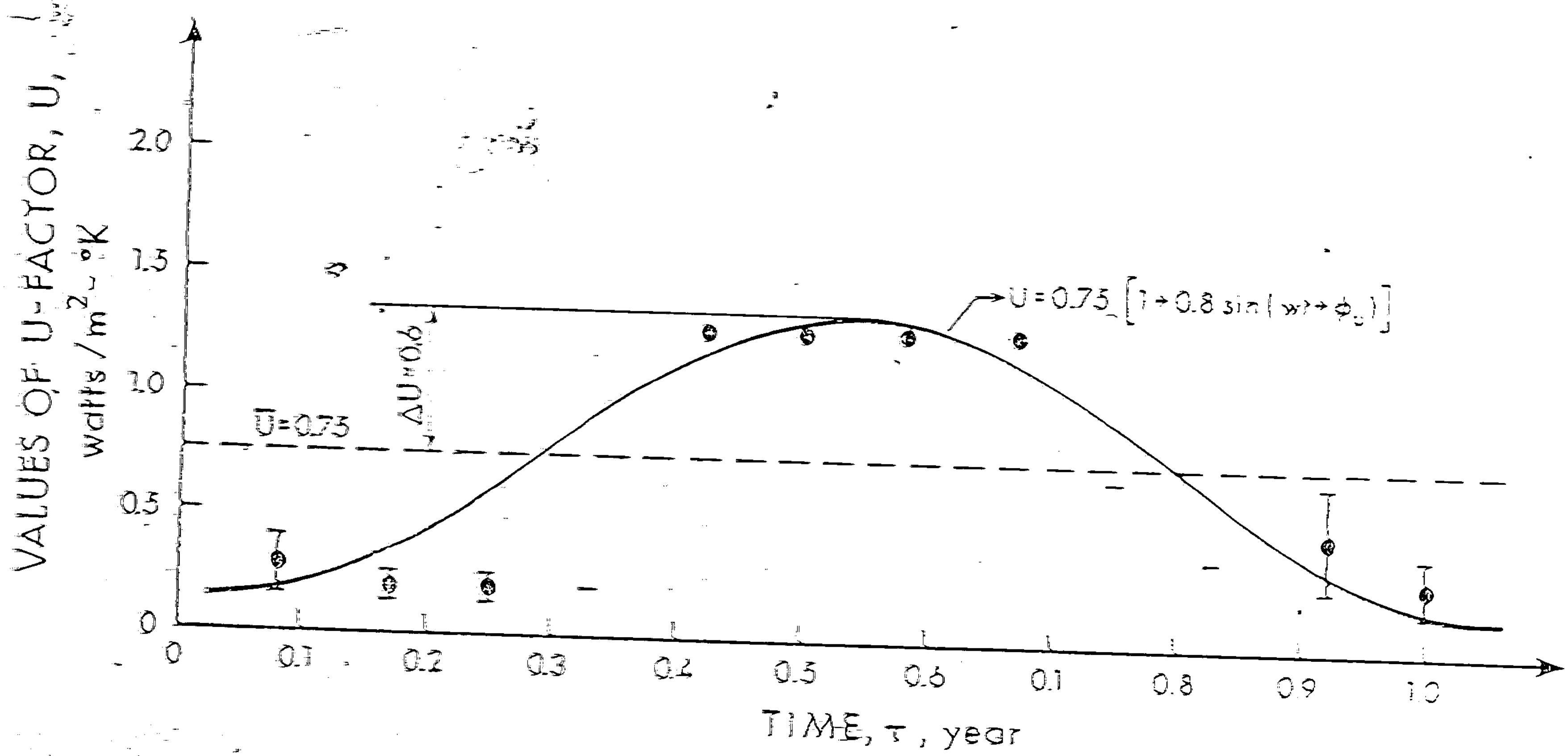

FIGURE 41 – Approximate values of the U - Factor for Norman Wells

TABLE 21. Values of U_b and U_w for the year

Year	U_b watt/m^2 °C	U_w watts/m^2 °C	
		$U_{w(max)}$	$U_{w(min)}$
0.08		0.40	0.16
0.17	–	0.26	0.13
0.25	–	0.25	0.13
0.33	–	–	0.20
0.42	1.28	–	–
0.50	1.28	–	–
0.58	1.28	–	–
0.67	1.28	–	–
0.75	–	–	0.68
0.83	–	–	0.37
0.92	–	0.68	0.26
1.00	–	0.40	0.17

The thermal properties of the snow cover used are 250 kg/m^3 for the density and 0.13 watt/m-°C for the thermal conductivity. These properties are dependent on many factors, such as, temperature, moisture content, fresh or settled snow and the method used in determining them, as such their values varied over a wide range. For example its density ranges from 72 to 400 kg/m^3 (40, 41) and its thermal conductivity ranges from 0.018 to 0.5 watt/m-°C. This wide range in values indicate .

variability in the thermal properties of snow. The thermal properties of peat as those for the snow cover are also dependent on many factors, such as, moisture content, porosity, plant structure, temperature and drainage. Peat, because of its nature, has a great ability to soak up water many times its own weight. The moisture content as such determines the thermal properties of peat to a great extent. The moisture content of the peat varies considerably, being less in the more decomposed types than with more fibrous types, and it also varies with season and the corresponding position of the ground water table. For pure peats, when saturated, the water content is more than 600 per cent of dry weight, generally varying between 750 and 1500 per cent but extremes of 50% and 3000% have been noted. However a small percentage of inorganic material in the peat will seriously affect the water content value, which will drop sharply as the mineral contamination increases. The dry unit weight of the peat also varies considerably ranging from 40 to 400 kg/m^3 depending on the type of peat (39). The observed thickness of the peat ranges from 30 cm to more than 6 m in the discontinuous permafrost zone. It usually does not exceed 1 m in the continuous permafrost zone.

APPENDIX IV

Climatic Conditions

Solar Short Wave Radiation

The range of values of short wave radiation (R_n) for a latitude of 65°N from 1943-1957 (42).

TABLE 22. Values of R_n for Norman Wells (65°17'N)

Months	Year	Mean Radiation (watts/m^2)	Mean Absolute Deviation (watts/m^2)
January	0.08	6.94	± 1.39
February	0.17	27.78	± 4.17
March	0.25	90.28	± 6.94
April	0.33	158.33	± 8.33
May	0.42	201.39	±15.28
June	0.50	208.33	±16.67
July	0.58	193.06	±11.11
August	0.67	138.89	±13.89
September	0.75	75.00	± 8.33
October	0.83	33.33	± 5.55
November	0.92	11.11	± 2.78
December	1.00	2.78	

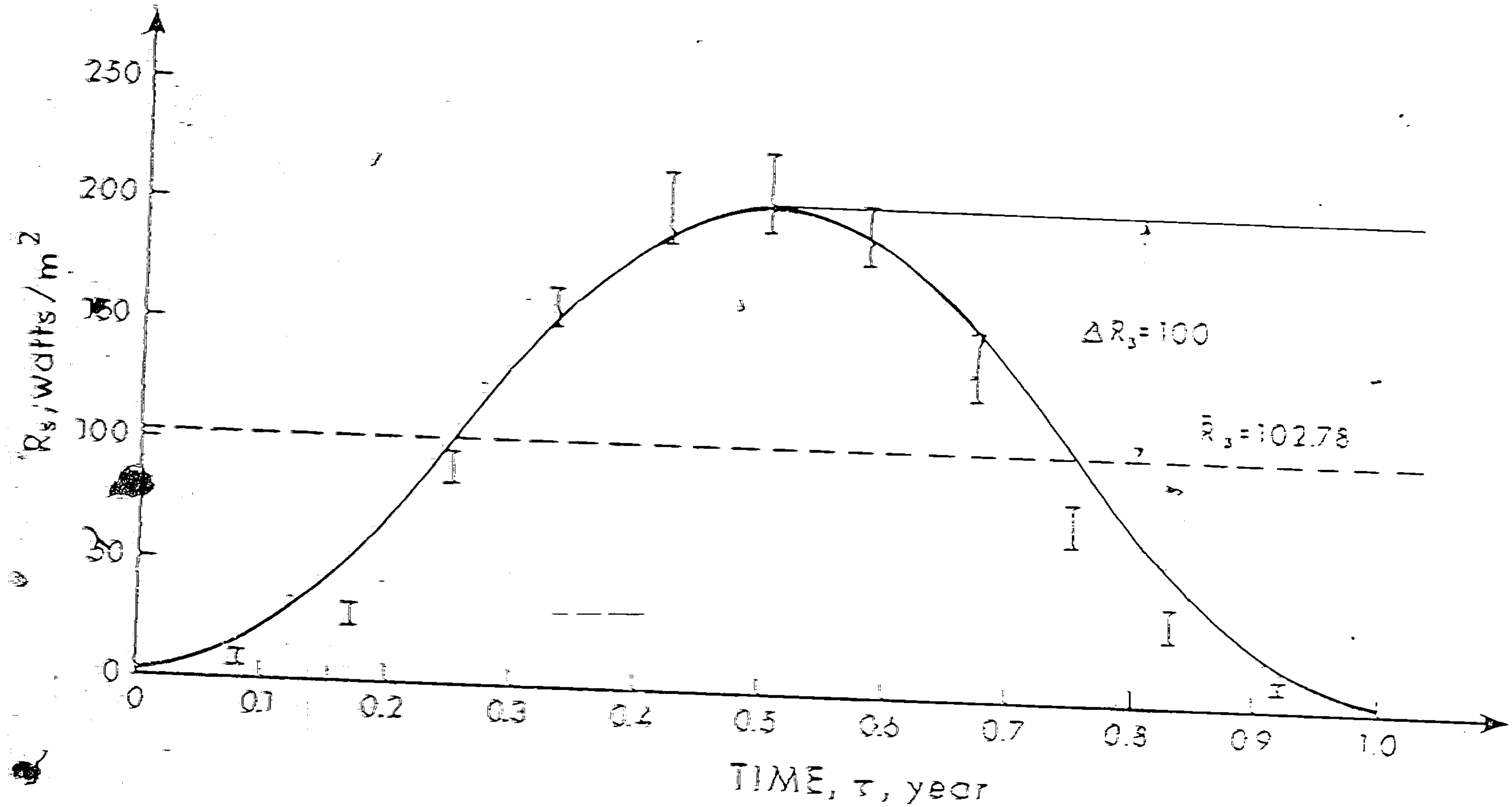

FIGURE 42 – Total radiation (Lat 65° N)
Source: Radiation climate of the Artic

APPENDIX V

Clausius Clapeyron equation expresses the relationship between the temperature T and the saturated vapor pressure e_{ss}. The equation is

$$\frac{de_{ss}}{e_{ss}} = X \frac{dT}{(T+273)^2}, \qquad (i)$$

Integrating equation (i) gives

$$\ln(e_{ss}) = -X/(T+273) + Y \qquad (ii)$$

where X and Y are constants.

TABLE 23. Values of T and e_{ss}

T(°C)	1/(T+273) (°K^{-1})	Sat. Vapor Press. (M_b)
20	0.00341	23.37
10	0.00353	12.27
0	0.00366	6.11
-10	0.00380	2.86
-15	0.00388	1.91
-20	0.00395	1.25
-25	0.00403	0.81
-30	0.00412	0.51
-40	0.00429	0.19

X and Y are obtained by obtaining values of e_{ss} and $1/(T+273)$ from Figure (43) and then substituting them into equation (41). The calculated values for X and Y are

$$X = 5900 \quad \text{and} \quad Y = 23.4$$

hence

$$e_{ss} = e^{23.4} \, e^{-5900/(T_a+273)}$$

The air vapor pressure is given by

$$e_a = w e_{ss}$$

or

$$e_a = w e^{23.4} \, e^{-5900/(T_a+273)}$$

where w is the relative humidity.

The surface vapor pressure is given by

$$e_s = M_s \, e_{ss} + (1-M_s) \, e_a$$

where M_s is the moisture content.

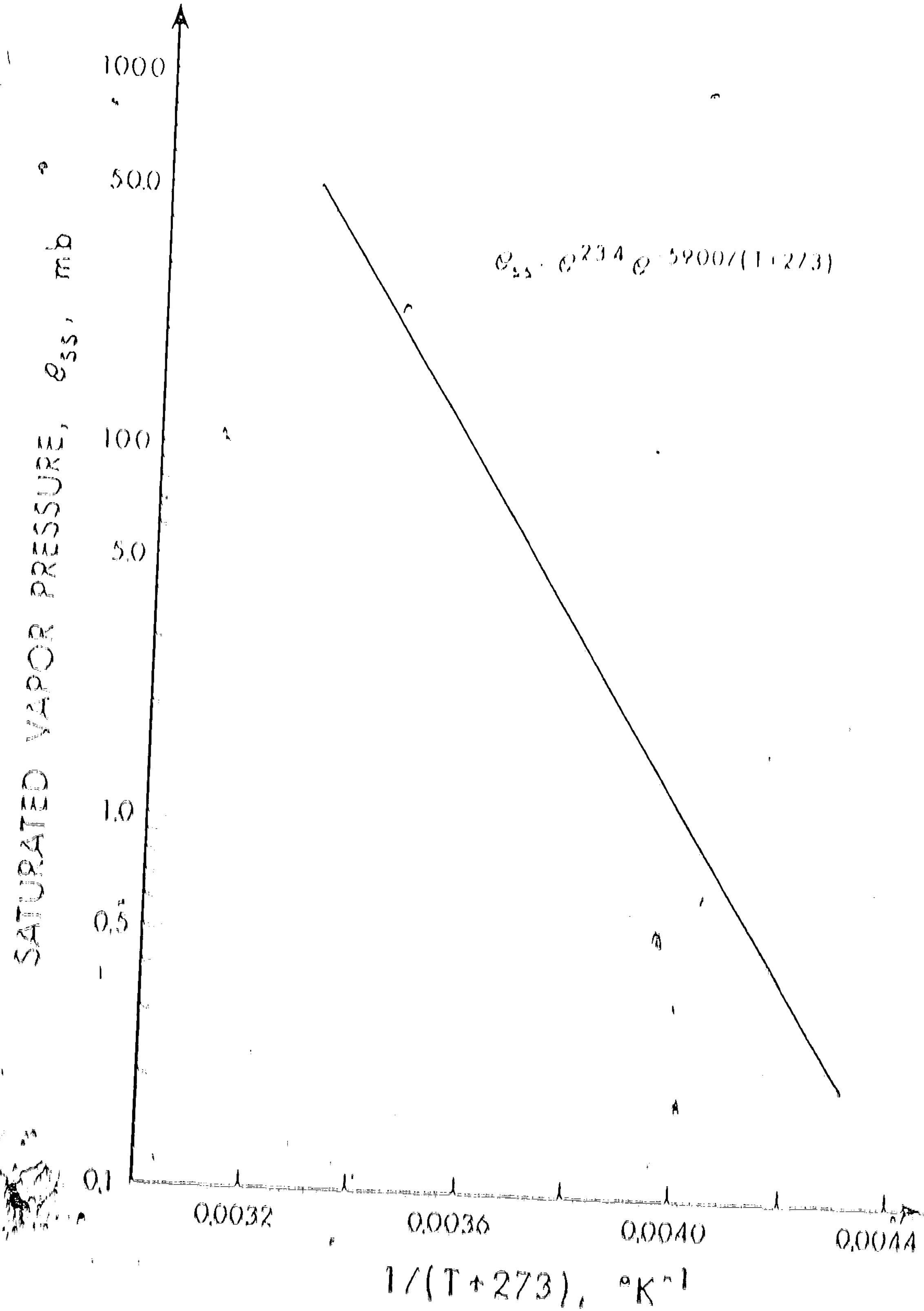

FIGURE 43 — Saturated vapor pressure (mb) vs 1/T ($°K^{-1}$)

TABLE [illegible]. Mean Relative Humidity for Norman Wells from Climatic Normals ([illegible])

Month	w
January	
February	
March	0.73
April	0.73
May	0.65
June	0.59
July	0.66
August	0.72
September	0.80
October	0.84
November	0.79
December	

Considering only the relative humidity w in the summer months, the average relative humidity is 0.65.

[illegible]

TABLE [illegible]. Mean monthly cloud cover for [illegible] from [illegible] Climatic Normal [illegible]

Month	W
January	0.5[illegible]
February	0.58
March	0.5[illegible]
April	0.55
May	0.65
June	0.64
July	0.67
August	0.69
September	0.72
October	0.73
November	0.67
December	0.60

The mean annual cloudiness was 0.63.

TABLE 26. Mean Monthly Wind Velocity (m/sec)

at Norman Wells [illegible] [illegible] ([illegible])

Month	Mean Monthly Wind Vel. (m/sec)	Standard Deviation (m/sec)
January	3.00	3.26
February	2.77	2.91
March	3.31	2.82
April	3.71	3.13
May	3.80	2.82
June	4.07	2.41
July	3.71	2.50
August	3.62	2.46
September	3.71	2.77
October	3.67	2.86
November	3.08	2.82
December	2.73	3.04

Mean annual wind velocity is 3.43 m/sec.

Mean annual standard deviation is 2.82 m/sec.

This value used in the calculations is u = 4.5 m/sec.

TABLE 27. Mean Sea Level Pressure P (mb) for Norman Wells from Climatic Normals (59)

Months	P (mb)
January	102[illegible]
February	1024
March	1022
April	1020
May	1018
June	1014
July	1013
August	1013
September	1014
October	1012
November	1018
December	1018

Annual mean sea level pressure P is 1018 mb. This corresponds to a tare air pressure at Norman Wells of 1000 mb.